SOME PROPERTIES OF D-REGION PARTIAL REFLECTIONS

A thesis presented for the
degree of Doctor of Philosophy in Physics
in the University of Canterbury,
Christchurch, New Zealand.

by

H.A. von Biel

1970

ABSTRACT

In this work the conditions and requirements that lead to a randomly phased angular spectrum of plane waves are investigated. An experimental technique is developed from which the complex spatial correlation of the electromagnetic fields at two spaced antennas may be obtained. It is shown that the complex correlation of these electromagnetic fields is strongly influenced by the amount of angular correlation within the spectrum of plane waves. From this theoretical development emerge criteria that may be used to test the hypothesis that a spectrum of plane waves was randomly phased. Experimental results from a multiple baseline field correlation experiment are presented. In this program the primary intent was to obtain data from D-region altitudes between 70 km and 90 km. The data from the E-region are primarily for comparison purposes.

It is shown that the angular spectrum due to scattering in the ionospheric D-region is probably not randomly phased. In comparison, the results obtained from E-region scatter appear to support

the validity of the randomly phased angular spectrum approximation.

It is further shown that the angular power spectrum due to scattering in the D-region contains a plane undiffracted wave component which accounts for approximately 25% of the received power.

Extensive effort was devoted to the identification of D-region echo amplitudes with a Rice probability density distribution. It is shown that the majority of the amplitude distributions analyzed were Rayleigh distributed.

The concept and credibility of the "off-set" Rayleigh distribution are investigated and a theoretical interpretation of the observed facts is presented.

ACKNOWLEDGEMENTS

I am greatly indebted to my employer, Cornell Aeronautical Laboratory of Buffalo, New York, U.S.A., who by granting me a prolonged sabbatical leave of absence, made my visit to New Zealand possible.

I further gratefully acknowledge the help and assistance of W.A. Flood and H.G. Camnitz, my colleagues from 1959 to 1967 at Cornell Aeronautical Laboratory, who provided me with ideas and theoretical approaches which ultimately culminated in the project reported here.

I was indeed fortunate to be associated with R.G.T. Bennett and G.J. Fraser while in residence at the University of Canterbury, and I am indebted to them for their help and constructive criticism during the performance of the experimental work.

Finally, I wish to express my greatest thanks to my wife, Margaret, who in addition to keeping the family running from day to day, also provided me with much needed encouragement. I am particularly indebted to her for typing the manuscript of this work.

TABLE OF CONTENTS

TABLE OF ILLUSTRATIONS

I. INTRODUCTION

The investigation of the ionospheric D-region by means of ground-based radar techniques has a relatively short history when compared to other ionospheric research work. Although the existence and some of the characteristics of the D-region have been well known for some time, it was probably not until Gardner and Pawsey's work (1953), that extensive ground-based D-region experiments were conducted by other investigators.

Soon after the Differential Absorption experiment was reported by Gardner and Pawsey, Fejer (1955) published his findings from a Wave Interaction experiment. These two radar techniques, with few exceptions (Parthasarathy et al. 1963) appear to be the most successful methods yet devised for a ground-based assessment of the D-region electron density concentration. While the accuracy and individual merits of these two techniques is a highly debatable subject, there seems to be little doubt that the electron density profiles obtained from either technique are representative of the true variation of free electrons with altitude in the D-region. From the point of view of relative simplicity of instrumentation and

interpretation of resulting data, it further appears that the partial reflection-differential absorption technique has been favored among the various investigators. Whether or not this assumption is truly representative of the status quo, for the purpose of introducing the subject matter of this work, the discussion will henceforth be confined to some of the problem areas that plague the Gardner Pawsey, or "D.A." experiment, even though some of the following comments may be apropos to a large portion of ionospheric investigations.

In their publication, Gardner and Pawsey (1953) postulate a partial reflection mechanism which, when viewed in its essentials, is one of reflection from discontinuities in the mean refractive index of the medium. While much has been written on the subject since 1953, probably the most comprehensive review and implementation of the D.A. experiment was published by Belrose and Burke (1964). These authors conclude that poor experimental results in the past were due to insufficient transmitted power and poor magneto-ionic mode discrimination upon reception. They recognized, as did Gardner and Pawsey, that backscatter from the D-region is probably caused by a mechanism of far greater complexity than the simple Fresnel

process postulated. Belrose and Burke attempted to generalize the scatter cross-section by means of "Booker (1959) scattering". This attempt was inconclusive because the calculations did not include the effects of absorption in the scattering volume.

From 1965 to 1968, this author, at Cornell Aeronautical Laboratory, Buffalo, New York, conducted a series of D.A. experiments and reported his findings. (von Biel 1965, 1966). The experiments were designed to overcome most of the objections to experimental technique which were pointed out by Belrose and Burke. In addition, and with the help of his colleagues (W.A. Flood and H.G. Camnitz), the data analysis technique was altered so as to include the effects of differential absorption in the scattering volume. From this work evolved the "D-Region Volume Scatter Theory" as reported by Flood (1968) and the "Partial Reflection Differential Phase Technique" as reported by von Biel, Flood, and Camnitz (1970).

There appears to be little doubt in the minds of most investigators that the D.A. experiment is the most accurate and reliable ground-based experiment available today for the determination of D-region electron density. While this statement may be regarded as an expression of confidence in an experi-

mental technique, it must also be accompanied by at least two or three clarifying remarks:

(a) The electron density derived from this experiment will probably be somewhere near plus or minus 100 per cent from the true electron density in the D-region if

(1) the analysis is restricted to an altitude interval between 70 km and 90 km, and

(2) the experimental data are carefully screened and all "contaminating" data are rejected.

(b) Within the limits of accuracy claimed for this experiment (i.e. a factor of 2), the experimental results are surprisingly immune to rather large errors in the (assumed) collisional frequency profile, and to attempts on the part of the investigator to refine the underlying theoretical formulation.

A few words of explanation in support of (b) seem appropriate at this time. Gardner and Pawsey made use of the classical magneto-ionic theory in which the expression for the complex refractive index is due to Appleton and Hartree. In this theory,

no allowance was made for the velocity distribution of free electrons in the medium under investigation. In 1960 Sen and Wyller proposed the generalized magneto-ionic theory in which the velocity distribution is assumed to be Maxwellian. There can be no doubt that recognition of, and due allowance for, the velocity distribution in the ionosphere has improved the theoretical formulation of the magneto-ionic theory. However, modification of data analysis procedures from the traditional theory to the Sen-Wyller theory has not improved the confidence limits of results from the D.A. experiment. In fact, modern results appear to be about the same as those given by Gardner and Pawsey. Again, Flood's (1968) "Revised Theory..." when applied as a refinement of D.A. data analysis does not appear to change the electron density results in a practical significant manner. At any rate, the confidence in the results remains within a factor of two.

After many unhappy hours devoted to the seemingly impossible task of improving the accuracy and reliability of results from the D.A. experiment, this author concluded that some, if not all, of the assumptions made about D-region scattering are based on wishful thinking rather than fact. To illustrate,

consider one of the primary assumptions made; namely, that the cone of back-scattered radiation from the D-region is narrow and centered on the vertical direction. Under these circumstances one would expect echoes from the vertical direction only; and yet, a common explanation for data "contamination" is the reception of "oblique" echoes. In fact, when this author conducted experiments in which a carefully controlled circularily polarized signal was transmitted, much too frequently was the returned signal linearily polarized (von Biel 1966). This observation is clearly not consistent with mode-coupling (Budden 1961). One would expect the ratio of the two magneto-ionic components to be of the order of 100 to 1 or greater, but certainly not 1 to 1. One must conclude, in a purely qualitative fashion, that the cone angle of arrival might in reality be neither narrow nor centered on the vertical direction.

In persuing this point, an attempt was made to obtain an estimate of the scale sizes of scatterers in the D-region. A review of the available literature on this subject soon revealed that the only extensive measurements were those by Briggs and Philips (1950) and these were primarily concerned

with the E and F regions. Furthermore, the experimental technique employed was that of finding the correlation of amplitudes at two spatially separated antennas. The usefulness of this technique requires that two assumptions be made; first, that the amplitudes are either Rayleigh distributed or else that they are "displaced" gaussian distributed, and second, that the angular spectrum is randomly phased. Only under these circumstances may the spatial correlation of the complex fields be associated with the spatial correlation of the amplitudes (Bramley 1950, Booker et al. 1950).

From an experimental point of view, there is little difficulty in ascertaining how the amplitudes are distributed. However, this author is not aware of any experimental methods that have been used to substantiate the premise that the angular spectrum was, in fact, randomly phased. To quote Ratcliffe (1956):

> "In much of the work on the ionosphere it has been assumed without sufficient proof that the angular spectrum was randomly phased. There are no established methods for testing this assumption, without examining in detail the distribution of ampli-

> tude and phase in f(x), and that is often prohibitively difficult. It is important that methods should be devised for determining when a spectrum is randomly phased."

It now appears that one is forced to substantiate two additional assumptions of a far more basic nature in order to substantiate the assumption made for the D.A. experiment. The obvious conclusion to be reached from the state of things was to abandon the art of "model making" for the D-region. Instead, it was decided to perform some basic measurements which, hopefully, might lead to a deeper insight into the intricacies of this elusive portion of the earth's ionosphere. Specifically, an experiment was designed and constructed from which the correlation of the complex field distribution could be deduced. The primary aim of the experiment was to obtain estimates of the correlation "length" and of the angular spectrum in a way that would avoid recourse to the assumption that the angular spectrum is randomly phased. In addition to this primary task, an extensive investigation was made of the statistical distribution of received echo amplitudes. Much of the theoretical effort for this program was directed toward the derivation of an expression for

the complex field correlation on the assumption that the angular spectrum is not randomly phased. As will be shown later, under these circumstances the spatial field correlation will be complex and dependent on the specific location of the experiment in the field pattern.

The overall goal of this project is to supply some basic answers with regard to the complex field distribution of echoes partially reflected from the D-region. It is not to be expected that these materials alone will cure the ills of the D.A. experiment, but certain of the results are indicative of past misconceptions about D-region scattering.

II. THEORETICAL ASPECTS

In the sections that follow, an attempt will be made to examine the theoretical formulations that lead to the concept of a spatial correlation function of two electromagnetic fields. It will be shown that if certain assumptions can be made with regard to the statistical relationship between the phases of individual waves within a spectrum of plane waves, then the resulting expression for the spatial correlation of two electromagnetic fields is simply the Fourier transform of the power spectrum of plane waves that gave rise to those fields. Furthermore, it will be shown that under these circumstances, the spatial correlation of the two fields is dependent only on the physical separation of two points at which the fields are defined, and is independent of the absolute position of these points within the field pattern.

The effects upon the formulation of the complex spatial field correlation under conditions when the above simplifying assumptions do not apply will next be examined. It will be shown (in section II-2) that a non-zero correlation within a spectrum of plane waves will manifest itself in the form of an "angular

filter function" which acts on the angular power spectrum of plane waves. It will be shown that under these circumstances the Fourier transform of the spatial field correlation is not equal to the angular power spectrum, but rather to the product of the angular power spectrum and this "angular filter function".

II(1). THE RANDOMLY PHASED ANGULAR SPECTRUM

Much of ionospheric research work conducted today has been made possible through a clear understanding of the stochastic processes that are inherent to electrical "noise" and other randomly fluctuating quantities. Thus, Booker, Ratcliffe, and Shinn (1950) were able to associate statistical theory with experimentally observable processes in the ionosphere on the basis of the fundamental work done by Rice (1944, 1945) and Uhlenbeck (1945). Probably the chief contribution of this work to an understanding of the upper atmosphere was their realization that a complex distribution of electromagnetic energy could be synthesized into a spectrum of plane waves and that the resulting angular spectrum was the Fourier transform of the "aperture distribution" that gave rise to it. Because their theory is general, it must hold true in any situation, and consequently it must be equally applicable for a situation in which the field distribution that gives rise to an angular spectrum can only be described in a statistical sense. It is at this point that the notion of the complex field correlation is introduced into their work, and it is

shown that the Fourier transform of this complex correlation of the electromagnetic fields is equivalent to the angular power spectrum of plane waves.

Many different diffracting screens may be postulated to exist in a medium such as the ionosphere. However, the one screen which appears to lend itself most readily to mathematical analysis and manipulation is assumed to consist of a continuum of uncorrelated scatterers. These scatterers are assumed to be related to one another only from the point of view that their "sizes" are the same. If such a screen were illuminated by a plane wave and the resulting field pattern were investigated by means of two antennas spaced from one another by some distance (r) at a large distance from the screen, how can the correlation of the voltages induced in the antennas be related to the characteristics of the screen itself? The answer to this question is most eloquently given by Bramley (1950).

Consider that the screen modifies the incident plane wave so that the result is a spectrum of n plane waves, each of which makes an angle $\frac{\pi}{2} - \theta_n$ with the line joining the two antennas. The voltage induced into antenna 1 will be E_1 so that

$$E_1 = \int_{-\pi/2}^{\pi/2} A(\theta) \cos\left\{\omega t + \frac{\pi r}{\lambda} \sin\theta + \phi(\theta)\right\} d\theta \qquad (1)$$

Likewise, the voltage induced into antenna 2 is E_2 and

$$E_2 = \int_{-\pi/2}^{\pi/2} A(\theta) \cos\left\{\omega t - \frac{\pi r}{\lambda} \sin\theta + \phi(\theta)\right\} d\theta \qquad (2)$$

In the above equations $A(\theta)$ represents the amplitude of a wave arriving at some angle θ, while $\phi(\theta)$ is assumed to be the phase of that wave upon emergence from the screen. The total power collected by each of the two antennas is proportional to the mean squared value of E_1 or E_2 so that

$$\overline{|E_1|^2} = \overline{|E_2|^2} = \frac{1}{2} \text{REAL}\left\{\int_{-\pi/2}^{\pi/2}\int_{-\pi/2}^{\pi/2} A(\theta) A(\theta')^* \exp i\left[\phi(\theta) - \phi(\theta') + \frac{\pi r}{\lambda}(\sin\theta - \sin\theta')\right] d\theta d\theta'\right\} \qquad (3)$$

Assume next that the $\phi(\theta)$'s are uniformly distributed between $-\pi$ and $+\pi$ and further assume that $\phi(\theta)$ is statistically independent from any other $\phi(\theta')$. For these conditions the only contribution to the integral in (3) occurs when $\theta = \theta'$. Thus:

$$\overline{|E_1|^2} = \overline{|E_2|^2} = \frac{1}{2} \text{REAL}\left\{\int_{-\pi/2}^{\pi/2} A(\theta)^2 \, d\theta\right\} \qquad (4)$$

The co-variance $\overline{E_1 E_2^*}$ can be obtained in a similar manner:

$$\overline{E_1 E_2^*} = \tfrac{1}{2}\,\mathrm{REAL}\left\{\int_{-\pi/\lambda}^{\pi/\lambda}\int_{-\pi/\lambda}^{\pi/\lambda} A(\theta)A(\theta')^* \exp\left[\phi(\theta)-\phi(\theta')+\frac{\pi r}{\lambda}(\sin\theta+\sin\theta')\right]d\theta\, d\theta'\right\} \tag{5}$$

Again, when the conditions that lead to (4) are assumed, one obtains:

$$\overline{E_1 E_2^*} = \tfrac{1}{2}\,\mathrm{REAL}\left\{\int_{-\pi/\lambda}^{\pi/\lambda} A(\theta)^2 \cos\left[\frac{2\pi r}{\lambda}\sin\theta\right]d\theta\right\} \tag{6}$$

Now, by definition, the spatial field correlation $\rho(r)$ is given by:

$$\rho(r) = \frac{\overline{E_1 E_2^*}}{|E_1|^2} = \frac{\tfrac{1}{2}\,\mathrm{REAL}\left\{\int_{-\pi/\lambda}^{\pi/\lambda} A(\theta)^2 \cos\left[\frac{2\pi r}{\lambda}\sin\theta\right]d\theta\right\}}{\tfrac{1}{2}\,\mathrm{REAL}\left\{\int_{-\pi/\lambda}^{\pi/\lambda} A(\theta)^2\, d\theta\right\}} \tag{7}$$

It will next be convenient to replace $\frac{1}{2}\,\mathrm{REAL}\left\{\int_{-\pi/\lambda}^{\pi/\lambda} A(\theta)^2 d\theta\right\}$ by $\int_{-\pi/\lambda}^{\pi/\lambda} P(\theta)\, d\theta$ and rewrite (7) so that

$$\rho(r) = \frac{\int_{-\pi/\lambda}^{\pi/\lambda} P(\theta)\cos\left[\frac{2\pi r}{\lambda}\sin\theta\right]d\theta}{\int_{-\pi/\lambda}^{\pi/\lambda} P(\theta)\, d\theta} \tag{8}$$

To reiterate the assumptions that have lead to (8): it was assumed that for the postulated angular spectrum of plane waves, the phase of every individual component was uniformly distributed between $-\pi$ and $+\pi$, and that the phase of each

individual plane wave was statistically independent of the phases of other waves in the spectrum. When the angular spectrum satisfies both of these assumptions, the angular spectrum is considered to be randomly phased. Also, if the amplitudes at antennas 1 and 2 are Rayleigh distributed, then Bramley (1950) has shown that the correlation of amplitudes from antennas 1 and 2 is approximately proportional to the square of the complex field correlation. On the other hand, if the distribution of amplitudes is nearly gaussian and the angular spectrum is randomly phased, then the correlation of amplitudes is equal to the complex field correlation. No definitive statement may be made about the relationship between the amplitude correlation and the field correlation if the above conditions are not satisfied.

Having arrived at a concise understanding regarding the requirements of the randomly phased angular spectrum (which henceforth will be abbreviated RPAS) one is next lead to investigate the consequences and implications of this concept. We shall assume that the field due to a spectrum of plane waves is given by

$$E(x) = \int_{-\infty}^{\infty} G(S) \exp i\{kSx\}\, dS \qquad (9)$$

where $S = \sin\Theta$

$$k = \frac{2\pi}{\lambda}$$

and (x) is a linear dimension in a plane parallel to the scattering screen.

It next follows that the field at a point (x+r) is given by

$$E(x+r) = \int_{-\infty}^{\infty} G(S) \exp i\{kS(x+r)\} dS \qquad (10)$$

The covariance is $\overline{E(x)E(x+r)^*}$, so that:

$$\overline{E(x)E(x+r)^*} = \int_{-\infty}^{\infty}\int_{-\infty}^{\infty} \overline{G(S)G(S')^*} \exp i\{kx(S-S')\} \exp -i\{krS\} dS dS' \qquad (11)$$

In order to satisfy the conditions stated earlier for RPAS we conclude that $\overline{G(S)G(S')^*} = P(S')\delta(S-S')$ and find that

$$\overline{E(x)E(x+r)^*} = \int_{-\infty}^{\infty}\int_{-\infty}^{\infty} P(S')\delta(S-S') \exp i\{kx(S-S')\} \exp -i\{krS\} dS dS' \qquad (12a)$$

$$\overline{E(x)E(x+r)^*} = \int_{-\infty}^{\infty} P(S') \exp -i\{kS'r\} dS' \qquad (12b)$$

The right hand member of (12b) is seen to be of the same form as was the right hand member of (6), and consequently both satisfy the RPAS conditions. Furthermore, the right hand member of (12b) is seen to be <u>independent of position</u> (<u>x</u>). We must conclude that $\overline{E(x)E(x+r)^*}$ must therefore also be independent

of (x) so that the RPAS conditions are satisfied. Some further thought devoted to this situation will reveal that when $\rho(r) = \frac{\overline{E(x)E(x+r)^*}}{\overline{|E(x)|^2}}$ is independent of (x), then it constitutes both a necessary and sufficient condition that the angular spectrum is randomly phased.

From the foregoing discussion it is reasonable to conclude that a fairly straightforward experiment could be conducted in order to test the hypothesis that the angular spectrum is randomly phased. To perform such a test it would be necessary to operate simultaneously two field-correlation experiments separated by some distance from each other. If the results from these two stations are identical to within experimental error, then the RPAS conditions are satisfied. While this is an appealing thought, the overall experiment would yield only a qualitative answer to the problem. Furthermore, the cost of constructing and operating two identical stations was considered prohibitive in view of the possible benefits to be derived.

Instead, it was decided to investigate another aspect of the problem: how would the spatial correlation be influenced if the angular spectrum

were not randomly phased? The theoretical derivation and results of this problem are presented in the next section.

II(2). THE COMPLEX FIELD CORRELATION

In the previous section the randomly phased angular spectrum (RPAS) was defined. It was also shown that a necessary and sufficient condition for the angular spectrum to be randomly phased is that the spatial field correlation be independent of position in a plane parallel to the scattering screen. In this section the spatial field correlation will be derived on the assumption that the angular spectrum is not randomly phased.[1] Specifically, it will be assumed that the angular correlation within the spectrum of the plane waves is a gaussian function rather than the delta function stipulated earlier.

For the purposes of this problem we shall assume a two-dimensional geometry so that a transmitter on the surface of the earth is located at $x=0$ and $z=-H_o$. The scattering screen is assumed to be large and illuminated by the transmitter from $-L_o \leq x \leq +L_o$. Before proceeding, it will prove helpful to normalize all linear dimensions to the operating

---

(1). This approach to the problem was suggested by W. A. Flood in 1967.

wavelength λ . We shall define all un-normalized linear dimensions by a subscript "0".

The electromagnetic field at (x) and (z), back-scattered from a screen at z=0 will, in general, be given by

$$E(x,z) = \int_{-\infty}^{\infty} F(S) \exp i\left[2\pi(xS + zC)\right] dS \qquad (13)$$

In (13) F(S) is the angular spectrum function, S=SINΘ, C=COSΘ, and Θ is an angle measured from the positive z direction. Since F(S) and E(x,0) are Fourier transform pairs, it follows that:

$$F(S) = \int_{-\infty}^{\infty} E(x,0) \exp -i\left[2\pi x S\right] dx \qquad (14)$$

The field due to the scattering screen at a point (x+r) is given by

$$E(x+r,z) = \int_{-\infty}^{\infty} F(S) \exp i\left[2\pi\left\{S(x+r) + zC\right\}\right] dS \qquad (15)$$

The covariance of these two fields will be given by (I) where

$$I = \overline{E(x,z)\, E(x+r,z)^*} \qquad (16a)$$

$$I = \int_{-\infty}^{\infty}\int_{-\infty}^{\infty} \overline{F(S)F(S')^*} \exp i\left\{2\pi\left[x(S-S') + z(C-C') - rS'\right]\right\} dS\, dS' \qquad (16b)$$

In equation (16) the asterisk is used to indicate the complex conjugate of a quantity, while the overbar indicates an ensemble average.

If in equation (16b), S or S' are much smaller

than one, then C may be replaced by $1-\frac{S^2}{2}$ and C' by $1-\frac{(S')^2}{2}$. A further useful substitution is to let $\sigma = S-S'$. We now obtain

$$C-C' \doteq \frac{(S')^2-S^2}{2} = -\sigma(\sigma+2S') \qquad (17)$$

The above assumption will cause an error of less than 1% in C-C' when $|\theta| \leq 32°$. We shall next identify the average value $\overline{F(S)F(S')^*}$ with the product of the mean squared value $\overline{|F(S')|^2}$ and the angular correlation within the spectrum of plane waves, $\rho(\sigma)$. Thus:

$$\overline{F(S)F(S')^*} = \overline{F(\sigma+S')F(S')^*} = \rho(\sigma)\overline{|F(S')|^2} \qquad (18)$$

After rewriting (16b) one obtains:

$$I = \int_{-\infty}^{\infty} \overline{|F(S')|^2} \exp\{-i[2\pi rS']\} I_1 \, dS' \qquad (19a)$$

where

$$I_1 = \int_{-\infty}^{\infty} \rho(\sigma) \exp\{-i[\pi z\sigma^2]\} \exp i\{2\pi\sigma(x-S'z)\} \, d\sigma \qquad (19b)$$

Inspection of (19a) reveals immediately that the RPAS conditions would be satisfied if $I_1 = 1.0$. Also, (19b) would be equal to 1.0 if $\rho(\sigma) = \delta(S-S')$. Evidently therefore, equation (19) is consistent with our conclusions from the previous section.

Let us next look at the angular spectrum function F(S). In equation (14) we defined F(S) so that

$$F(S) = \int_{-\infty}^{\infty} E(x,0) \exp -i\{2\pi x S\}\, dx \qquad (14)$$

Likewise:

$$F(S') = \int_{-\infty}^{\infty} E(x',0) \exp -i\{2\pi x' s'\}\, dx' \qquad (20)$$

the covariance $\overline{F(S)F(S')^*}$ will then be I_2:

$$I_2 = \int_{-\infty}^{\infty}\int_{-\infty}^{\infty} \overline{E(x)E(x+r)^*} \exp i\{2\pi r s'\} \exp -i\{2\pi x(s-s')\}\, dx\, dr \qquad (21)$$

where x' = x+r. We shall next let

$$\rho(r) = \frac{\overline{E(x)\,E(x+r)^*}}{\overline{|E(x)|^2}} .$$

Substitution into (21) yields the result

$$I_2 = \int_{-\infty}^{\infty}\int_{-\infty}^{\infty} \overline{|E(x)|^2}\,\rho(r) \exp i\{2\pi r s'\}\, dr \exp -i\{2\pi\sigma x\}\, dx \qquad (22a)$$

or:

$$I_2 = \overline{|F(S')|^2} \int_{-\infty}^{\infty} \overline{|E(x)|^2} \exp -i\{2\pi\sigma x\}\, dx \qquad (22b)$$

Equation (22b) follows directly from (22a) since $\rho(r)$ and the "angular power spectrum" $\overline{|F(S')|^2}$ are Fourier transforms of one another. Likewise, $\rho(\sigma)$ and $\overline{|E(x)|^2}$ are Fourier transform pairs so that (22b) reduces to

$$I_2 = \rho(\sigma)\ \overline{|F(S')|^2} \qquad (18)$$

and

$$\rho(\sigma) = \int_{-\infty}^{\infty} \overline{|E(x)|^2} \exp -i\{2\pi\sigma x\}\, dx \qquad (23)$$

In order to make any further progress in this derivation we are forced to make an assumption with regard to either $\rho(\sigma)$ or the aperture power distribution $\overline{|E(x)|^2}$. Since the choice of a delta function for $\rho(\sigma)$ was earlier shown to satisfy the RPAS requirements, we shall now choose $\rho(\sigma)$ to be a gaussian function, namely:

$$\rho(\sigma) = \frac{1}{(2\pi\beta^2)^{1/2}} \exp -\tfrac{1}{2}\left\{\frac{\sigma}{\beta}\right\}^2 \qquad (24)$$

In (24) we associate with β the angular "width" of correlation within the spectrum of plane waves. (Note: β is the sine of some angle.) Now:

$$\overline{|E(x)|^2} = \int_{-\infty}^{\infty} \rho(\sigma) \exp i\{2\pi\sigma x\}\, d\sigma \qquad (25a)$$

or:

$$\overline{|E(x)|^2} = \exp -\tfrac{1}{2}\left\{\frac{X}{L}\right\}^2 \qquad (25b)$$

The quantity (L) in (25b) is a measure of the "size" of the illuminated portion of the scattering screen and is related to β by

$$L = \frac{1}{2\pi\beta} \qquad (26a)$$

Consequently,

$$\beta = \frac{\lambda}{2\pi L_o} \qquad (26b)$$

where L_o is in meters.

We shall next substitute the assumed functional value for $\rho(\sigma)$ into equation (19b) and obtain:

$$I_1 = \frac{1}{(2\pi\beta^2)^{1/2}} \int_{-\infty}^{\infty} \exp\left\{-\frac{1}{2}\left[\frac{\sigma^2}{\beta^2}\right]\right\} \exp\left\{-i\left[\pi z\sigma^2\right]\right\} \exp\left\{i\left[2\pi\sigma(x-s'z)\right]\right\} d\sigma \qquad (27)$$

Equation (27) can next be reduced to the form:

$$I_1 = \frac{1}{(1+2\pi i\beta^2 z)^{1/2}} \exp\left\{-\frac{1}{2}\left\{\frac{(2\pi\beta[x-s'z])^2}{(1+2\pi i\beta^2 z)}\right\}\right\} \qquad (28)$$

It should be noted that when $\beta = 0$, then $I_1 = 1.0$. Since this condition also existed when $\rho(\sigma) = \delta(s-s')$, (28) is not inconsistent with the traditional treatment of the problem.

One should furthermore note that equation (28) is complex. It is interesting at this point to estimate an upper bound for L_o so that the imaginary part of (28) can be neglected. Thus, for $2\pi\beta^2 z \ll 1$ we require that $\frac{z}{2\pi L^2} \ll 1$. Consequently, $L_o \gg \left(\frac{z_o\lambda}{2\pi}\right)^{1/2}$. As an example, assume that $\lambda = 125$ meters and that $Z_o = 80$ kilometers. Then the inequality requires that $L_o \gg 1.26$ km. This condition can be met in D-region when L_o is of the order of 5 km. to 10 km. While it appears feasible to neglect the imaginary part of (28) there is no apparent merit in doing so at this time. Instead, we shall let

$$c^2 = (1 + 2\pi i\beta^2 z) \qquad (29a)$$

so that equation (28) becomes

$$I_1 = \frac{1}{c} \exp -\frac{1}{2}\left\{\frac{2\pi\beta(X-S'z)}{c}\right\}^2 \qquad (29b)$$

Our next step will be to compute the covariance $\overline{E(x,z)E(x+r,z)^*}$ as given by equation (19a). In so doing, one is once again forced to make an assumption with regard to a mathematical model for the angular power spectrum $\overline{|F(S')|^2}$. We shall choose a gaussian function for the sake of mathematical convenience only. Thus we shall assume that:

$$\overline{|F(S')|^2} = \frac{P_o}{(2\pi S_o^2)^{1/2}} \exp -\frac{1}{2}\left\{\frac{S'-A}{S_o}\right\}^2 \qquad (30)$$

where S_o is a measure of the "width" of the power spectrum, and A is the sine of some angle θ_o at which the magnitude of the power spectrum maximizes. Also, we shall define the correlation "distance" ℓ of the various scatterers within the screen so that

$$\ell = \frac{1}{2\pi S_o} \qquad (31)$$

From equation (29b) and (19b) we now obtain:

$$I = \frac{P_o}{c\{2\pi S_o^2\}^{1/2}} \int_{-\infty}^{\infty} \exp -\frac{1}{2}\left\{\frac{S'-A}{S_o}\right\}^2 \exp -\frac{1}{2}\left\{\frac{2\pi\beta(X-S'z)}{c}\right\}^2 \exp -i\{2\pi S'r\}\, dS' \qquad (32)$$

The evaluation of (32) is straightforward but requires a considerable amount of subcalculation. Suffice it to say that the equation can be reduced to the form:

$$I = K \exp -N \int_{-\infty}^{\infty} \exp -\frac{1}{2}\left[\frac{(S'+M)^2}{B}\right] dS' \qquad (33)$$

where M, N, K, and B are independent of S'. The integral in (33) has a well known solution. In the final evaluation of I, use is made of the definition for $\mathcal{L}$ in (31). The result can then be shown to be:

$$I = \frac{P_0}{c(Q+1)^{1/2}} \exp -\frac{1}{2}\left\{\frac{r^2}{\mathcal{L}^2(1+Q)}\right\} \exp -\left\{2\pi^2\mathcal{L}^2\left(A-\frac{X}{2}\right)^2\left(\frac{Q}{Q+1}\right)\right\} \exp -i\left\{\frac{2\pi r\left(A+\frac{X}{2}Q\right)}{Q+1}\right\} \qquad (34)$$

The quantity Q in (34) is given by

$$Q = \left\{\frac{\beta z}{\mathcal{L} c}\right\}^2 \qquad (35)$$

where c is complex and defined in (29a). Since (34) is a relationship for the covariance of E(x,z) and E(x+r,z), the mean squared value of E(x,z) may be directly evaluated from (34) by letting r = 0. Thus:

$$\overline{|E(x,z)|^2} = \frac{P_0}{c(Q+1)^{1/2}} \exp -\left\{2\pi^2\mathcal{L}^2\left(A-\frac{X}{2}\right)^2\left(\frac{Q}{Q+1}\right)\right\} \qquad (36)$$

We can now define the spatial field correlation as

$$\rho(r,x,z) = \frac{\overline{E(x,z)\,E(x+r,z)^*}}{\overline{|E(x,z)|^2}} = R \exp -i\phi \qquad (37)$$

where:

$$R = \exp - \frac{r^2}{2\ell^2(1+Q)} \qquad (38a)$$

and

$$\phi = \frac{2\pi r}{Q+1}\left\{A + \frac{x}{z}Q\right\} \qquad (38b)$$

It is evident from the definition for Q that when $\beta = 0$, $Q = 0$. Under these circumstances, and because of the particular model chosen for $\overline{|F(S')|^2}$, the spatial correlation is seen to be a gaussian function and dependent on the separation (r) only. Similarly, the phase angle ϕ will under these circumstances reduce to $\frac{2\pi r_0}{\lambda}\sin\theta_0$, where θ_0 is the mean "geometrical" angle of arrival. It was shown earlier that, for variables appropriate to the ionospheric D-region, the factor c as defined by (29a) will probably be real and equal to one. Under these circumstances, Q will be real and equal to $\frac{\beta^2 z^2}{\ell^2}$. If, in addition, one can assume that Q is much smaller than one, then

$$R \doteq \exp - \frac{r^2}{2\ell^2} \qquad (39a)$$

and

$$\phi \doteq 2\pi r\left(A + \frac{x}{z}Q\right) \qquad (39b)$$

From (39) it is now evident that the major effect of a non-zero β will be that of influencing the argument of the complex spatial correlation function.

One should further recognize that when Q is complex and when c is not equal to unity, then both R and ϕ in (38) will be complex. This assumption would yield an R' (say) which would depend on r^2 and on r; and likewise, a ϕ' that would vary non-linearily with r.

In summary, one may conclude the following properties of Q from the magnitude and argument of the complex correlation when $x \neq 0$:

(a) When ϕ does not appreciably depart from the geometrical value (i.e. $\phi = \frac{2\pi r_0}{\lambda} \sin\theta_0$), then Q must be negligible and the RPAS requirements are satisfied.

(b) When ϕ is a linear function of r but exhibits a value that is larger than that predicted from purely geometrical considerations, then Q is finite and real and the angular spectrum is not randomly phased. If, in addition, Q is small, then the value of "ℓ" deduced will be representative of the "size" of the scattering irregularities.

(c) When ϕ is a non-linear function of r, then Q is non-zero and complex and the angular spectrum is not randomly phased. The value of the scale size of irregularities deduced

from R will be in serious error.

Once more, we wish to point out the assumptions made to arrive at the above conclusions:

1. The back-scattered energy is contained within a cone for which the cone angle does not exceed 64^{0}.
2. The angular correlation within the spectrum of plane waves is a gaussian function, rather than a delta function.
3. The angular power spectrum is of a gaussian form centered on $A = \mathrm{SIN}\,\theta_{o}$.

Within the limitations imposed by these assumptions, a, b, and c above are proposed as valid tests for the determination of a randomly phased angular spectrum.

II(3). THE MAGNITUDE OF THE COMPLEX FIELD CORRELATION

In the preceeding sections we have defined the properties of a randomly phased angular spectrum and have given certain criteria for the complex field correlation which must be satisfied if the angular spectrum were randomly phased.

In arriving at the conclusions in the previous section, we were forced to assume a functional form for the angular power spectrum $\overline{|F(S')|^2}$. It was pointed out that the choice of a gaussian function was purely arbitrary and was made for mathematical convenience only. Because of this choice, the magnitude of the complex field correlation, R, is a gaussian function of separation (r). However, in view of the model stipulated for the scattering screen, it does not appear to be physically unrealistic to expect the angular power spectrum to be "gauss-like". Even though the specific shape of the power spectrum is irrelevant to the conclusions of the last section, it is nevertheless of interest to pursue the point a few steps further and to examine the implications of the assumed shape.

It has been pointed out by Ratcliffe (1956)

and others that scattering screens may either influence the amplitude only, or the phase only, or cause a combination of the two. Thus, nature being what it is, one must consider the third possibility; namely, that the scattering screen introduces amplitude "modulation" as well as phase "modulation" upon the incident wave field.

In evolving a model of the scattering screen, it appears appropriate to identify the characteristics to be associated with a "pure" amplitude screen and a "pure" phase screen. Whale and Gardiner (1966) define an amplitude scattering screen as one that gives rise to scattered components only, and a phase scattering screen as one that gives rise to scattered waves as well as to a plane, undiffracted wave. It now stands to reason (depending on the "depth" of phase modulation introduced) that the emerging wave from the composite screen will exhibit a spectrum of scattered plane waves in addition to a steady, undiffracted plane wave. In general, one cannot predict how much of the power in the spectrum of plane waves is due to "phase-screen" scattering and how much is due to "amplitude-screen" scattering.

In an effort to circumvent this dilemma, Whale and Gardiner (1966) postulated two hypothetical

uncorrelated scattering screens. The first of these is an amplitude screen and it is assumed to be the cause of all of the scattered waves. The second screen is assumed to be a "zero order" phase screen which causes no scattered waves and gives rise to a plane undiffracted wave. Since these two screens are totally uncorrelated, Whale and Gardiner predict a spatial field correlation so that

$$\rho(r) = \frac{B+R(r)}{B+1} \qquad (40)$$

In (40) B is defined as the ratio of the power in the undiffracted plane wave to the total power in the spectrum of scattered plane waves. R(r) will then be the spatial correlation function of the hypothetical amplitude screen which causes the observed spectrum of scattered plane waves. By a somewhat different argument, Bramley (1950) arrives at the same functional form for $\rho(r)$ as is given in equation (40).

While equation (40) appears to be generally acceptable as a representation of the spatial <u>field</u> correlation, Whale and Gardiner (1966) and Bramley (1950) proceed beyond this point with great caution. It is not the purpose of this section to compare the various theoretical models in the literature; suffice it to say that all three authors specifically

assume that the spectrum of plane waves is randomly phased and their subsequent conclusions are true only when this condition can be satisfied.

It is worth noting at this time that Bramley (1954) developed another expression for the complex field correlation in which he based his computations on the assumption that scattering was due to a phase scattering screen. His result is somewhat similar to (40):

$$\rho(r) = \exp - \left\{ \phi_o^2 [1 - R(r)] \right\} \qquad (41)$$

In (41) ϕ_o^2 represents the mean squared phase fluctuation caused by the screen, and R(r) is the spatial correlation of scatterers in the screen. By including the effects of absorption within the scattering volume, Bramley (1954) shows that the value of ϕ_o^2 is modified by a factor $(1 + \frac{\nu^2}{\omega^2})$ where ν is the mean collisional frequency of the medium.

It will be observed that both (40) and (41) have a value of 1.0 when R(r) = 1, and both approach some constant value when R(r) = 0. If one assumed, as was done in the previous section, that $R(r) = \exp - \frac{r^2}{2\ell^2}$ then equation (40) will be recognized as a "gaussian on a pedestal", while equation (41) reduces to a very complex function of r and ϕ_o^2. In addition, one is forced to observe that the various formulas for D-region

backscatter [Flood (1968), Belrose and Burke (1964)] indicate that both the phase and the amplitude of incident radiation is altered upon reflection. Consequently, it is felt that the relation for $\rho(r)$ in (41) is inappropriate for D-region scattering.

Consider next the functional relationship

$$R(r) = \frac{B + \exp-\left[\frac{r^2}{2\sigma^2(1+Q)}\right]}{(B+1)} \qquad (42)$$

The stipulation of a non-zero value for the undiffracted wave now introduces certain complications as regards the assumed form for the angular power spectrum $\overline{|F(S)|^2}$ in equation (30). Thus, the non-zero value for (B) in (42) implies that there exists a line in the angular power spectrum of relative strength $\frac{B}{B+1}$, and that this line does not coincide with S = A unless the angular spectrum is randomly phased. Specifically, if one were to assume that

$$\rho(r, x, z) = R(r) \exp -i\phi \qquad (37b)$$

and then substitute the values for R and ϕ as given in (42) and (38b) respectively, then the angular power spectrum $\overline{|F(S)|^2}_{z=0}$ will contain a delta function so that

$$\overline{|F(S)|^2}_{z=0} = \frac{B}{B+1}\delta\left[S - A\left(1 + \frac{Q}{Q+1}\right)\right] + \frac{1}{(B+1)(2\pi S_0^2)^{1/2}} \exp -\frac{1}{2}\left\{\frac{(S-A)^2}{S_0^2}\right\} \qquad (43)$$

Equation (43) implies that $\overline{|F(S)|^2}$ is not symmetrical about the value S=A unless Q=0. The seriousness of this implication of course, depends on the power in the undiffracted plane wave, the value of Q, and on the credibility of the assumed form for $\rho(r,x,z)$.

One is tempted at this point to investigate the consequences on the complex correlation $\rho(r,x,z)$ if a symmetrical angular power spectrum at z=0 were assumed. Thus, let

$$\overline{|F(S)|^2}_{z=0} = \frac{B}{B+1}\delta(S-A) + \frac{1}{(B+1)(2\pi S_0^2)^{1/2}} \exp -\frac{1}{2}\left\{\frac{(S-A)^2}{S_0^2}\right\} \qquad (44)$$

Under these circumstances it can be shown that

$$\rho(r,x,z) = \left\{\frac{B\exp i\Delta\phi + R}{B+1}\right\} \exp -i\phi \qquad (45)$$

where R and ϕ are defined in equation (38) and where

$$\Delta\phi \doteq 2\pi r A\left[\frac{Q}{Q+1}\right] \qquad (46)$$

Since the quantity $(B\exp i\Delta\phi + R)$ is complex, it will be convenient to let

$$R' = \left| \frac{B\exp i\Delta\phi + R}{B+1} \right| \qquad (47a)$$

and

$$\gamma = Arg\left\{B\exp i\Delta\phi + R\right\} \qquad (47b)$$

One then obtains:

$$R' = \left\{\frac{B+R}{B+1}\right\}\left\{1 - \frac{4RB}{(B+R)^2}\sin^2\frac{\Delta\phi}{2}\right\}^{1/2} \qquad (48a)$$

and

$$\gamma = \tan^{-1}\left\{\frac{B\sin\Delta\phi}{B\cos\Delta\phi + R}\right\} \qquad (48b)$$

The phase angle γ as given in (48b) is seen to be dependent on the separation (r) as well as on the magnitudes of B and R. This angle will therefore exhibit a non-linear variation with r and will cause the argument of $\rho(r,x,z)$ also to change in a non-linear fashion. One must conclude therefore, that when the angular power spectrum at z=0 is assumed to contain a delta function and is symmetrical about this line, then the phase of the complex spatial field correlation will be a non-linear function of (r) unless the angular spectrum is randomly phased.

It will be shown later that experimentally determined values for $\rho(r,x,z)$ exhibit magnitudes that can be well fitted by the functional relationship

$$|\rho(r,x,z)| = \frac{B + \exp-\left\{\frac{r^2}{L^2}\right\}}{B+1}$$

Furthermore, it will be shown that the phase of $\rho(r,x,z)$ is linearily dependent on (r), and that it has a slope which is generally greater than predicted from geometrical considerations. These observations are indicative of an asymmetrical angular power spectrum at z=0, which in addition, is not randomly phased.

III. EXPERIMENTAL ASPECTS

The results obtained from the previous sections suggest that an experiment be performed from which the complex field correlation $\rho(r,x,z)$ might be derived. Such an experiment was designed and operated and the desired complex field correlation was computed from the data. The purpose of the following sections is to discuss the philosophy of this experiment and to describe the experimental technique, instrumentation, and data analysis employed.

III(1). EXPERIMENTAL PHILOSOPHY

The conclusions from section II(2) are best summarized in equation (38) which relates the magnitude of the complex field correlation to a gaussian function for which the variance is given by $\ell^2(1+Q)$. Likewise, in (38b) the argument of the complex field correlation was shown to be dependent on x, so that:

$$\phi = 2\pi r \left\{ \frac{\sin\theta_o + \frac{x}{z} Q}{1+Q} \right\} \qquad (38b)$$

From (38b) and from the definitions in section II(2) of x and z, the ratio $\frac{x}{z}$ will be recognized as:

$$\frac{x}{z} = 2 \tan\theta_o \qquad (49)$$

where θ_o was previously defined as the mean "geometrical" angle of arrival.

It is now evident from equation (38a) that the correlation "length" ℓ can be computed only when the value of Q is known. Also, from (38b) Q can only be assessed when θ_o is not equal to zero. In other words, to obtain an estimate of Q, an experiment must be conducted some distance x from the reference point, which was given in II(2) as the location of the transmitter.

In section II(3) it was pointed out that no a priori assumptions can be made regarding the functional form of the complex field correlation. While it is not unreasonable to suspect a "gauss-like" shape for the variation of the spatial correlation with distance, one is forced to consider the possibility of a plane undiffracted wave in the angular spectrum of waves reaching the antennas. Since the magnitude of the spatial field correlation is, in general, a function of the parameters B and $L^2 = 2\ell^2(Q+1)$, it was deemed necessary to sample the field pattern for at least three different values of separation r. Furthermore, it was shown in section II(2) and II(3) that there exists a possibility that the variation of phase difference might not be linearily related to the antenna separation r. Again, this possibility requires that the phase difference be assessed for several different baseline lengths. Consequently there emerged three basic requirements that had to be satisfied by the contemplated experiment. These are:

(1). The experiment must be conducted at a considerable distance from the transmitter.

(2). The experiment must be capable of yielding

data for several different antenna separations.

(3). The experimental instrumentation must be capable of yielding data from which the complex spatial field correlation can be computed.

While requirements (1) and (2) could be satisfied rather easily, requirement (3) presented a challenge in concept and in instrumentation. It is precisely for this reason that so much theoretical effort has been devoted in the past (Bramley 1950, Booker, Ratcliffe and Shin 1950) toward relating the magnitude of the complex field correlation to the spatial correlation of the magnitude of the fields. As was pointed out earlier, this process requires that assumptions be made which have not yet been adequately defended.

Consequently, a large portion of the total effort in this program was devoted toward the development of an experimental technique for the determination of the complex field correlation. The method that was finally developed resembles in concept the "mono-pulse" technique used in high resolution radars, and is discussed in the following section.

III(2). EXPERIMENTAL TECHNIQUE

A chief requirement of the experiment was that it yield data from which the cross-correlation and phase difference between two time varying vector fields could be computed. While some techniques exist that would accomplish this goal, the final choice of method resulted from a consideration of the statistical properties of the quantities to be measured. To be specific, the time varying quantities under consideration were the voltages from two antennas, separated by a distance (r) from one another, and positioned on a line that joined the receiving station with the transmitting station.

Illumination of the ionospheric D-region with pulsed electromagnetic energy will cause a scattered field to exist at each of the receiving antennas. The scattering process is believed to be caused by stochastic fluctuations of the complex refractive index about its mean value at some height (h) within the medium under consideration. Consequently, the instantaneous field at each of the receiving antennas may be synthesized from a spectrum of plane waves that arrive within a (narrow) cone of

angles. The antenna terminal voltage is directly related to the instantaneous value of the scattered field, and in general, fluctuates in magnitude over a range of approximately 13 db. In addition to this fading range, ionospheric echoes from the D-region exhibit fading rates of the order of seconds.

It is therefore clear that if the "rearranging" process of the individual scattering elements is of a statistical nature, then the resulting field distribution can only be treated in a statistical sense.

In view of the fading time and fading range that characterize ionospheric echoes, a direct phase comparison technique between antenna voltages was rejected. The primary reason for this verdict was the anticipated difficulty in constructing two receivers with identical linear phase characteristics over the required bandwidth and dynamic amplitude range. Other reasons against a "phasemeter" technique were found in the interpretations of eventual data, which because of their stochastic character, would make data analysis extremely difficult.

In an effort to circumvent some of these problems, it was decided to measure the phase

difference and cross-correlation by means of a technique which involves predetection linear vector addition. For such a system one requires only one receiver, or more accurately, a sensitive linear radio frequency voltmeter.

Upon reception, the phase of one of the (vector) antenna voltages is altered by some known angle (α) and the resulting voltage is added, vectorially, to the other antenna voltage. A quantity proportional to the resulting vector magnitude will then appear at the output of the receiver.

To gain more insight into this technique, assume that an antenna voltage v_1 is due to a field $E(x)$ at antenna (1). Antenna voltage v_2 will then be caused by a similar field $E(x+r)$ at antenna (2).

Assume next that the phase of v_2 is altered by an amount (α) so that $v_2' = v_2 \exp i\alpha$. The sum of v_1 and v_2' will then be given by

$$v(\alpha) = v_1 + v_2' = v_1 + v_2 \exp i\alpha = C\{E(x) + E(x+r)\exp i\alpha\} \tag{49}$$

where C is a proportionality constant which relates the antenna voltages to their respective fields.

The output from the receiver is assumed to be linearily proportional to the magnitude of $v(\alpha)$ so that

$$v_{out} \propto |v(\alpha)| \tag{50a}$$

and consequently

$$v_{out}^2 = K\,|v(\alpha)|^2 \tag{50b}$$

It now remains to derive a relationship between the receiver output voltage (a video quantity) and the antenna voltages (radio frequency quantities). The required relationship is given by

$$|v(\alpha)|^2 = |v_1|^2 + |v_2|^2 + v_1 v_2^* \exp(-i\alpha) + v_2 v_1^* \exp(i\alpha) \tag{51}$$

The asterisk signifies the complex conjugate of a quantity.

It now follows that the mean squared value of v_{out} is proportional to

$$\overline{|v(\alpha)|^2} = \overline{|v_1|^2} + \overline{|v_2|^2} + \overline{v_1 v_2^*} \exp(-i\alpha) + \overline{v_2 v_1^*} \exp(i\alpha) \tag{52}$$

Note that in (52) the quantities $\overline{|v_1|^2}$ and $\overline{|v_2|^2}$ are proportional to the average power received at (x) and (x+r) while $\overline{v_1 v_2^*}$ is the unnormalized covariance of the fields at (x) and (x+r) and is proportional to $\overline{E(x)E(x+r)^*}$. Now the spatial correlation between E(x) and E(x+r) is, in general, given by

$$\rho(x,r) = \frac{\overline{E(x)E(x+r)^*}}{\left\{\overline{|E(x)|^2}\cdot\overline{|E(x+r)|^2}\right\}^{1/2}} \qquad (53)$$

Equation (53), in terms of the antenna voltages v_1 and v_2, may be written as

$$\rho(x,r) = \frac{\overline{v_1 v_2^*}}{\left\{\overline{|v_1|^2}\cdot\overline{|v_2|^2}\right\}^{1/2}} = \rho(r)\exp i[\beta(r)] \qquad (54)$$

where $\rho(r)$ and $\beta(r)$ are the magnitude and argument of $\rho(x,r)$.

Rewriting of equation (52) in terms of the spatial correlation yields

$$\overline{|v(\alpha)|^2} = \overline{|v_1|^2} + \overline{|v_2|^2} + 2\left\{\overline{|v_1|^2}\cdot\overline{|v_2|^2}\right\}^{1/2}\rho(r)\cos[\alpha-\beta(r)] \qquad (55)$$

Equation (55) relates the mean squared value of the receiver output voltage, as a function of α, to the magnitude and the phase of the spatial field correlation at (x) and (x+r).

During the execution of the experiment, the value of output voltage was sequentially recorded for a fixed echo height (h) and for four values of α from 0° to 270°. Letting α_1 and α_2 be 0° and 180° respectively, one obtains

$$\overline{|v(\alpha_1)|^2} = \overline{|v_1|^2} + \overline{|v_2|^2} + 2\left\{\overline{|v_1|^2}\ \overline{|v_2|^2}\right\}^{1/2} \rho(r) \cos[\beta(r)] \tag{56a}$$

$$\overline{|v(\alpha_2)|^2} = \overline{|v_1|^2} + \overline{|v_2|^2} - 2\left\{\overline{|v_1|^2}\ \overline{|v_2|^2}\right\}^{1/2} \rho(r) \cos[\beta(r)] \tag{56b}$$

It then follows that

$$M = \frac{\overline{|v(\alpha_1)|^2} - \overline{|v(\alpha_2)|^2}}{\overline{|v(\alpha_1)|^2} + \overline{|v(\alpha_2)|^2}} = \frac{2\left\{\overline{|v_1|^2}\ \overline{|v_2|^2}\right\}^{1/2}}{\overline{|v_1|^2} + \overline{|v_2|^2}} \rho(r) \cos[\beta(r)] \tag{57}$$

Likewise, for $\alpha_3 = 90^\circ$ and $\alpha_4 = 270^\circ$

$$N = \frac{\overline{|v(\alpha_3)|^2} - \overline{|v(\alpha_4)|^2}}{\overline{|v(\alpha_3)|^2} + \overline{|v(\alpha_4)|^2}} = \frac{2\left\{\overline{|v_1|^2}\ \overline{|v_2|^2}\right\}^{1/2}}{\overline{|v_1|^2} + \overline{|v_2|^2}} \rho(r) \sin[\beta(r)] \tag{58}$$

In the above equations, the values of M and N may be directly evaluated from the appropriate receiver output voltage since the same receiver is used to produce all four quantities, and since receiver linearity was specifically stated as a requirement.

At this point it is worth mentioning that the values of $\overline{|v_1|^2}$ and $\overline{|v_2|^2}$ are, for all practical purposes, identical. Under these circumstances, the ratio

$$\frac{2\left\{\overline{|v_1|^2}\,\overline{|v_2|^2}\right\}^{1/2}}{\overline{|v_1|^2}+\overline{|v_2|^2}} \equiv 1.0$$

However, since two separate antennas were employed, along with their associated instrumentation (such as balun transformers and coaxial cables) the possibility existed that $\overline{|v_1|^2}$ might not be identical to $\overline{|v_2|^2}$. It is, therefore, fortunate that the ratio

$$\frac{2\left\{\overline{|v_1|^2}\,\overline{|v_2|^2}\right\}^{1/2}}{\overline{|v_1|^2}+\overline{|v_2|^2}}$$

is very nearly equal to unity for a fairly large departure of $\dfrac{\overline{|v_1|^2}}{\overline{|v_2|^2}}$ from unity. To illustrate this point, assume that $\overline{|v_1|^2}$ differed from $\overline{|v_2|^2}$ by as much as 3 db. Evaluation of the ratio

$$\frac{2\left\{\overline{|v_1|^2}\,\overline{|v_2|^2}\right\}^{1/2}}{\overline{|v_2|^2}+\overline{|v_2|^2}}$$

will then yield 0.945 instead of 1.0. Thus, under these extreme circumstances, the error would only be 6.5% if one arbitrarily set N equal to $\rho(r)\sin\beta(r)$ and M equal to $\rho(r)\cos\beta(r)$. It should be noted that in the actual experiment three separate antennas were used to yield three values of separation (r). It was possible, therefore, to calculate the value of

$\frac{2\left\{\overline{|V_1|^2}\,\overline{|V_2|^2}\right\}^{1/2}}{\overline{|V_1|^2}+\overline{|V_2|^2}}$ for each baseline length and to apply the appropriate correction to the value of M and N. This refinement in data evaluation proved to be superfluous in view of the fact that the correction factor only very rarely exceeded one or two per cent.

Returning once more to equations (57) and (58) it is clear that the ratio N/M is equal to the tangent of the argument (r), irrespective of the values (measured or assumed) of $\frac{2\left\{\overline{|V_1|^2}\,\overline{|V_2|^2}\right\}^{1/2}}{\overline{|V_1|^2}+\overline{|V_2|^2}}$. The ambiguity in the value of $\beta(r)$ is therefore $2n\pi$, a fact that becomes bothersome only for phase differences that exceed 360°.

On the assumption that $\frac{2\left\{\overline{|V_1|^2}\,\overline{|V_2|^2}\right\}^{1/2}}{\overline{|V_1|^2}+\overline{|V_2|^2}} = 1$, it is now possible to solve for the magnitude of the spatial correlation by substitution of the argument $\beta(r)$ into either (57) or (58). A third possibility is to compute the square root of the sum of the squares of M and N. This particular method was used to evaluate $\rho(r)$.

The experimental approach outlined in this section is in many respects similar to that of a "phase swept", or "phase switched" interferometer system. It differs, however, from these systems in

that four preselected phases are used in conjunction with an averaging process. Since the individual voltages $v(\alpha)$ are used only in the form of their mean squared value, there is no need to record simultaneously the four configurations that give rise to $v(\alpha)$. In fact, if the fading time is indicative of the decorrelation time in the medium under investigation, data recorded at time intervals that are shorter than the decorrelation time are redundant bits of information because they are not statistically independent of one another. In this experiment, as will be shown later, individual data points were obtained every six seconds, which at D-region altitudes, represents a time interval equal to about 3 "decorrelation times".

III(3). INSTRUMENTATION

There appears to be little doubt that the quality and interpretation of experimental results is contingent on the characteristics of the instrumentation used in an investigative program. Consequently, a large portion of the total technical effort was devoted toward experimental technique and the design, construction, and testing of the required apparatus.

While a detailed description of individual pieces of equipment is frequently necessary in order to assess the validity of certain conclusions from experimental results, it is felt that a brief description of the overall system and its capabilities is generally quite satisfactory. For this reason only the highlights of the experimental apparatus will be discussed in this section. Specific details, including circuit diagrams of the various components, will be found in Appendix A.

The transmitter for this experiment was located at Birdlings Flat (lat: $43^{o}49.6'$ S; long. $172^{o}41.2'$ E). It was operated at a frequency of 2.4 mc/s and had a peak pulse power capability of 100 kilowatts for a pulse repetition frequency of 50 per second, and

FIGURE - 1

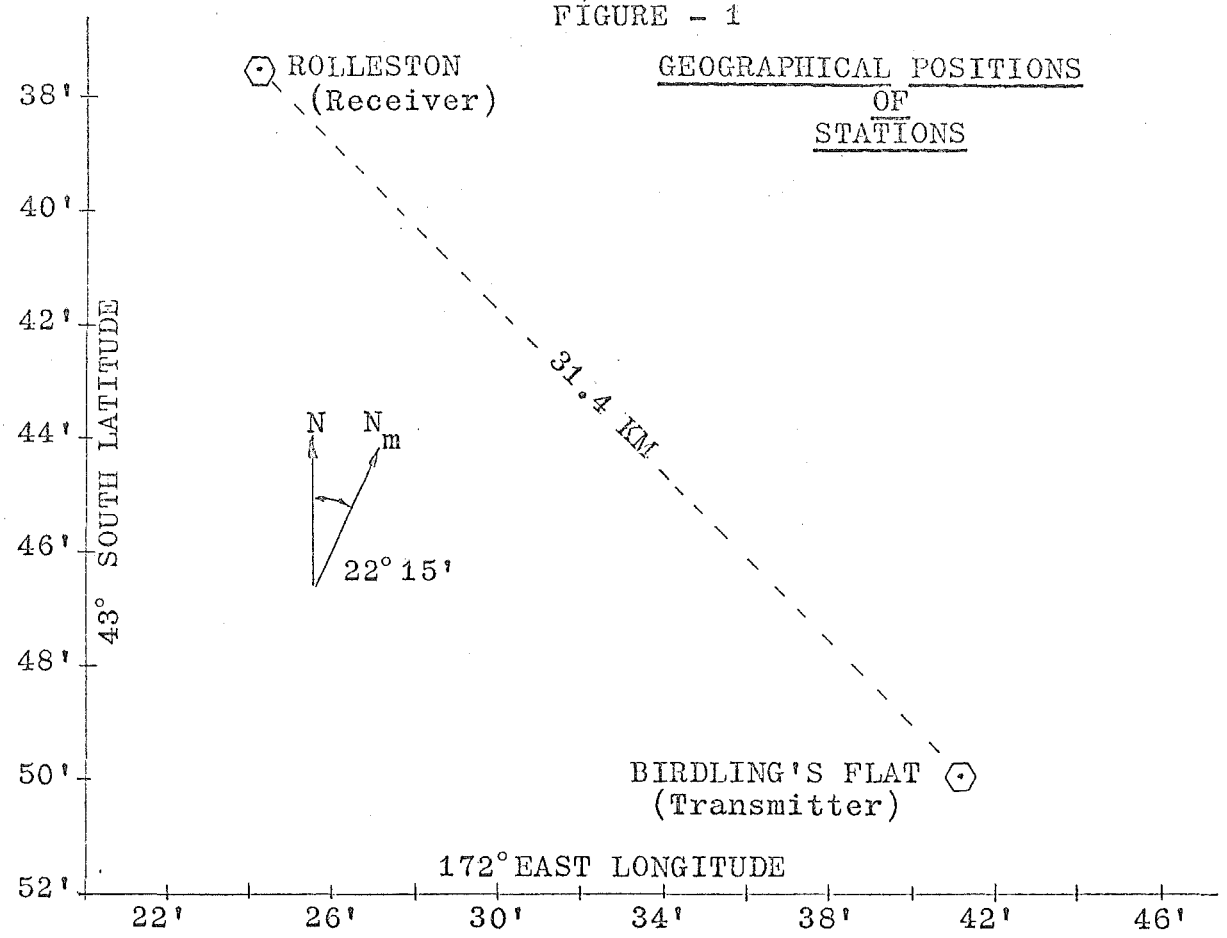
GEOGRAPHICAL POSITIONS OF STATIONS
ROLLESTON (Receiver)
31.4 KM
N
Nm
22° 15'
BIRDLING'S FLAT (Transmitter)
38'
40'
42'
44'
46'
48'
50'
52'
43° SOUTH LATITUDE
172° EAST LONGITUDE
22'
26'
30'
34'
38'
42'
46'

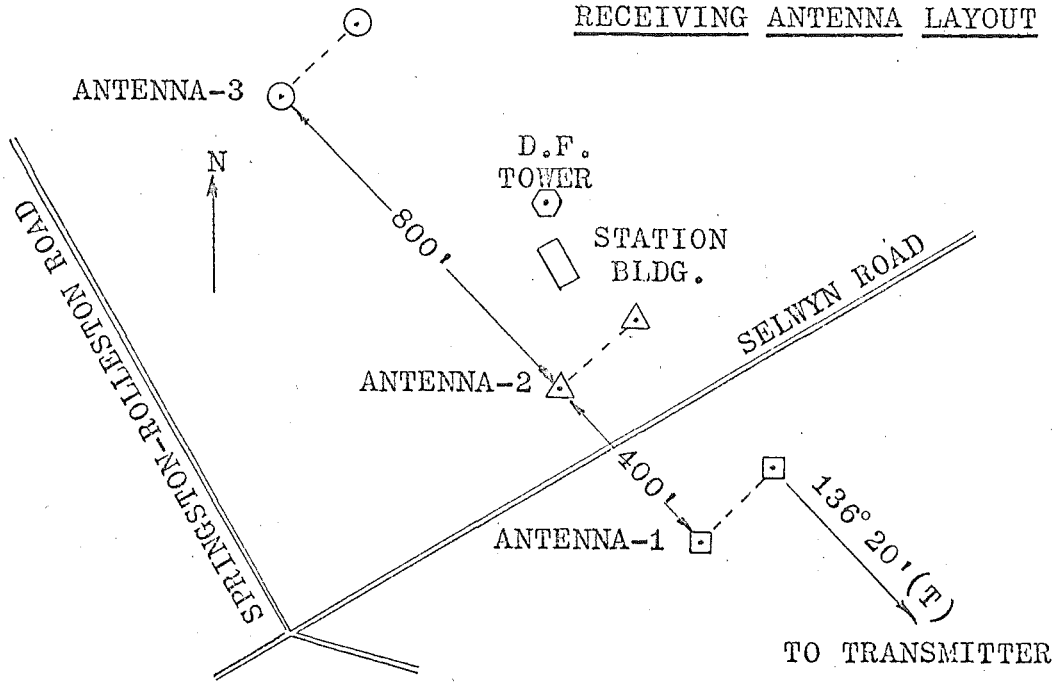
RECEIVING ANTENNA LAYOUT
ANTENNA-3
N
D.F. TOWER
800'
STATION BLDG.
SELWYN ROAD
SPRINGSTON-ROLLESTON ROAD
ANTENNA-2
400'
ANTENNA-1
136° 20' (T)
TO TRANSMITTER

a pulse width of 20 microseconds. The transmitting antenna consisted of a linearily polarized array of 8 dipoles that were arranged in a colinear and broadside configuration.

The receiving site was located at Rolleston, a distance of 31.4 km on a true bearing of 315^{o} from Birdlings Flat (see figure 1). Three half-wave dipole antennas were located on the line joining the transmitting site with the receiving site. These receiving antennas were spaced so that antenna separations of one, two, and three wave lengths were available. The antennas were connected to the remaining instrumentation by three identical lengths of RG 58/U coaxial cable, each approximately 1000 feet long. (The cable was generously made available to this experiment by Cornell Aeronautical Laboratory in Buffalo, New York.) The details of balun transformers used to convert the balanced antenna impedance to an unbalanced impedance of 50 ohms, will be found in Appendix A.

Because of the 30 km separation between the transmitter and receiver sites, a problem arose in connection with pulse synchronization between the two stations. This problem was solved through the use of a 69 mc/s telemetry link between Birdlings Flat and Rolleston. The transmitter

in this link consisted of a World War II radar transmitter for which the peak pulse power was about 100 kilowatts, and which was located at the Rolleston Field Station. The output from this transmitter was directed towards Birdlings Flat through the use of a 9 element yagi antenna. A folded dipole antenna was used for reception at Birdlings Flat.

Upon reception of the 69 mc/s signal, the video output from the receiver was appropriately shaped by a monostable multivibrator and was then used to trigger the modulator section of the 2.4 mc/s transmitter. Thus, except for a fixed time delay, corresponding to the 31.4 km station separation, the 69 mc/s pulse at Rolleston was coherent with the transmitted 2.4 mc/s pulse at Birdlings Flat. An additional benefit was realized from this arrangement in that the 69 mc/s signal received at Birdlings Flat was used to energize the 2.4 mc/s transmitter power supplies. This latter feature resulted in a savings of approximately 120 miles of travel every time the experiment was conducted.

The specific instrumentation requirements at the receiving site emerged earlier from the discussion of the experimental technique. In review, the primary requirement was for a sensitive

receiver, for which the output voltage is linearily proportional to the magnitude of the input signal. Secondly, some means had to be provided for summing the appropriate receiving antenna voltages, and to introduce the predetermined phase differences (α). Thirdly, a time reference had to be established for transmission and reception to facilitate the sampling of ionospheric echoes from the desired scattering height. Finally, some means had to be provided for recording the four different measurements required for each of the three interferometer configurations. A brief description of each of these system components follows.

1. Receiver

The receiver for this experiment was fully transistorized and operated on the superheterodyne principle. Its predetection band width was approximately 100 kc/s, for which the threshold sensitivity was -120 dbm. Two unique features of the receiver were its linearity and the inclusion of a pulse-commandable "track and hold" circuit.

A detector linearity of approximately 56 db was accomplished by means of a "perfect diode" circuit which consisted of a silicon diode in the feedback element of an operational amplifier. The

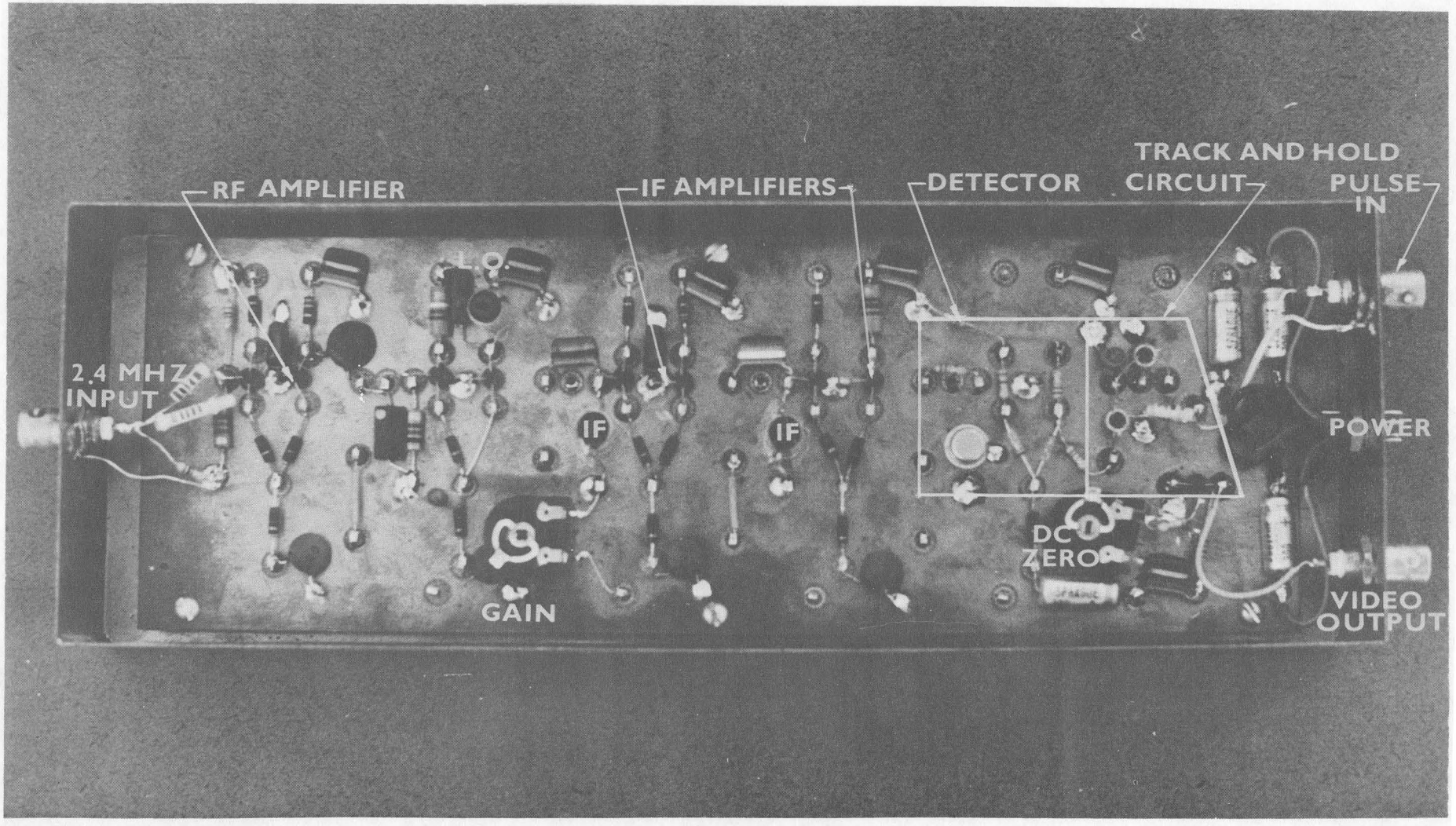

2.4 MHz RECEIVER

FIGURE - 2

operational gain of the device was unity.

The track and hold feature of the receiver was made possible through the use of a silicon FET which served to change the post detection time constant from 15 microseconds in the "track" mode to approximately 5 minutes in the "hold" mode. A modified "Darlington" circuit configuration was used to isolate the recording instrumentation from the video filter capacitor. The Darlington circuit, which utilized a silicon FET and a silicon transistor, exhibited an input impedance in excess of 10^{12} ohms. This resulted in a drift free "hold time" of well over 5 seconds. The power gain of the circuit was such that a maximum output voltage of 5 volts could be developed across a 2000 ohm load resistance.

Figure 3 shows the sensitivity, linearity, and impulse response for the overall receiver.

It should be mentioned at this time that considerable attention was given to the receiver input impedance, which as will be seen shortly, had to exhibit a purely resistive value of 100 Ω at 2.4 mc/s. This requirement was satisfied over a bandwidth of about 200 kc/s.

FIGURE - 3

2.4 Mc/s RECEIVER RESPONSE

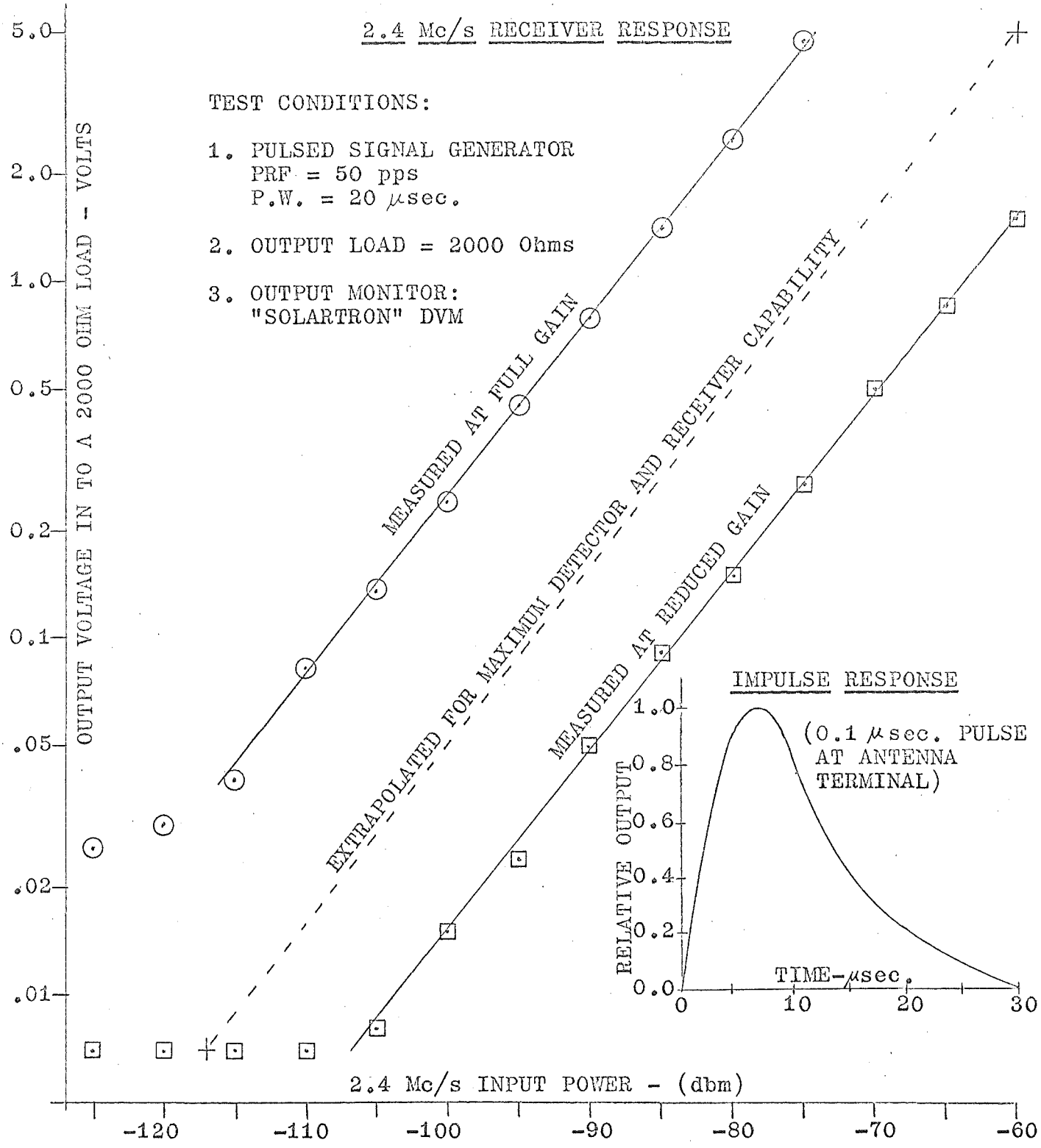

2. Lumped-Constants Hybrid Circuits

The problem of combining the two antenna voltages and of introducing the required phase shift between them was solved by means of two different configurations of hybrid combiner circuits.

The hybrid combiner circuit is probably best known in wave guide technology as a "Magic T" or as a "Series-Shunt T". Irrespective of its physical manifestation, it is a four terminal device that contains pure reactances in a variety of possible series and shunt configurations.

To demonstrate the operation and properties of such a device, assume that three quarter-wave sections of transmission line, having characteristic impedance $Z=\sqrt{2}\,Z_0$, are joined end to end. A fourth section of transmission line, three quarter wavelengths long, is then added and connected in such a way that a ring of circumference equal to 1.5 wave lengths results. This connection is demonstrated in the sketch. Assume next that terminals 2 and 4

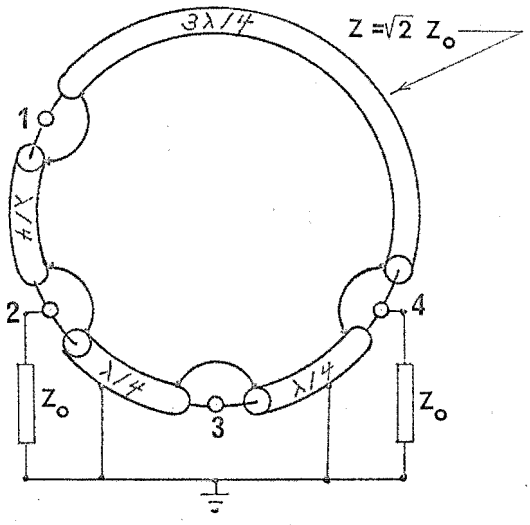

are connected to resistive loads of impedance Z_o, and that a generator with internal impedance Z_o is connected to terminal 3. It now follows that the generator will deliver equal power to the two load impedances, and that the voltages at 2 and 4 are in phase and lag behind the voltage at 3 by 90^o. It will furthermore be recognized that the voltage at terminal 1 is identically zero for the conditions stated here. It has been shown, therefore, that terminals 1 and 3 are independent of one another.

Let the generator next be connected to terminal 1. Then, the power will again be shared equally by the two loads at 2 and 4, but the voltages at these two terminals will now differ by 180^o. Also, the voltage at 3, due to a voltage at 1, will be zero. If finally, a source of voltage v_1 is connected to terminal 1, and a source of voltage v_3 is connected to terminal 3, then the voltage at 2 will be $v_1 + v_3$ and the voltage at 4 will be $v_3 - v_1$. In other words, $v_4 = v_3 + v_1 \exp(i\pi)$, and likewise, $v_2 = v_3 + v_1 \exp(i2\pi)$. Without going into details, it should be noted that this hybrid (ring) has a considerable bandwidth. That is to say, while the actual phase at terminals 2 and 4 varies linearily with frequency, the <u>phase difference</u> between voltages at 2 and 4

remains constant over nearly one octave (for the transmission line hybrid).

A device that has these characteristics satisfies one of the requirements imposed by the experimental technique. If the antenna voltages are introduced at terminals 1 and 3, then $v(\alpha_1)$ will appear at terminal 2 and $v(\alpha_2)$ will appear at terminal 4, where α_1 and α_2 are 0° and 180° respectively. We shall refer to this hybrid ring as "cosine hybrid".

It should be evident that this particular configuration cannot introduce phase differences of 90° and 270°, as is required for α_3 and α_4. Fortunately, there exists another version that will do exactly this. The sketch shows its configuration, in terms of quarter-wave transmission line sections, and on the assumption that terminals 1 and 2 are terminated in resistive loads of Z_0.

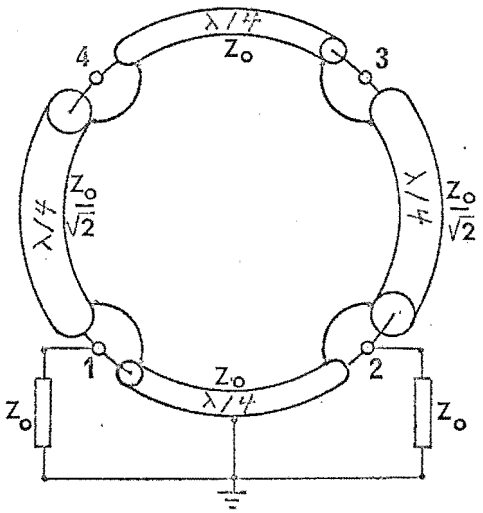

From a consideration of elementary circuit theory, it can be shown that

$$v_2 = iv_3 - v_4 = i\left[v_3 + v_4 \exp\left(i\pi/2\right)\right]$$

and that

$$V_1 = iV_4 - V_3 = -\left[V_3 + V_4 \exp\left(i\frac{3\pi}{2}\right)\right]$$

Also, as in the case of the $\frac{3\lambda}{2}$ transmission line ring, the input terminals (in this case 3 and 4) are independent of one another, as long as terminals 1 and 2 are terminated in Z_0. We shall refer to this configuration as the "sine hybrid" because of its ability to produce the phase angles α_3 and α_4 of 90° and 270° respectively.

While transmission lines were specified for purposes of discussion, they would obviously be impractical at a frequency of 2.4 mc/s, where one wave length (in vacuum) equals 125 meters.

A convenient method for constructing the two different hybrid configurations presents itself when constant-K or m-derived delay lines are substituted for the quarter-wave sections of transmission line. Suffice it to say that constant-K sections were used to construct three cosine-hybrids and three sine-hybrids (see figures 4 and 5). The characteristic impedance for all of these hybrid circuits was chosen to be 100 ohms, a choice which permitted the input terminals of the sine- and cosine-hybrid to be connected in parallel so that the combination presented itself as a 50 ohm resistive load to the 50 ohm transmission lines from

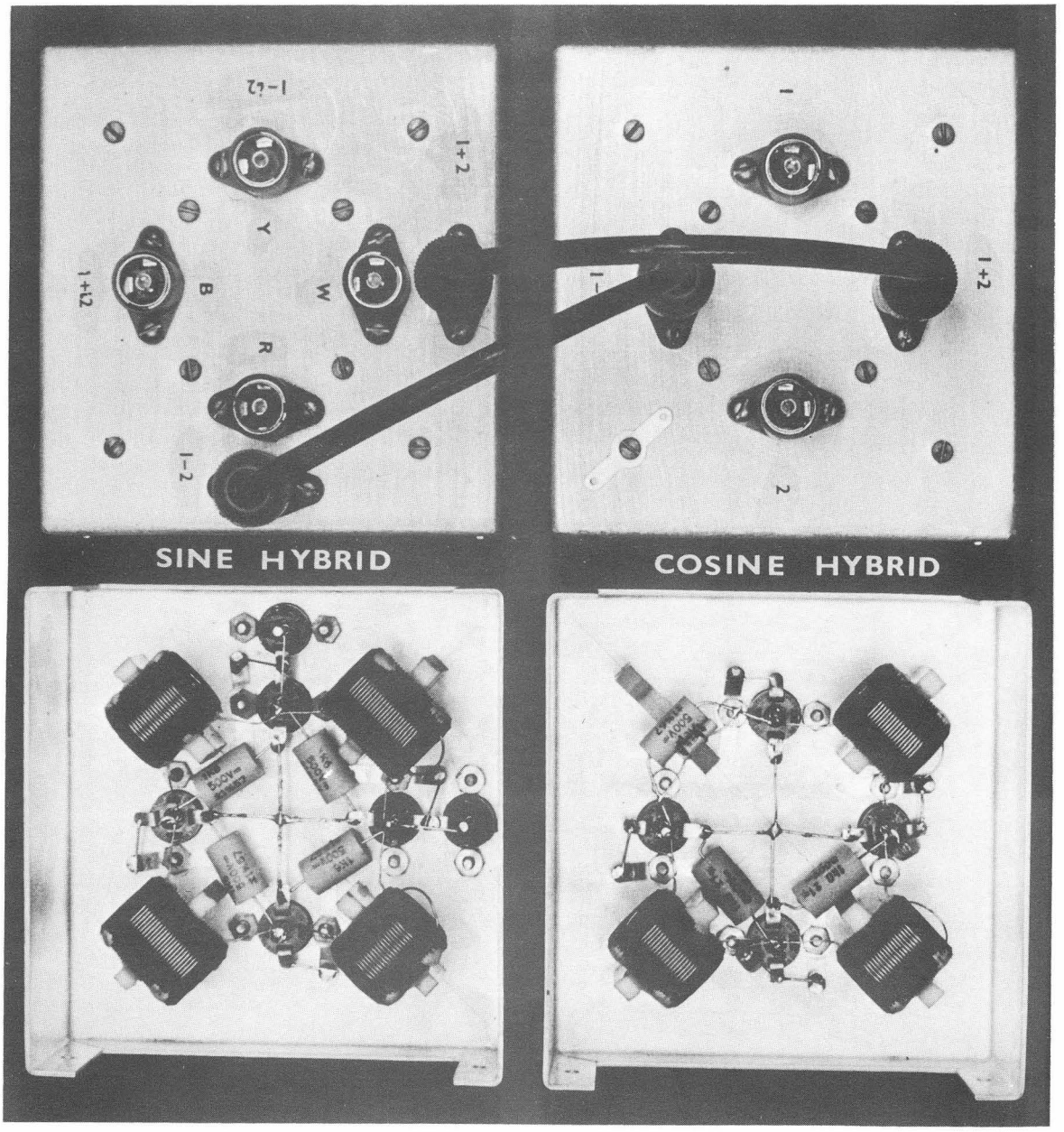

HYBRID COMBINERS

FIGURE - 4

the antennas.

The performance of these hybrid combiners has been most gratifying. Their bandwidth is approximately 1 mc/s, centered on 2.4 mc/s, and the phase error was measured to be less than 1.5° r.m.s. The amplitude balance between the two output ports was within 98% when identical signals were present at the input terminals.

In view of the relative simplicity of these circuits, it was decided to use a "cosine type hybrid" as an antenna transformer to match the (balanced) feedpoint impedance of the halfwave dipoles to the 50 ohm coaxial cable. In this application the hybrid circuit was again most satisfactory.

Figure 5 represents the functional block diagram for the hybrid combiners and the associated switching arrangement. The logic circuitry used to (sequentially) energize the relays has been omitted here since it is an integral part of the digital data recording system to be discussed later.

It will be noted that the output ports of both hybrids are terminated by 100 ohm resistive loads. It is primarily because of careful attention given to the termination requirements of these hybrid circuits that the phase and bandwidth

HYBRID COMBINERS AND TIAL SWITCH

FIGURE

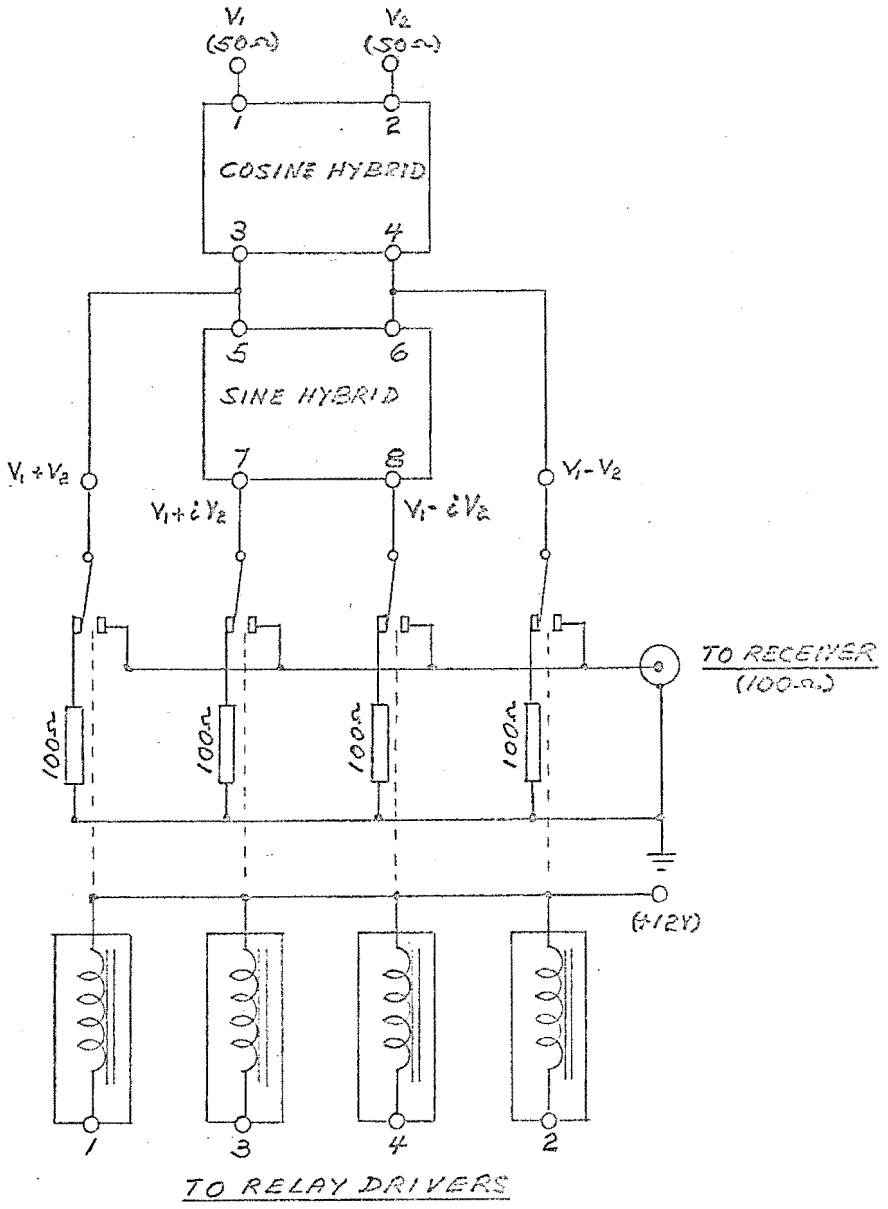

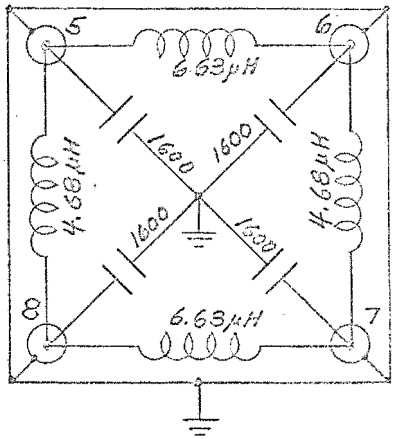

$Z_o = 100\Omega$

SINE HYBRID

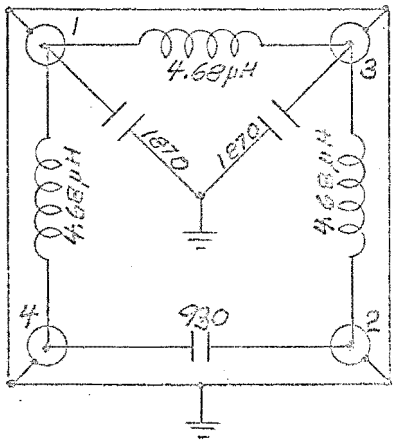

$Z_o = 50\Omega$

COSINE HYBRID

characteristics were achievable. For this reason, as was mentioned earlier, the input impedance of the receiver, which acts as a load impedance to the hybrid circuits, had to be a close match to a 100 ohm resistance.

In the physical manifestation of the sequential sampling switch (figure 6), three banks of four relays each were connected in parallel to facilitate the simultaneous sampling of corresponding functions for three different antenna separations. This mode of operation required three receivers and three chart recorders. Because of the difficulty experienced in data reduction from paper recording charts, the recording system was subsequently altered to permit analog-to-digital data "readout". In this mode corresponding channels for the three separate base-line lengths were sequentially sampled, thus giving twelve different measured quantities per data cycle. Even though the individual relays in the sampling switch were located as closely as physically possible to one another, measurements have shown that a minimum of 43 db isolation was achieved between all of the twelve channels. This figure was judged adequate for the purposes of this experiment.

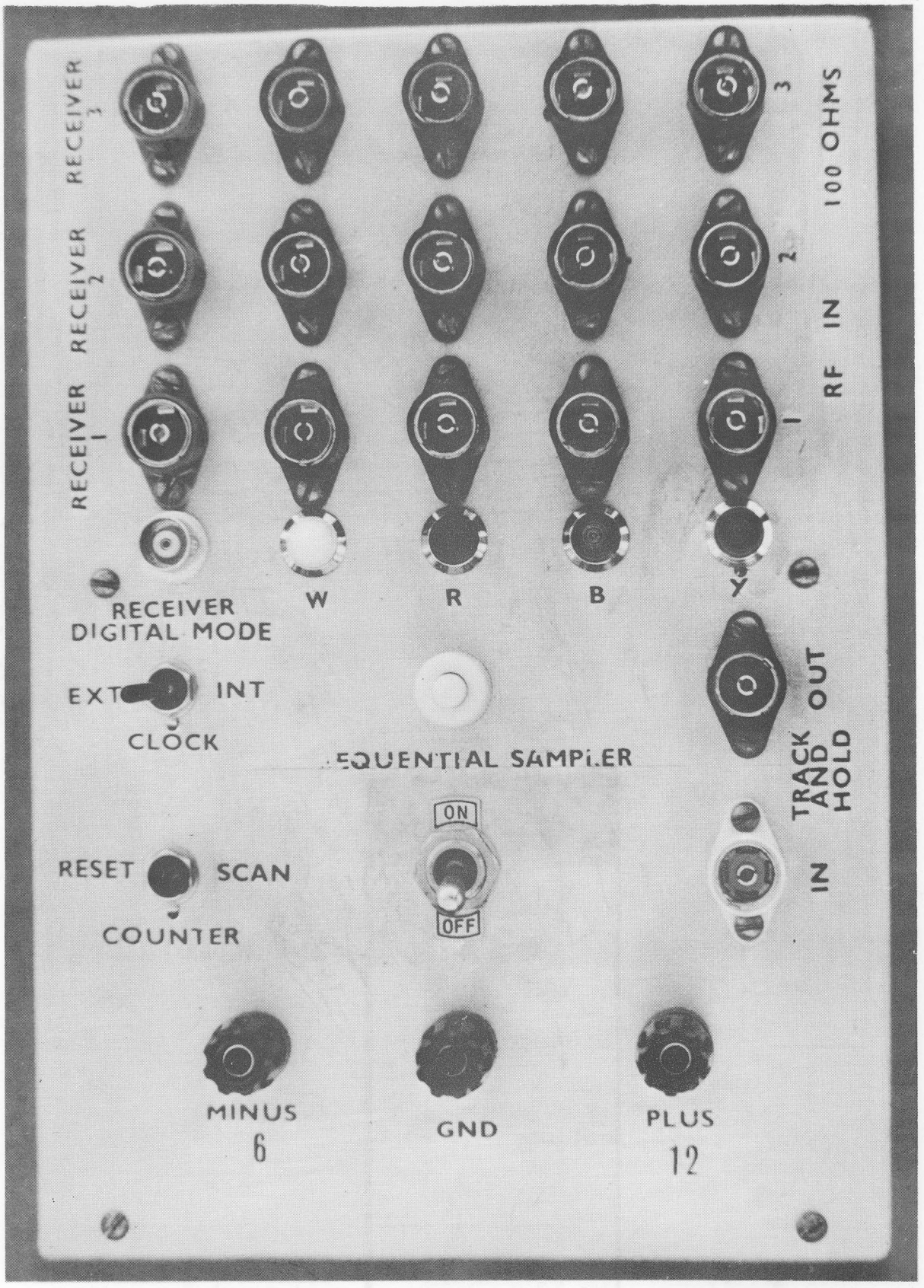

SEQUENTIAL SAMPLER

FIGURE - 6

3. Timing and Pulse Synchronization

The master time reference for this experiment was a crystal oscillator, phase locked to the power line frequency of 50 cps. This oscillator, in conjunction with various pulse shaping circuits, furnished the pulse repetition frequency for the 69 mc/s telemetry transmitter at Rolleston.

The only specific timing requirement for the receiving instrumentation was a "track and hold" pulse to facilitate reception of signals from a predetermined height. The pulse generator constructed for this purpose is shown in figure 7. Provisions were made, in the nature of a "Range Delay" circuit, to compensate for the time difference between the pulse leaving Rolleston (at 69 mc/s) and the time at which the 2.4 mc/s pulse was transmitted from Birdlings Flat.

The time at which the receiver was commanded to switch from a "track" function to a "hold" function was set by the "Range Gate" control. Both the Range Delay and the Range Gate consisted of monostable multi-vibrator circuits. A convenience feature was added in the form of a meter calibrated for a PRF of 50 per second. This meter indicated the echo height that corresponded to the time at which the "hold" function commenced. The meter

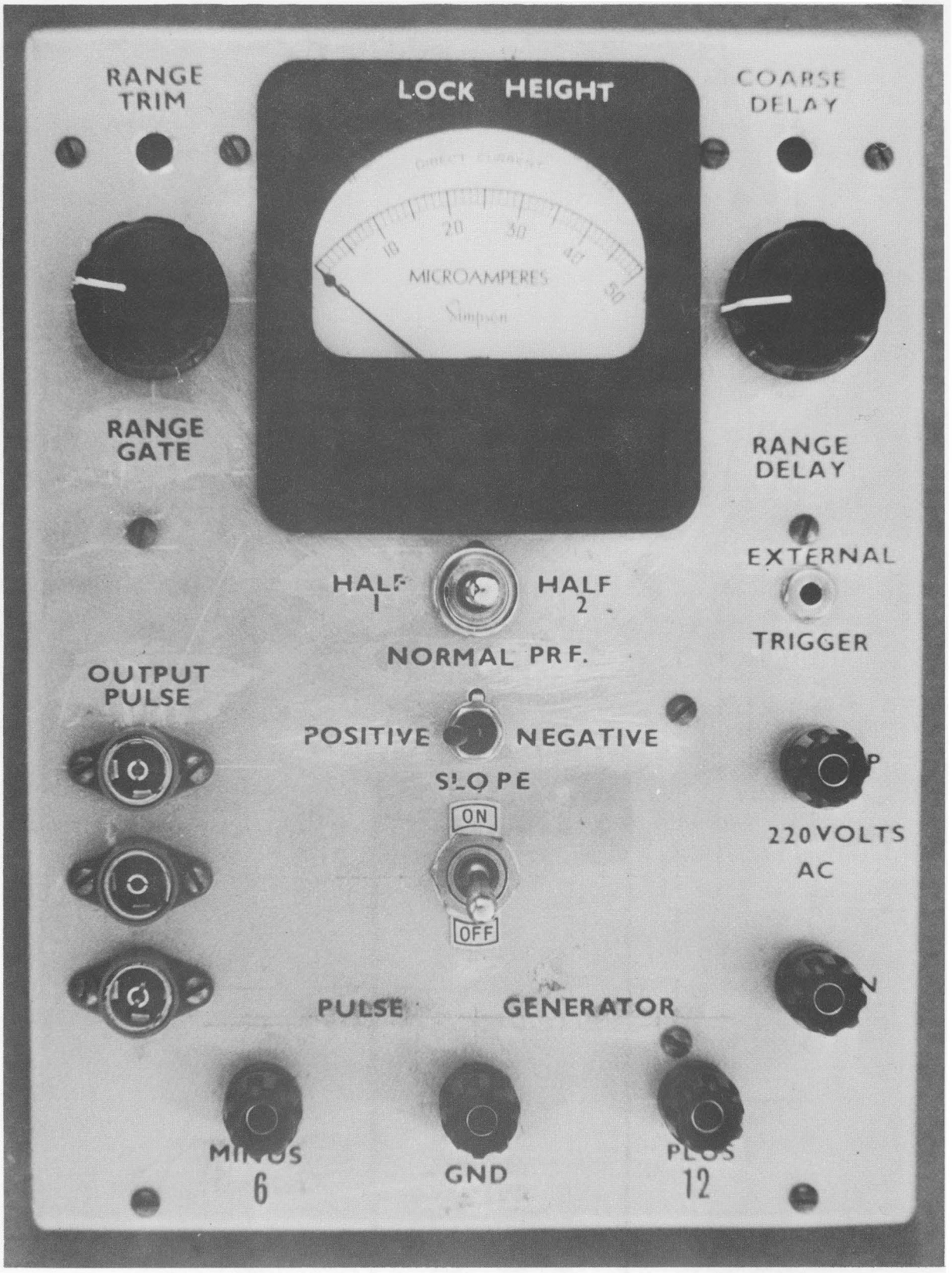

TRACK-AND-HOLD
PULSE GENERATOR
FIGURE - 7

scale in figure 7 should be multiplied by 2 to obtain the equivalent echo height (in kilometers).

The output pulse from the pulse generator changed from minus 6 volts to plus 12 volts at the instant the 2.4 mc/s transmitter at Birdlings Flat was pulsed. The pulse amplitude then remained at plus 12 volts for the duration of the receiver "track" time, and changed to minus 6 volts for the "hold" time interval.

Because of the fast rise time of this command pulse, in conjunction with the response time inherent to field effect transistors, the receiver mode changed from "track" to "hold" in less than 0.1 microseconds. The use of high quality polystyrene capacitors served to reduce time "jitter" in the monostable multivibrators to a negligible value. Consequently, the selected echo height was maintained constant to well within one kilometer.

4. Analog-to-Digital Recording System

It was mentioned earlier that the originally planned (and used) method of recording amplitude data on paper recording charts was subsequently changed to a digital recording system. It was indeed fortunate that an IBM paper-tape punch and associated driving circuitry, as well as a Solartron

digital voltmeter, were temporarily available to this project. The voltmeter proved to be ideal for the contemplated A to D recording system in that BCD information, as well as an external "read" command, were available at a terminal board. All that remained to be done was to design and construct the necessary "interface" circuitry for the system.

Without going into details, a brief description of the overall system follows:

The command to convert the analog data voltage from the receiver into BCD was given by the Sequential Sampler to the DVM. Approximately 180 milliseconds were required for this conversion. Buffering circuits then directed the digital data to the paper punch where they were printed as a 12 bit word. In addition, the appropriate channel identification number, corresponding to channels 1 to 12, and also generated by the sequential sampler, was punched on the paper tape. At the completion of printing, the paper punch furnished a "punch complete" signal. This signal, when combined with the sample-and-hold pulse, caused the cycle to be repeated.

Because of the slow action of the paper punch and the long conversion time required by the DVM,

the time to digitize one data point was 0.5 seconds. One complete data cycle of 12 points, therefore, required six seconds. While this performance is slow in comparison with modern A to D converters, it was entirely adequate for this program. In fact, the slow sampling rate of the system guaranteed that each data point would be statistically independent of its predecessor.

Figures 8 and 9 show a composite of the receiving station instrumentation. As mentioned earlier, details and circuit diagrams are to be found in Appendix A.

DIGITAL RECORDING SYSTEM

FIGURE - 8

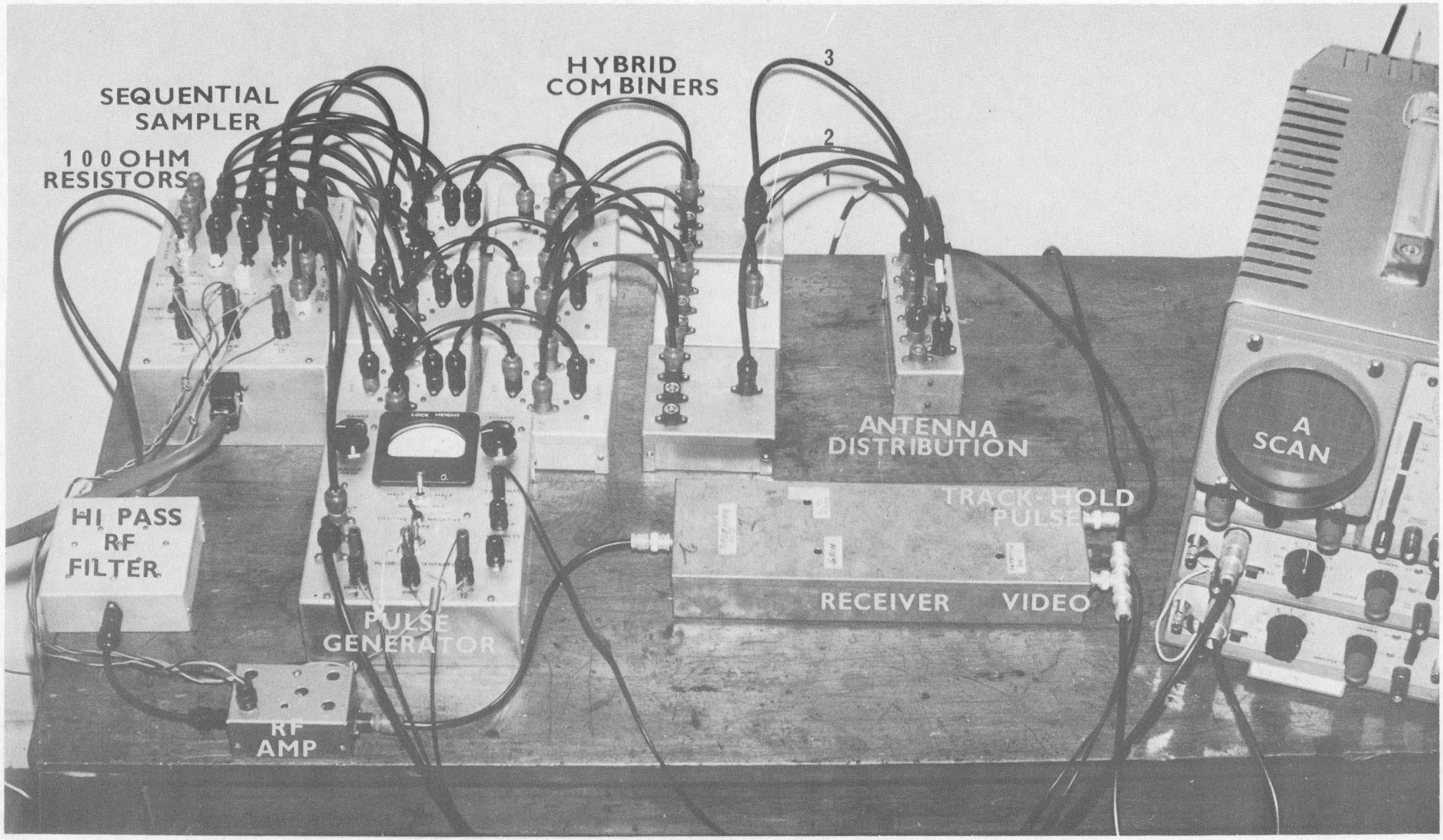

EXPERIMENTAL INSTRUMENTATION

FIGURE - 9

III(4). DATA COLLECTION AND ANALYSIS

From the discussion of experimental instrumentation it will be recognized that the receiving station required little operator attention during data collection. A routine was established, however, and was strictly adhered to during the time interval when data were collected (i.e. May 1969 to December 1969).

Prior to commencement of data collection, each of the three antenna feed lines was tested for proper insulation and continuity. This precaution was necessary in view of the fact that the antenna cables traversed areas where pigs and sheep were grazing, and since occasionally some inquisitive porker would chew on a section of cable.

In order to test the correct functioning of all the equipment, a standard data run was made each day in which the ground wave from the 2.4 mc/s transmitter at Birdlings Flat was recorded. The results were used for calibration purposes of subsequent data from the D-region.

Data from a preselected scattering height were recorded for eight minutes during a normal data run. In addition, one minute before and one minute after

ionospheric data were collected, the 2.4 mc/s transmitter was turned off, and the noise due to the receiver and the background was recorded. It was mentioned earlier that the digital recording system required 0.5 seconds to record one data value. Consequently, during a normal data run, 240 noise values were sampled, as well as 80 complete data sets (4 data values per set) for each of the three different antenna configurations. The information was stored in digital form on punched papertape for subsequent analysis by the Canterbury University Computer System (IBM 360/44).

The general procedure for data analysis was outlined in section III(2). A few modifications and refinements were added, however, to the analysis program. Thus, the raw data were first "stored" for repeated references to individual values. Then the average, mean squared, and variance values were computed for each of the 12 data channels and for the noise data. The mean square and variance values of the noise data were next subtracted from the corresponding quantities in each of the 12 data channels, and the average value of the noise was subtracted from each individual data point stored in the computer memory. The object of adjusting each individual data point by the mean value of the noise was to facilitate

statistical studies of the amplitude in the 12 data channels. It is recognized that removal of the "noise data" mean from the individual "composite" data points does not entirely render these data points noise-free. It does, however, serve to remove systematic errors that could be artificially introduced by a D.C. offset in the receiver output and in the digital voltmeter.

Beyond this preliminary "data conditioning" routine, the analysis program was split into two distinct phases. In the first of these phases the computations as outlined in section III(2) were carried out. Thus, the output from this portion of the analysis routine were the magnitude and the argument of the spatial correlation, evaluated for antenna separations of one, two, and three wave lengths.

During the design of this analysis phase, it was recognized that if one could assume that the various $v(\alpha)$ were members of the same statistical parent distribution (a Rice distribution was specifically assumed) then the values of M and N computed from the variance values should agree with those computed from the mean squared values.

To test this hypothesis, the magnitudes and arguments of the spatial field correlation were

computed for both the mean squared values and variance values. The agreement between corresponding results was generally very good.

The second phase of the analysis program had as its primary goal the identification of each of the 12 amplitude distributions with a Rice parameter "a" between 0 and 4.0. Rice (1945) defines a^2 as the ratio of power of a sinusoidal signal to the total power of random noise. The parameter "a" therefore relates the signal voltage to r.m.s. noise voltage. By definition, the Rayleigh amplitude distribution is one for which a=0. In essence, the program performed a sorting function in which the individual data from each of the 12 channels were compiled into amplitude distribution histograms. These histograms were computed for five amplitude cells, each of which corresponded to one standard deviation of the data in the appropriate channel. By means of a chi-square test each of the resulting histograms was compared with pre-computed histograms that would be expected for Rice distributions of parameter "a" between 0.0 and 4.0. In this comparison routine, the parameter "a" was successively incremented by 0.1 and the value of "a", for which the agreement between the theoretical and the experimental histograms was greatest, was then chosen as the identifying parameter. An experimental

histogram for which the best fit resulted in χ^2 larger than 6.75 was rejected as "unfittable". (See section III(5) for a further discussion of this point.) Two examples of histograms for which χ^2 was exactly equal to 6.75 are shown in figure (10). It is estimated that less than 20% of all of the histograms processed was discarded as unfittable ($\chi^2 = 6.75$, with four degrees of freedom, corresponds to a "confidence" of 0.15).

The computed values for the magnitude and phase of the spatial field correlation, as well as the Rice parameters, were returned by the computer on punched cards. In addition, the computer printout contained a variety of other related facts about the particular data run. Among these were such items as the signal to noise ratio, individual histograms, the baseline corrections (see discussion in section III(2), and other data of interest to the experimenter.

The discussion of data analysis has thus far been concerned with the day to day processing of the raw experimental data. It was not until the overall experiment had been completed that the final analysis program was executed. At that time, the correlation and statistical data were sorted on the basis of scattering height and baseline length. A cursory examination of the results revealed that the magnitude

THRESHOLD FIT TO A RAYLEIGH DISTRIBUTION

(MAXIMUM ACCEPTABLE DEPARTURE FROM THE ASSUMED DISTRIBUTION)

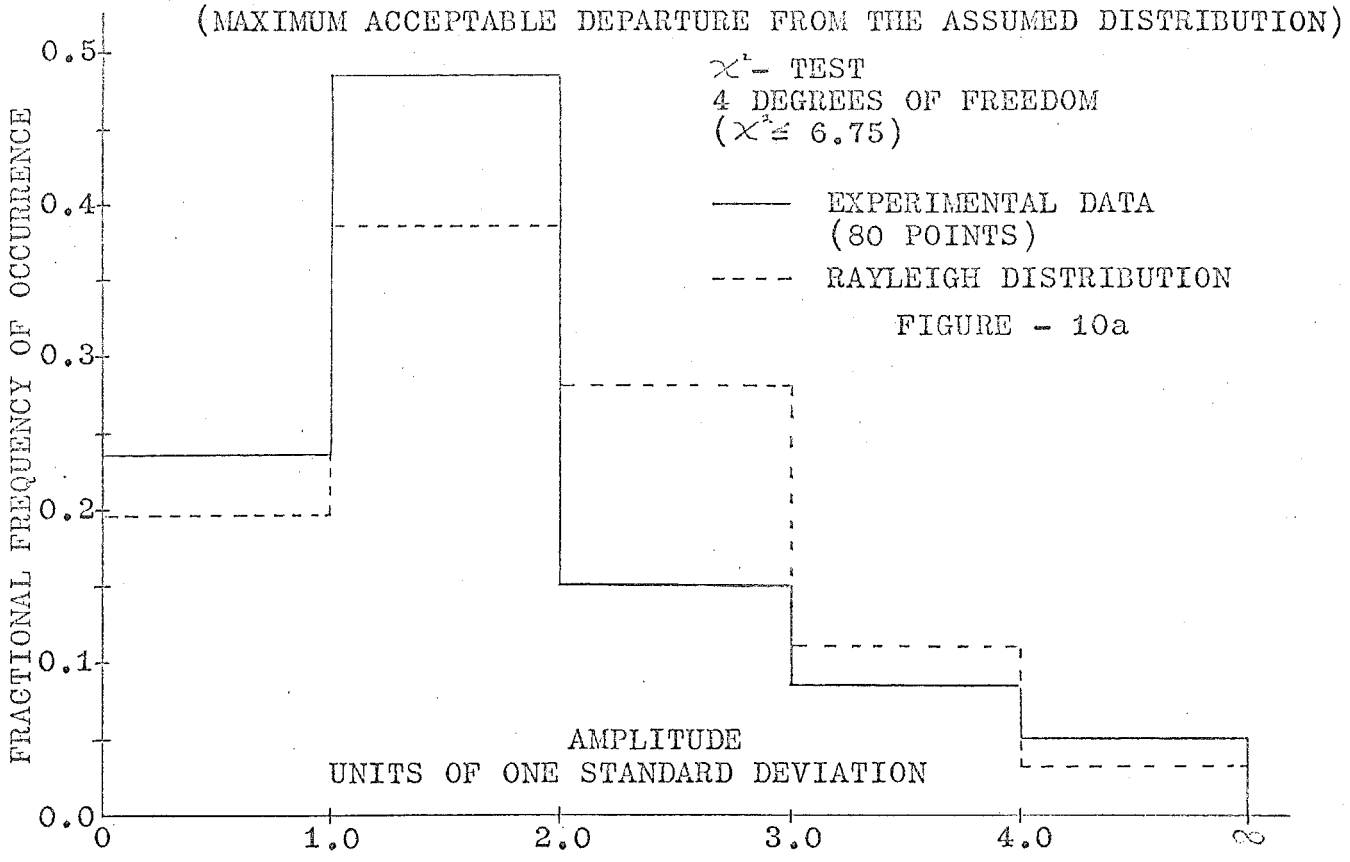

FIGURE - 10a

THRESHOLD FIT TO A RICE (a = 1.9) DISTRIBUTION

(MAXIMUM ACCEPTABLE DEPARTURE FROM THE ASSUMED DISTRIBUTION)

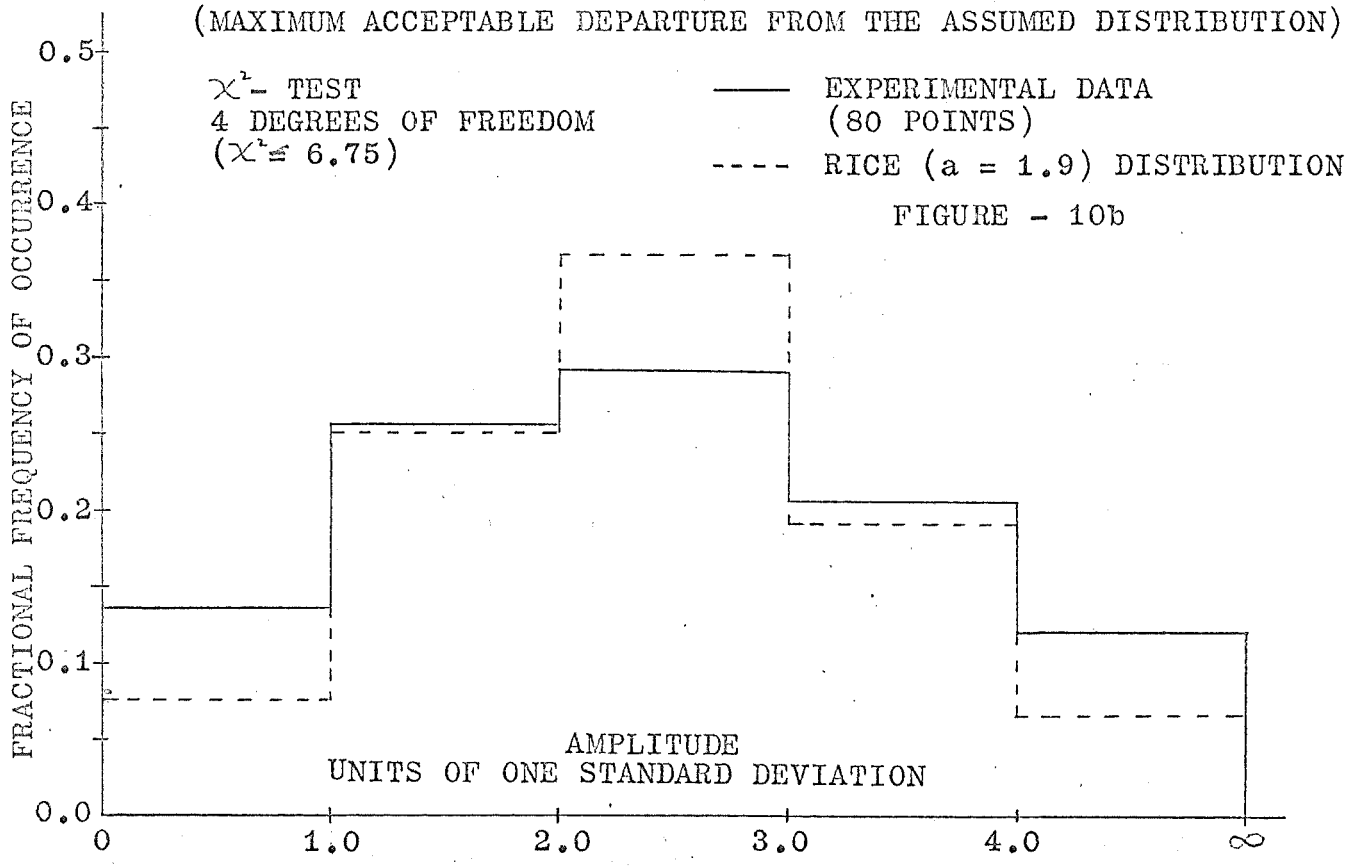

FIGURE - 10b

of the spatial field correlation did not decrease to zero for large antenna separations. Instead, it appeared to approach some constant value. This finding, of course, is in accord with the conclusions reached in section II(3) where the correlation magnitude was assumed to be of the form

$$\rho(r) = \frac{B + \exp-\left[\frac{r^2}{L^2}\right]}{B + 1}$$

To fit the data to this assumed functional form, a non-linear least squares fit routine was required. Without going into the details of the resulting computer program, suffice it to say that the value of $\exp-(1/L^2)$ was determined by means of the Newton-Raphson iterative technique (Golden 1965). The output from this program were the values of B and L.

The fit routine was used for each individual set of correlation magnitude data, whether computed on the basis of mean squared values or variance values. In addition a fit was made to the average values of all the experimental data points for a given antenna separation and scattering height. Also, where possible, those points representing the average plus or minus one standard deviation were fitted by this routine. One should recognize that simultaneous values for B and L may be obtained from a least squares routine

only when three or more data points are used. In this experiment only three points were available, and these points were obtained in a way that made any one point statistically independent of the remaining two points. It is therefore not surprising that occasionally a point, or even two points, in a set of three was in obvious error. A situation such as this can be explained on the basis of noise pulses, or interference, that could conceivably affect only one of the 12 independent data channels. Consequently, it was sometimes not possible to fit a set of three data points with the assumed functional relationship. Even though a hypothetical fit might be possible, the resulting values of B and L would be in serious error. For this reason a set of three data points was deemed "unfittable" if the r.m.s. error of fit exceeded 0.1. Thus, the values of B and L derived from the individual fits are those for which the r.m.s. deviation of the data points from the curve was smaller than this tolerance limit. In fitting the average data, this problem did not arise since the "bad" points were deemphasized by the much greater number of "good" data points.

In comparison with the non-linear fit routine just described, analysis of the "phase" data was considerably easier. A least squares, polynomial

fit routine was used on each set of three phase values. It was subsequently found that the r.m.s. error of fit was not appreciably affected when the quadratic term was omitted. For this reason it was concluded that the phase varied linearily with antenna separation. Since the phase difference for an antenna spacing of zero also had to be zero, and because each of the three phase values was obtained independently of the remaining two, it was decided to compute a mean phase slope from the three points rather than fitting them to a straight line by the method of least squares. As it turned out, the difference in phase slope obtained by these two methods was negligibly small.

Before proceeding to the next section, it is worthwhile to mention the results obtained from certain system calibration experiments. It was stated earlier that a normal data run was made for the "ground pulse" signal every day the experiment was conducted. The result from 32 such experiments was that the correlation for each of the three antenna configurations was $0.99 \pm .01$ and that the phases were $+14.1 \pm 3.8^{o}$, -21.8 ± 3.3^{o} and -7.6 ± 3.5^{o} for the one, two, and three wave lengths spacing respectively. While the correlation values are to be expected from a coherent signal, the phase values

were interpreted as errors in the baseline lengths. Thus the baselines were in reality 1.04λ, 1.94λ, and 2.98λ long. This conclusion was subsequently verified to within ±5 feet.

While these results are most gratifying, they do apply to a steady signal and to a large signal-to-noise ratio. A second series of system tests was therefore conducted in which random noise was used as the signal source. Specifically, two nominally identical amplifiers were constructed. The gain of these amplifiers was about 30 db, and their frequency response was "flat" from 0 to 10 mc/s. With no input signal to these amplifiers, their output voltage was a band limited white noise signal. When these two amplifiers were substituted for any two of the three antennas, the resulting correlation was 0.03 ± 0.02. The phase difference obtained from this test had a mean value of 357^{o} and an r.m.s. deviation of $\pm 58^{o}$. Six such tests were conducted. In an effort to ascertain the response of the system to a coherent noise signal the above test was repeated, but the output from one of the noise sources was divided into two equal channels. (The second amplifier was not used.) The result from this test was a correlation value of 0.996 ± 0.003 and a phase of 359.48 ± 0.75. Again, six

such tests were conducted. The test results speak for themselves and are indicative of the capability of the experimental instrumentation.

III(5). THE "OFF-SET" RAYLEIGH DISTRIBUTION

It was stated earlier that certain experimentally obtained amplitude distributions could not be satisfactorily fitted to any Rice distribution between a=0 and a=4.0. It was also pointed out that distributions for which the smallest value of χ^2 exceed an arbitrarily chosen value of 6.75 were rejected as "unfittable". Upon further examination of these "unfittable" distributions a rather curious fact emerged; namely, that while none of them could be properly fitted to a Rayleigh distribution or to a Rice distribution, the majority could be fitted to the function

$$P(V) = \frac{(V-C)}{\sigma^2} \exp-\left[\frac{(V-C)^2}{2\sigma^2}\right] \qquad (59)$$

In equation (59) C is a constant, and P(V) is zero for negative (V-C).

This particular functional dependence was first reported by von Biel (1965) and again in (1966). That certain amplitude distributions obtained from ionospheric experiments do not conform to either Rayleigh or Rice distributions was also recognized by Whitehead (1962) who tried to explain the phenomenon in terms of a focussing mechanism. More recently, Austin and

Thorpe (1969) have addressed themselves to the problem of unusual amplitude distributions. Their approach was similar to that of Whitehead (1962) and is based on geometrical optics arguments. These authors also point out that their mechanism is probably not applicable to D-region echoes.

Before proceeding with the development and discussion of a process which, it is felt, is responsible for the experimentally observed distributions, a few words in defense of the functional relation given by equation (59) seem appropriate. Consider the histogram in figure (11a) which represents a plot of frequency of occurrence in successive amplitude intervals of one data standard deviation. This particular histogram was obtained on September 21, 1969, for a scattering height of 75 km. It is typical of an "unfittable" distribution and was chosen for that reason only.

Probably the least controversial treatment of amplitude distribution data is to compute the cumulative probability as a function of amplitude. Thus, for each value of amplitude, it is possible to compute the probability that the amplitude will be smaller than this value. At the same time, one may compute a value of R in a Rayleigh distribution $\left[P(R) = R \exp -\frac{R^2}{2}\right]$

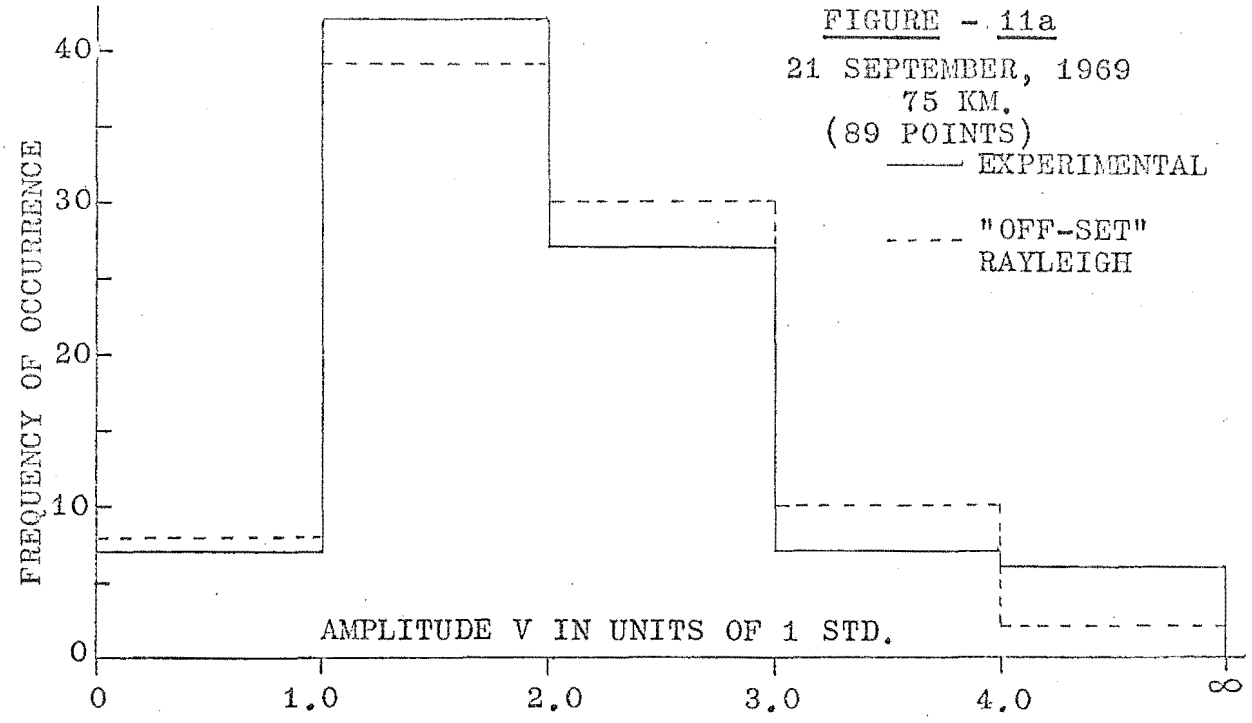

FIGURE - 11a

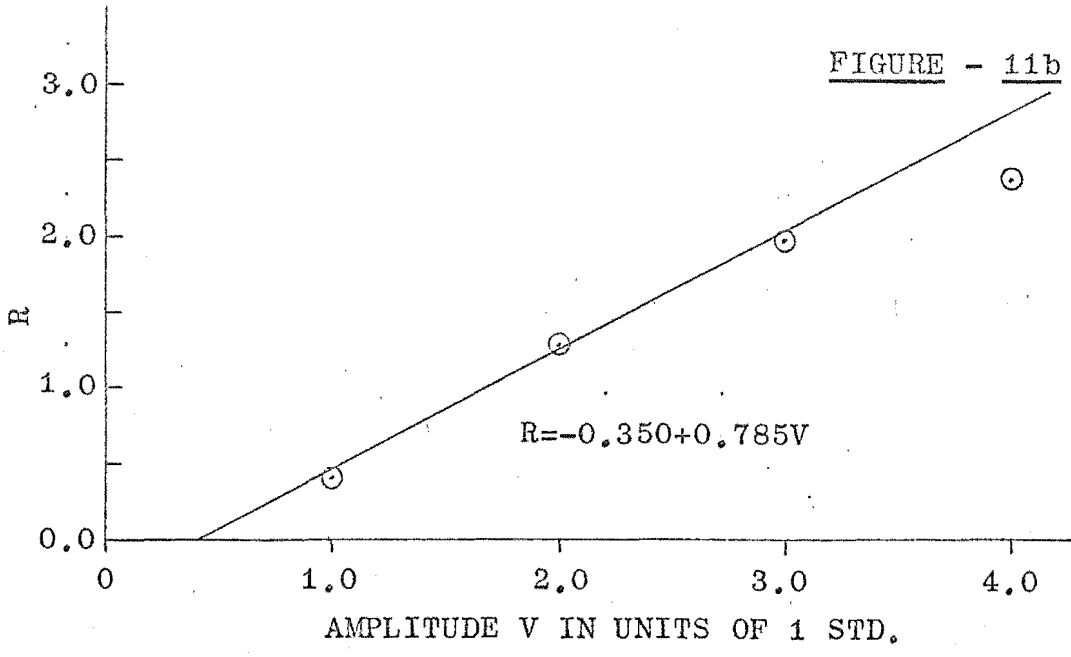

FIGURE - 11b

which would represent the same cumulative probability as was computed for a given amplitude (V) from the experiment. Next, if the values of R were plotted as a function of the experimental amplitudes V (the cumulative probability being the same for both R and V), then the points obtained will fall on a straight line which passes through zero if the experimentally obtained values of V were Rayleigh distributed. Under these circumstances the value of C in equation (59) would be zero, and the slope of the straight line would equal $\frac{1}{\sigma}$. On the other hand, if the points fall on a straight line which does not pass through the origin, the amplitude distribution can be fitted with the function in equation (59) for which $\frac{1}{\sigma}$ is the slope of the line, and C is the intercept with the R-axis divided by the slope. Since it is not likely that all of the points will fall on a straight line, a compromise is to fit the best straight line to points for which the cumulative probability is between 10% and 90%. This range, again, is a purely arbitrary one. The process is illustrated in figure (11b).

The dotted lines in figure (11a) show the expected frequency of occurrence for each of the amplitude intervals when the histogram is assumed to be an "offset Rayleigh" distribution. It will be observed

that the fit is remarkably good. Further substantiations for the "goodness" of fit is that $\chi^2 = 4.65$ in constrast to $\chi^2 \doteq 10$ when the same histogram was fitted to the "best" Rice distribution.

It should be evident that the "offset" Rayleigh distribution is a purely empirical relationship that cannot be explained in terms of any physical processes. At the same time, it must be recognized that amplitude data from ionospheric experiments frequently exhibit a noticeable departure from distributions that can be physically justified. Consequently, one is forced to look for a realistic reason for the observed facts. Since the experimental data under discussion here were derived from the ionospheric D-region, one is hesitant to stipulate a focussing process as the cause for the observed distributions. Thus, the explanations advanced by Whitehead (1962) and Austin and Thorpe (1969) might well apply to the E and F regions but are not likely to be valid for the D-region where scattering is assumed to be caused by under-dense irregularities.

Instead, consider the fact that ionospheric echoes exhibit decorrelation times of the order of seconds. This fact is equivalent to saying that the noise band width of ionospheric signals is extremely small: a fraction of one cycle per second. Since

in most back scatter experiments height resolution is usually important, the receiving equipment is designed for band widths comparable to the reciprocal of the pulse resolution time. D-region experiments, for example, would require a receiver band width of about 100 kc/s. Thus, the output from the receiver I.F. amplifier consists of band limited white noise having a band width of the order of 100 kc/s, plus the ionospheric echo signal which has a band width of a fraction of one cycle per second. If this composite signal is sampled at the usual pulse repetition rate of about 20 samples per second then the output from the detector will be Rice distributed; that is to say, the ionospheric echo amplitude will change very little over several sample intervals but the band limited noise signal will be a random component added to this pseudo-steady signal.

Next assume that the detector output is filtered and recorded. The filtering process may simply be the mechanical response of a chart recorder which normally is of the order of one or two cycles per second. Alternatively, filtering might be accomplished by means of a low-pass video filter. The net result will be the same for either method of filtering: the voltage recorded is the average value of the composite

voltage at the detector output. Naturally, this averaging process will be primarily determined by the band width of the post detection filter. For purposes of discussion, it will be assumed that the band width of the filter is comparable to the noise band width of the ionospheric signal, but is much narrower than the predetection band width of the receiver. This assumption will yield a "worst case" situation, and in the following discussion this fact should be periodically recalled.

Assume next that the amplitude V_s of the ionospheric signal is Rayleigh distributed so that its r.m.s. value is $\sqrt{2}\sigma_s$. Likewise, it is assumed that the band limited noise signal amplitude is Rayleigh distributed and has an r.m.s. value of $\sqrt{2}\,\sigma_o$. In view of the vast difference in band width of these two signals, the detector output over several sample intervals will be Rice distributed, and its mean value[1] (the voltage recorded on the chart) is given by Rice (1944) as

$$V = \sqrt{2}\sigma_0 \left[\frac{3}{2}\right] {}_1F_1\left(-\tfrac{1}{2};1;-\frac{V_s^2}{2\sigma_0^2}\right) \qquad (60)$$

In equation (60) ${}_1F_1$ is the confluent hypergeometric

(1). This approach to a "limiting case" filter was suggested by R. G. T. Bennett.

function of the arguments and may be replaced by

$$ {}_1F_1(-\tfrac{1}{2};1;-z) = e^{-z/2}\left[(1+z)I_0(\tfrac{z}{2}) + zI_1(\tfrac{z}{2})\right] \qquad (61) $$

In equation (61), $z = \frac{V_s^2}{2\sigma_o^2}$, and I_0 and I_1 are the Bessel functions of imaginary argument. Rewriting (60) in terms of (61) one obtains:

$$ V = \sqrt{\tfrac{\pi}{2}}\,\sigma_o \exp-(\tfrac{z}{2})\left[(1+z)I_0(\tfrac{z}{2}) + zI_1(\tfrac{z}{2})\right] \qquad (62) $$

Now:

$$ P(V_s)dV_s = P(z)dz = P(V)dV \qquad (63a) $$

and

$$ P(V) = P(V_s)\left[\frac{dV_s/dz}{dV/dz}\right] \qquad (63b) $$

Differentiation of V with respect to z yields:

$$ \frac{dV}{dz} = \frac{\sqrt{\frac{\pi}{2}}\,\sigma_o}{2} \exp-(\tfrac{z}{2})\left[I_0(\tfrac{z}{2}) + I_1(\tfrac{z}{2})\right] \qquad (64) $$

And, from the definition of z one obtains

$$ \frac{dV_s}{dz} = \frac{\sigma_o^2}{V_s} \qquad (65) $$

Consequently:

$$ P(V) = P(V_s)\left[\frac{2\sqrt{2}}{\sqrt{2\pi z}}\right] \frac{1}{\exp-(\frac{z}{2})\left[I_0(\frac{z}{2})+I_1(\frac{z}{2})\right]} \qquad (66) $$

Recalling that V_s was assumed to be Rayleigh distributed (an assumption which is not necessary to the results shown in equation 66) one obtains:

$$P(V_s) = \frac{V_s}{\sigma_s^2} \exp-\left[\frac{V_s^2}{2\sigma_s^2}\right] \qquad (67)$$

Next, define the signal-to-noise ratio so that $b = \frac{\sigma_s}{\sigma_0}$, and further let $x = \frac{V_s}{\sigma_s}$ and $y = \frac{z}{2} = (\frac{bx}{2})^2$. Then:

$$P(V) = \frac{4}{\sqrt{2\pi}\, b\, \sigma_s} \exp-(\tfrac{x^2}{2}) \; \frac{1}{e^{-y}\left[I_0(y)+I_1(y)\right]} \qquad (68a)$$

$$V = \frac{\sigma_s}{b}\sqrt{\frac{\pi}{2}} \exp-(y)\left[I_0(y)+2y\left\{I_1(y)+I_0(y)\right\}\right] \qquad (68b)$$

$$P(V)dV = x \exp-(\tfrac{x^2}{2})dx \qquad (68c)$$

Equation (68a) gives the probability density distribution for the recorded voltage V. Both P(V) and V are seen to be functions of the signal-to-noise ratio b and of the normalized ionospheric signal amplitude $x = \frac{V_s}{\sigma_s}$. Thus, when x=0, it follows that $P(V) = \frac{4}{\sqrt{2\pi}\, b\, \sigma_s}$ and $V = \frac{\sigma_s}{b}\sqrt{\frac{\pi}{2}}$. In other words, the probability of finding V smaller than $\frac{\sigma_s}{b}\sqrt{\frac{\pi}{2}}$ is identically zero. As b becomes large, $P(V) \rightarrow P(x)$ and $V \rightarrow x$.

The distribution given in equation (68) is obviously not a Rayleigh, but in the limit as b becomes large, converges to the Rayleigh process.

The extent to which the process in (68) resembles an "offset" Rayleigh distribution is shown for various signal-to-noise ratios in the following 10 figures. (Note: the S/N in db is equal to $20\log_{10}b$). In computing these distributions, σ_s was first assumed to be equal to 1.0. Then the resulting histogram was treated in the same way as was the experimentally derived histogram for the "offset" Rayleigh distribution. This process was explained earlier, and does not require repeated explanation. All of the curves and histograms shown enclose a unit area. One should recall at this time that the curves presented here are for a "worst case" situation. A realistic assessment would require that the actual video band width be taken into consideration. Even a casual attempt to accomplish such a task will reveal the magnitude of the job. It was therefore decided to be satisfied with the identification of this very likely process that gives rise to "offset" amplitude distributions. The obvious conclusion must be that a substantial signal-to-noise ratio is required before a distribution can positively be identified with the Rayleigh process. It has also been shown that when a distribution can be associated with an "offset" Rayleigh, then it is not inconceivable that

the distribution of the echo amplitude was, in fact, Rayleigh distributed.

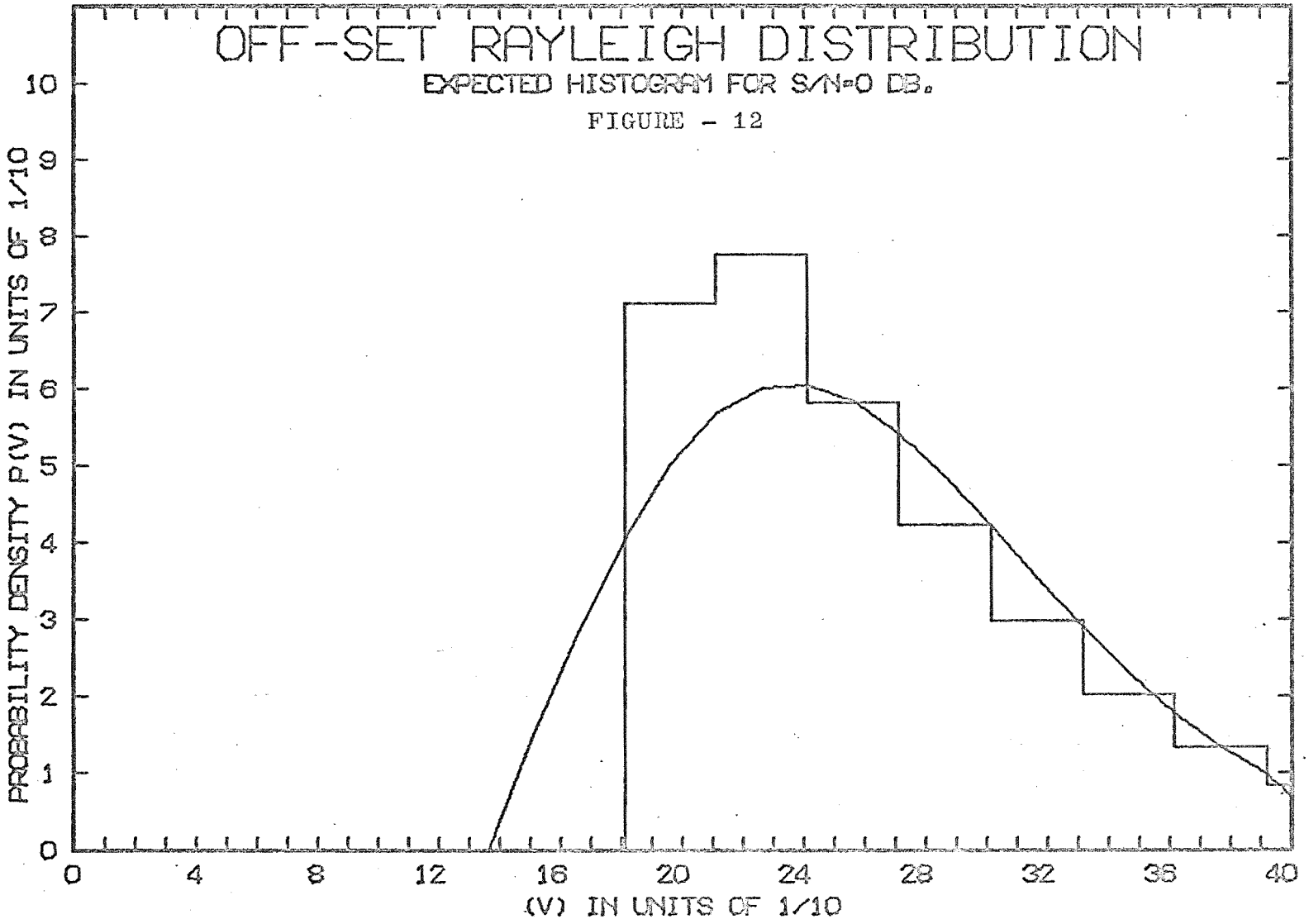
OFF-SET RAYLEIGH DISTRIBUTION
EXPECTED HISTOGRAM FOR S/N=0 DB.
PROBABILITY DENSITY P(V) IN UNITS OF 1/10
0
1
2
3
4
5
6
7
8
9
10
0
4
8
12
16
20
24
28
32
36
40
(V) IN UNITS OF 1/10

FIGURE - 12

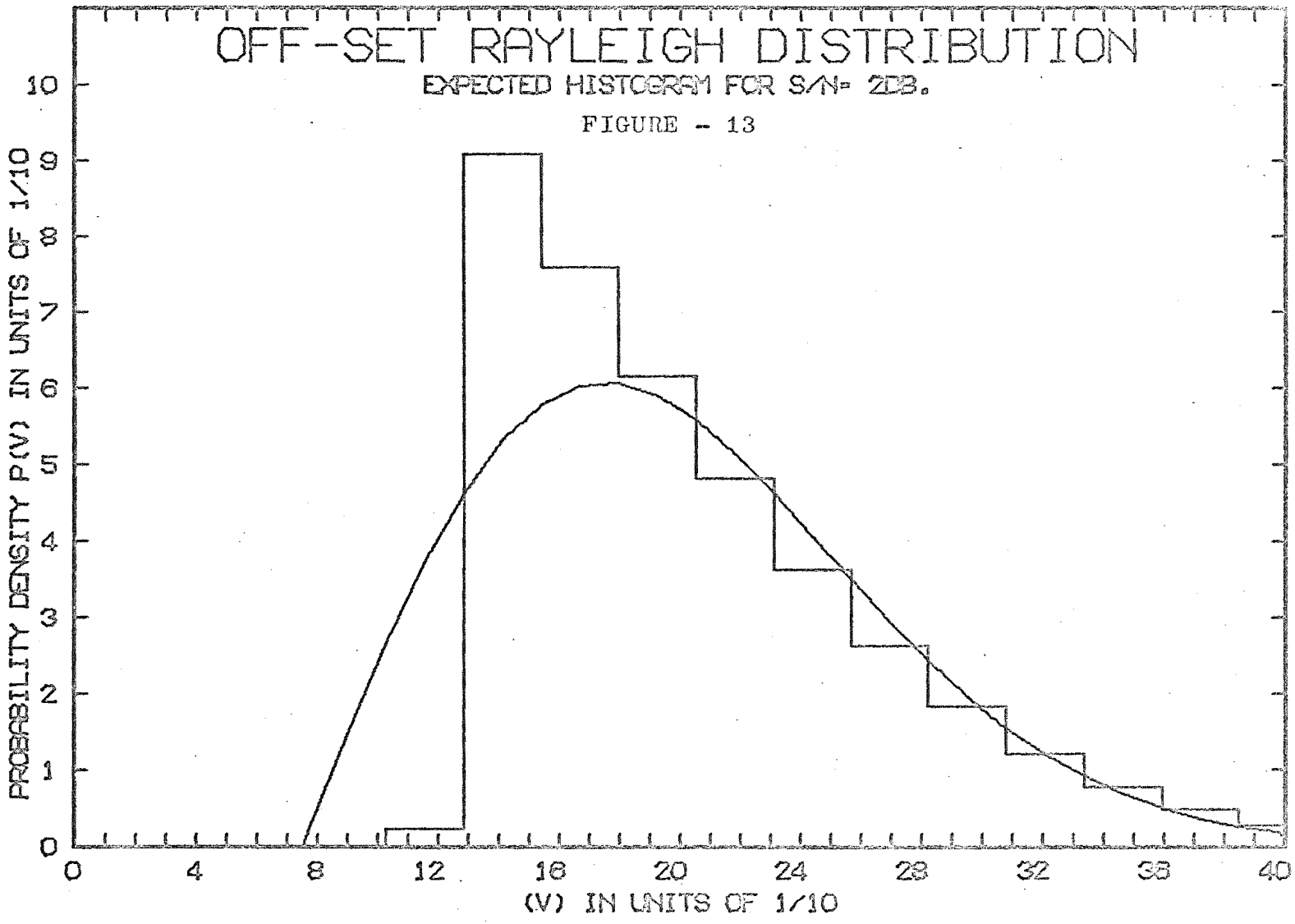
OFF-SET RAYLEIGH DISTRIBUTION
EXPECTED HISTOGRAM FOR S/N= 2DB.
PROBABILITY DENSITY P(V) IN UNITS OF 1/10
0
1
2
3
4
5
6
7
8
9
10
0
4
8
12
16
20
24
28
32
36
40
(V) IN UNITS OF 1/10

FIGURE - 13

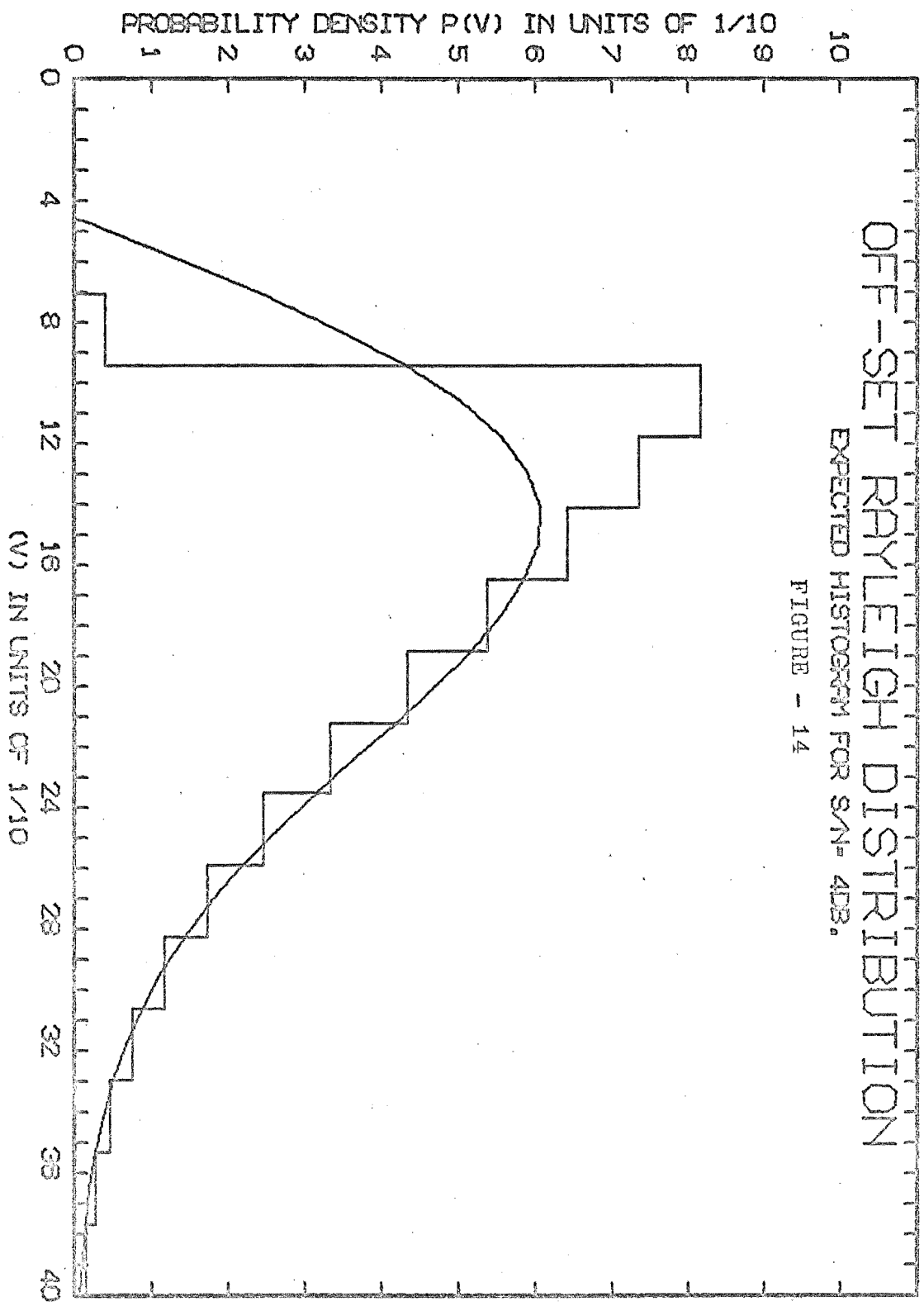

FIGURE - 14

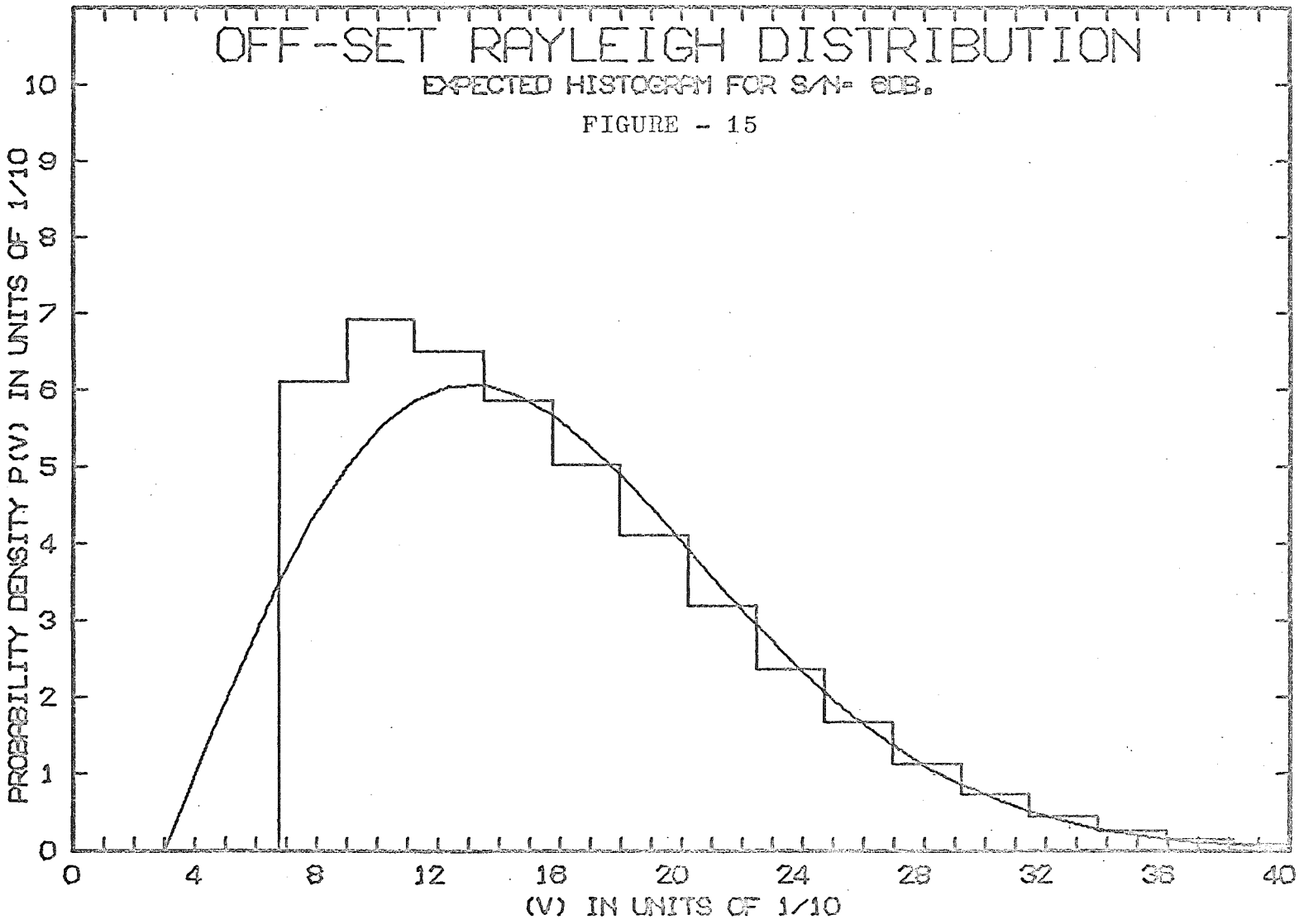
OFF-SET RAYLEIGH DISTRIBUTION
EXPECTED HISTOGRAM FOR S/N= 6DB.
PROBABILITY DENSITY P(V) IN UNITS OF 1/10
0
1
2
3
4
5
6
7
8
9
10
0
4
8
12
16
20
24
28
32
36
40
(V) IN UNITS OF 1/10

FIGURE - 15

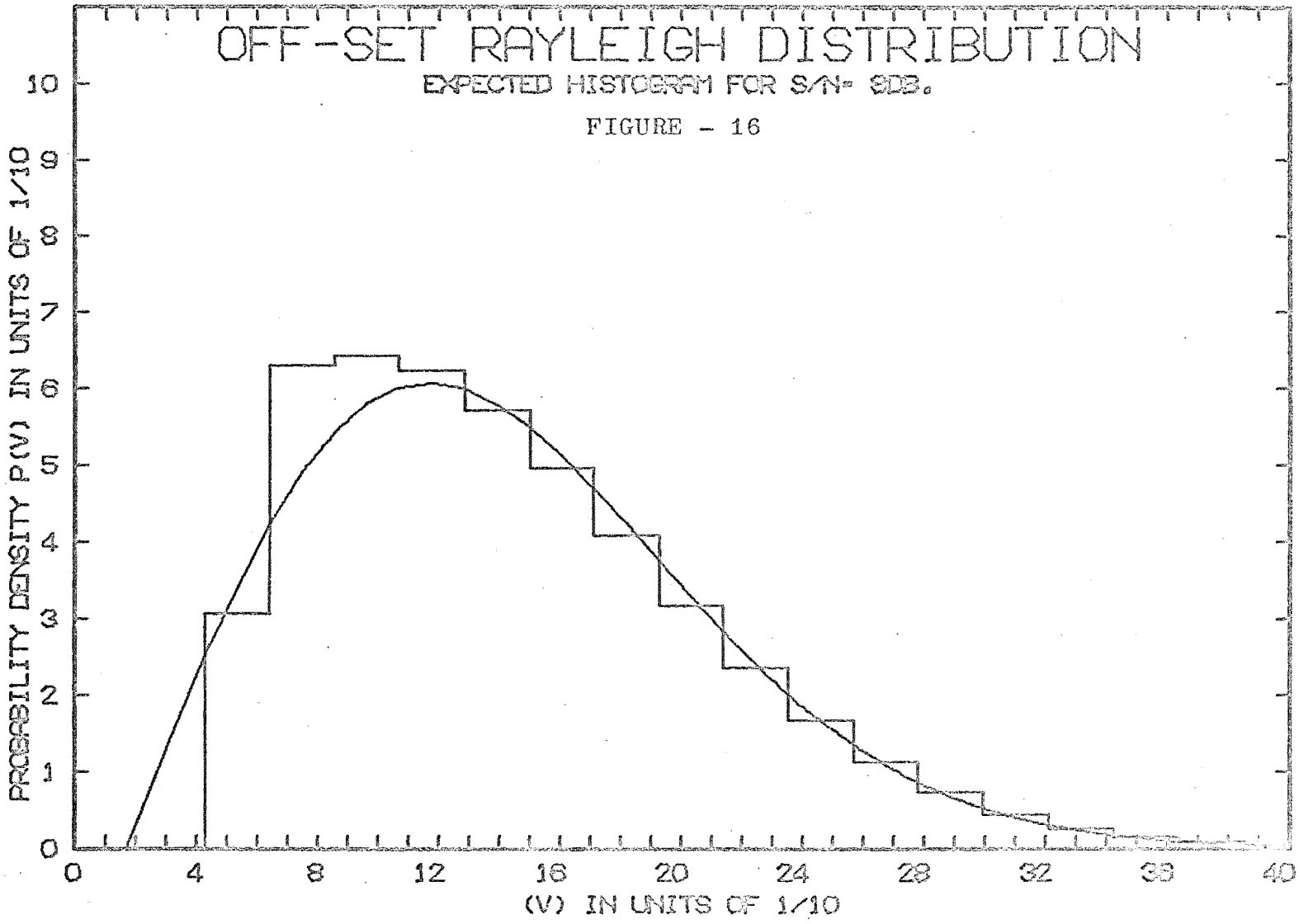
OFF-SET RAYLEIGH DISTRIBUTION
EXPECTED HISTOGRAM FOR S/N= 9DB.
PROBABILITY DENSITY P(V) IN UNITS OF 1/10
0
1
2
3
4
5
6
7
8
9
10
0
4
8
12
16
20
24
28
32
36
40
(V) IN UNITS OF 1/10

FIGURE - 16

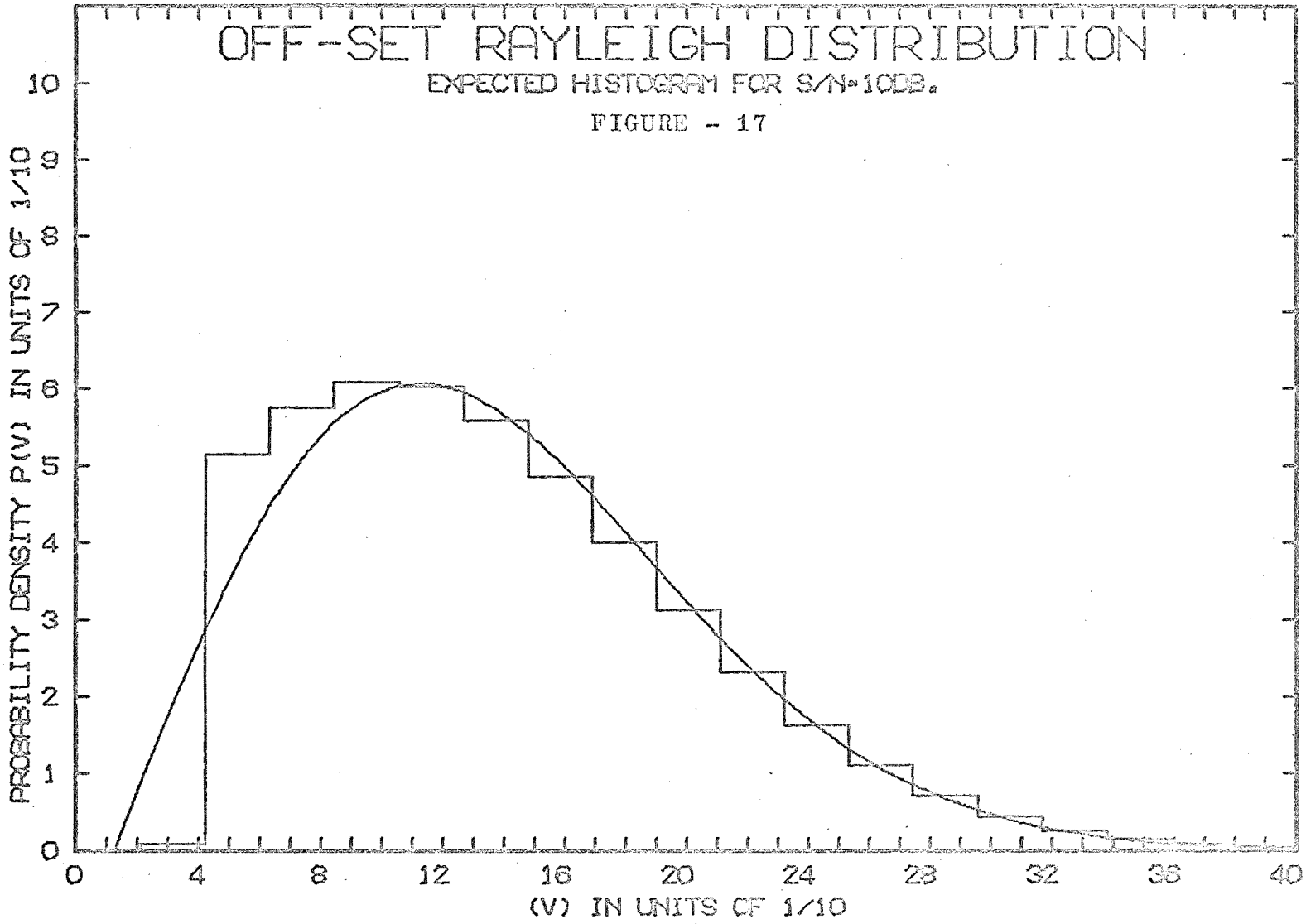
OFF-SET RAYLEIGH DISTRIBUTION
EXPECTED HISTOGRAM FOR S/N=10DB.
PROBABILITY DENSITY P(V) IN UNITS OF 1/10
0
1
2
3
4
5
6
7
8
9
10
0
4
8
12
16
20
24
28
32
36
40
(V) IN UNITS OF 1/10

FIGURE - 17

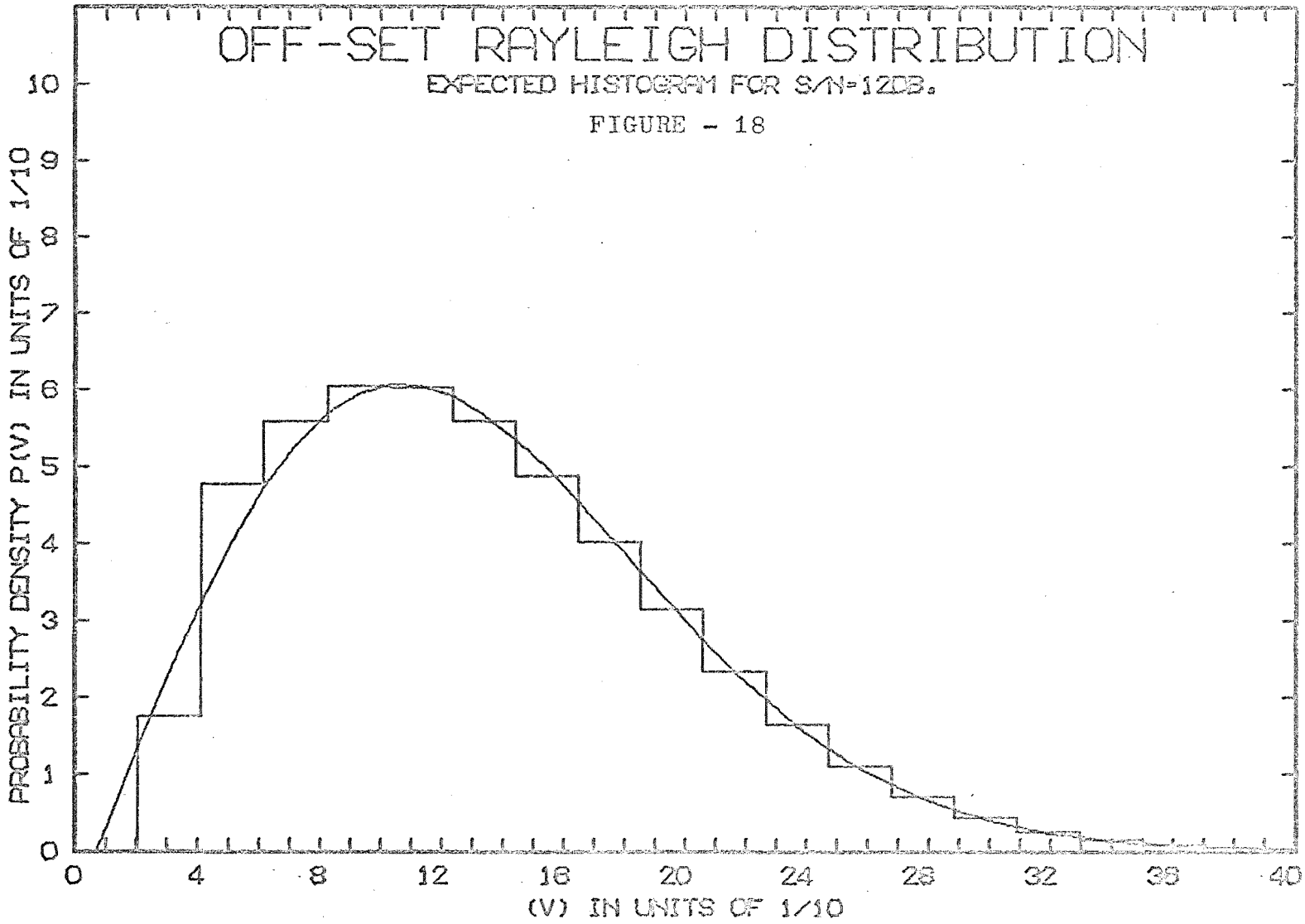
OFF-SET RAYLEIGH DISTRIBUTION
EXPECTED HISTOGRAM FOR S/N=12DB.
PROBABILITY DENSITY P(V) IN UNITS OF 1/10
0
1
2
3
4
5
6
7
8
9
10
0
4
8
12
16
20
24
28
32
36
40
(V) IN UNITS OF 1/10

FIGURE - 18

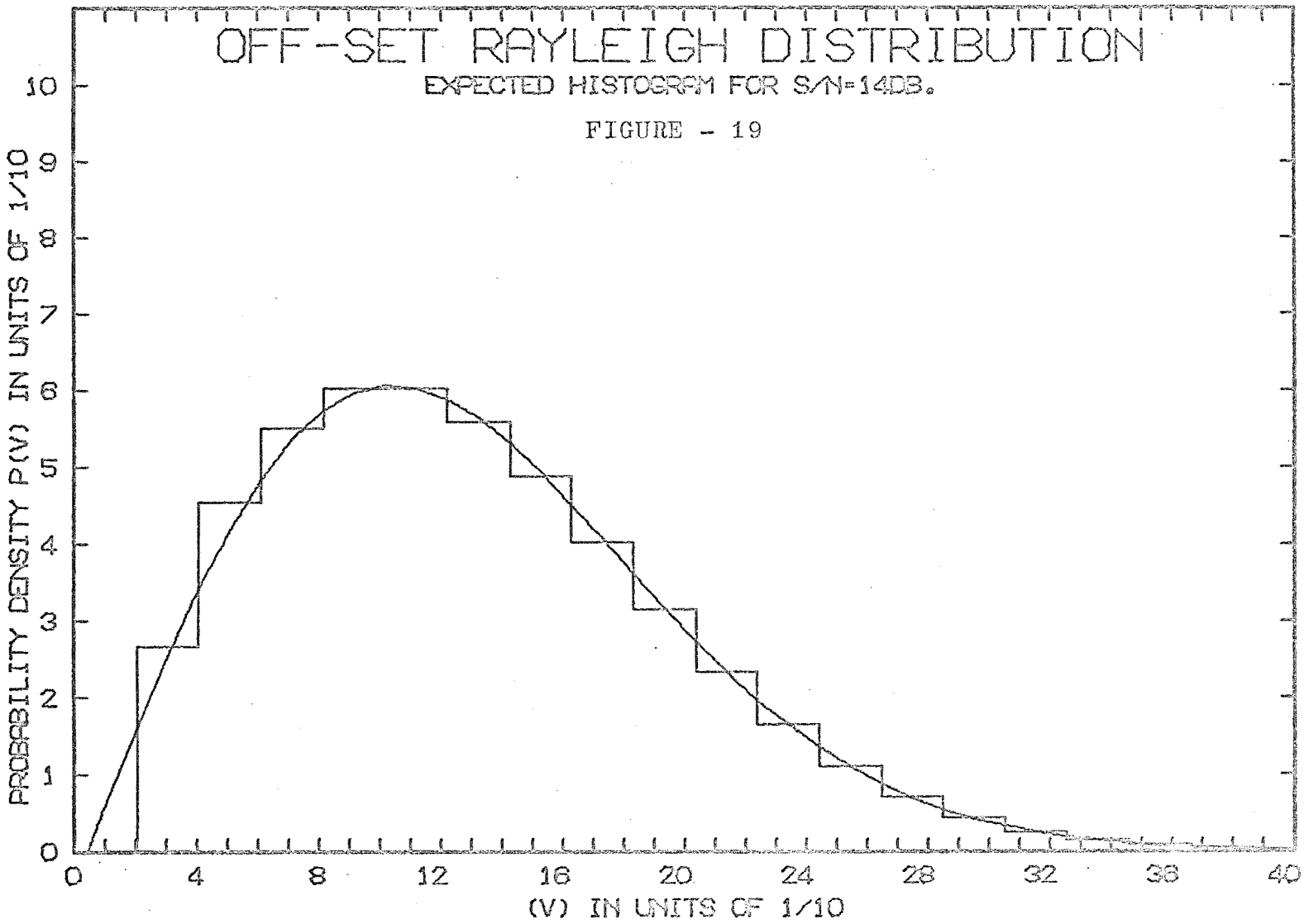
OFF-SET RAYLEIGH DISTRIBUTION
EXPECTED HISTOGRAM FOR S/N=14DB.
PROBABILITY DENSITY P(V) IN UNITS OF 1/10
0
1
2
3
4
5
6
7
8
9
10
0
4
8
12
16
20
24
28
32
36
40
(V) IN UNITS OF 1/10

FIGURE - 19

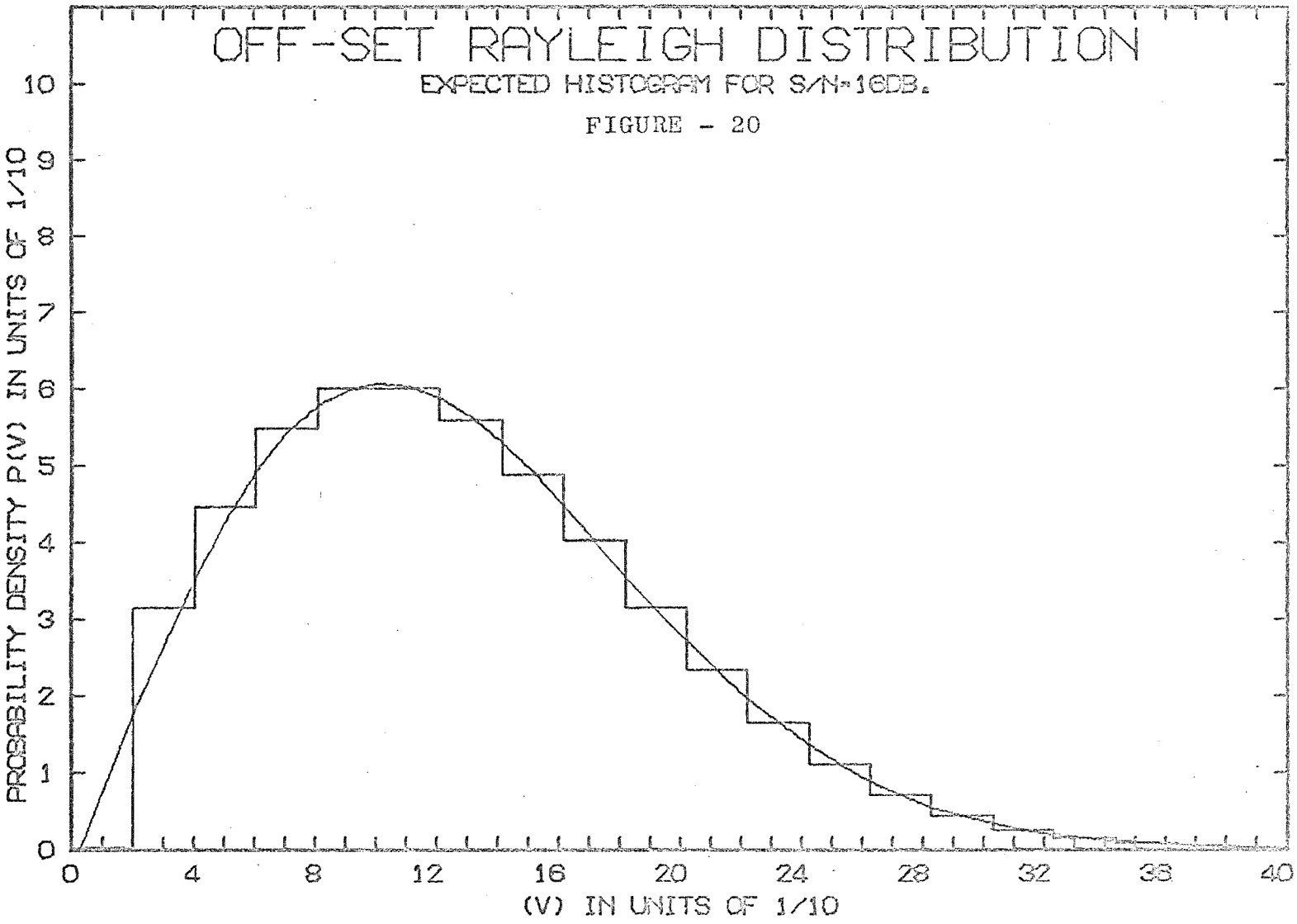
OFF-SET RAYLEIGH DISTRIBUTION
EXPECTED HISTOGRAM FOR S/N=16DB.
PROBABILITY DENSITY P(V) IN UNITS OF 1/10
0
1
2
3
4
5
6
7
8
9
10
0
4
8
12
16
20
24
28
32
36
40
(V) IN UNITS OF 1/10

FIGURE - 20

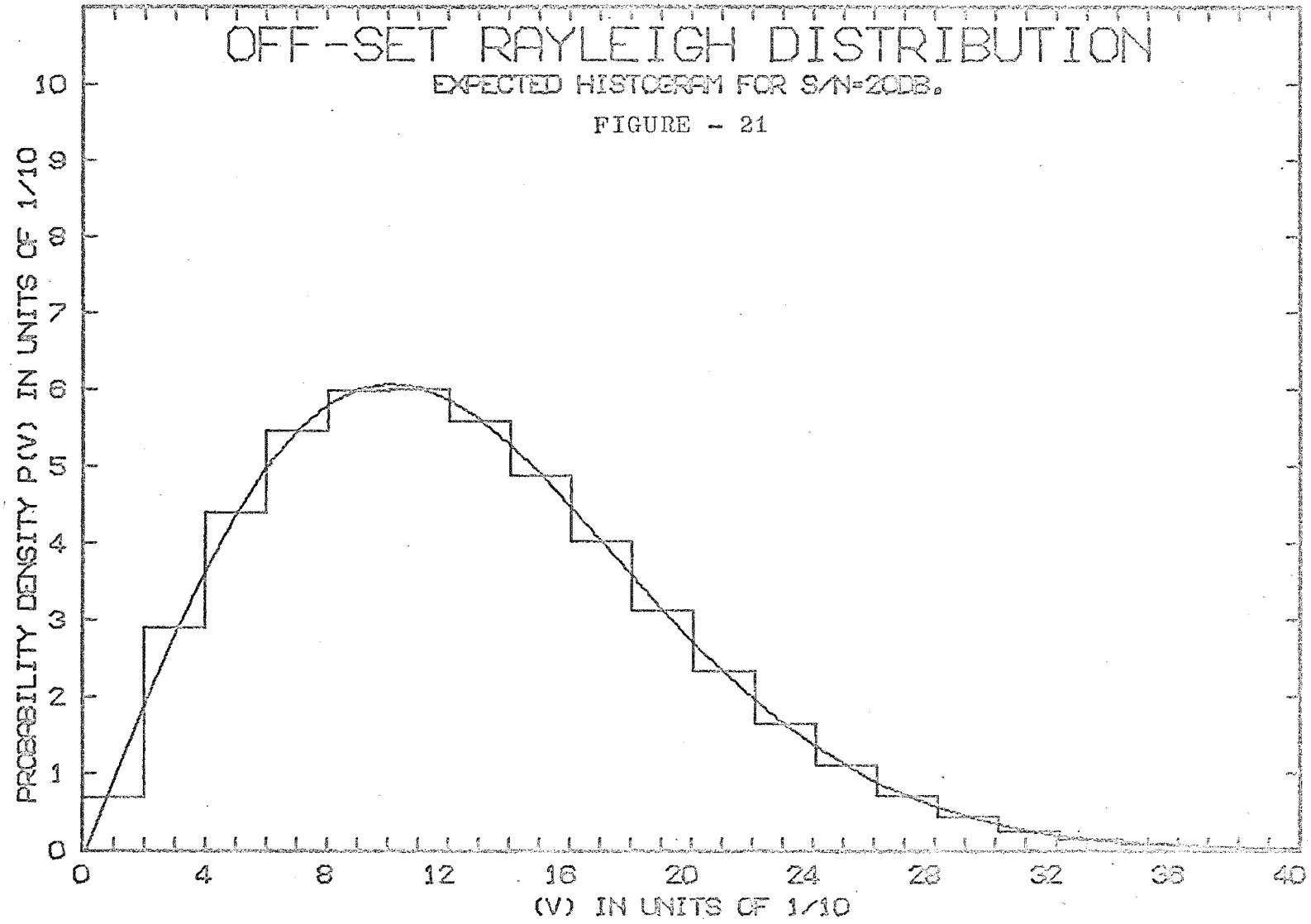
OFF-SET RAYLEIGH DISTRIBUTION
EXPECTED HISTOGRAM FOR S/N=20DB.
PROBABILITY DENSITY P(V) IN UNITS OF 1/10
0
1
2
3
4
5
6
7
8
9
10
0
4
8
12
16
20
24
28
32
36
40
(V) IN UNITS OF 1/10

FIGURE - 21

IV. EXPERIMENTAL RESULTS AND DISCUSSION OF RESULTS

The theoretical development presented earlier led to certain predictions with regard to the manifestation of the experimental results. It should prove helpful at this time to review briefly these conclusions and to state once more their implications.

In section II(2) it was shown that the argument of the complex field correlation would, in general, be greater than expected from geometrical considerations, unless the angular spectrum was randomly phased. In section II(3) it was pointed out that the presence of an undiffracted plane wave in the angular spectrum could conceivably lead to a non-linear dependence of the correlation phase on antenna separation. Under these circumstances, the implication was that the angular spectrum should be symmetrical and not randomly phased. On the other hand, a linear phase dependence on antenna separation, in addition to a plane wave, would imply an unsymmetrical angular spectrum at the scattering height. The extent of this dissymmetry was shown to depend on the magnitude of a factor Q which relates to the amount of angular correlation within the spectrum of plane waves.

For all the cases discussed in sections II(2) and II(3) it was shown that a non-randomly phased angular spectrum would give rise to a non-zero value of Q. Consequently, the value of the correlation length deduced from the magnitude of the spatial field correlation would be in error, unless the randomly phased angular spectrum requirements could be satisfied.

In the following sections, the experimental results from the program will be presented. It will be shown that these results are in accord with the theoretical predictions, and that they may be interpreted in terms of the theoretical model stipulated.

IV(1). SPATIAL FIELD CORRELATION RESULTS

The method of data collection and analysis was discussed in section III(4). Figures (22) to (27) show the results obtained from the "phase analysis program". In each of these figures, the "geometrical" slope was evaluated from the relationship

$$S_G = 180 \frac{D}{H} \quad \text{(degrees/wave length)}$$

Here D=31.4 km and represents the distance between the transmitter and the receiving antennas. H is the nominal scattering height appropriate to the particular figure, and corresponds to one-half the product of time difference between transmission and reception and the velocity of light in vacuum. The value $\frac{D}{2H}$ will be recognized as the sine of the mean geometrical zenith angle of arrival.

Calculation of the mean "experimental" slope was discussed in section III(4). The value shown represents the average of the phase difference per wave length for the six points in each figure. The phase differences indicated by the error bars in each figure represent the average value plus or minus one standard deviation of the combined (mean

FIGURE - 22

70 Km PHASE RESULTS

(18 EXPERIMENTS)

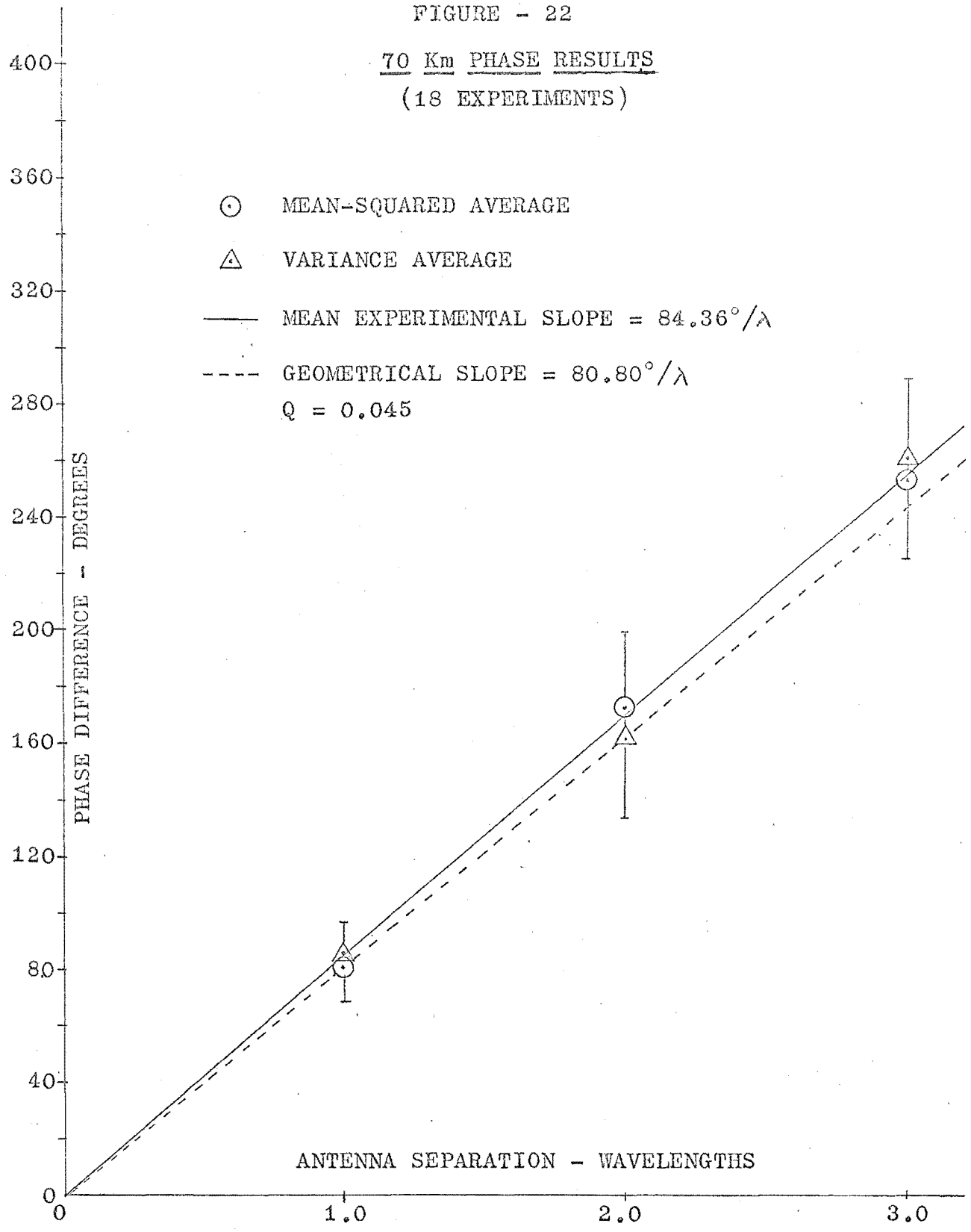

FIGURE - 23

75 Km PHASE RESULTS

(26 EXPERIMENTS)

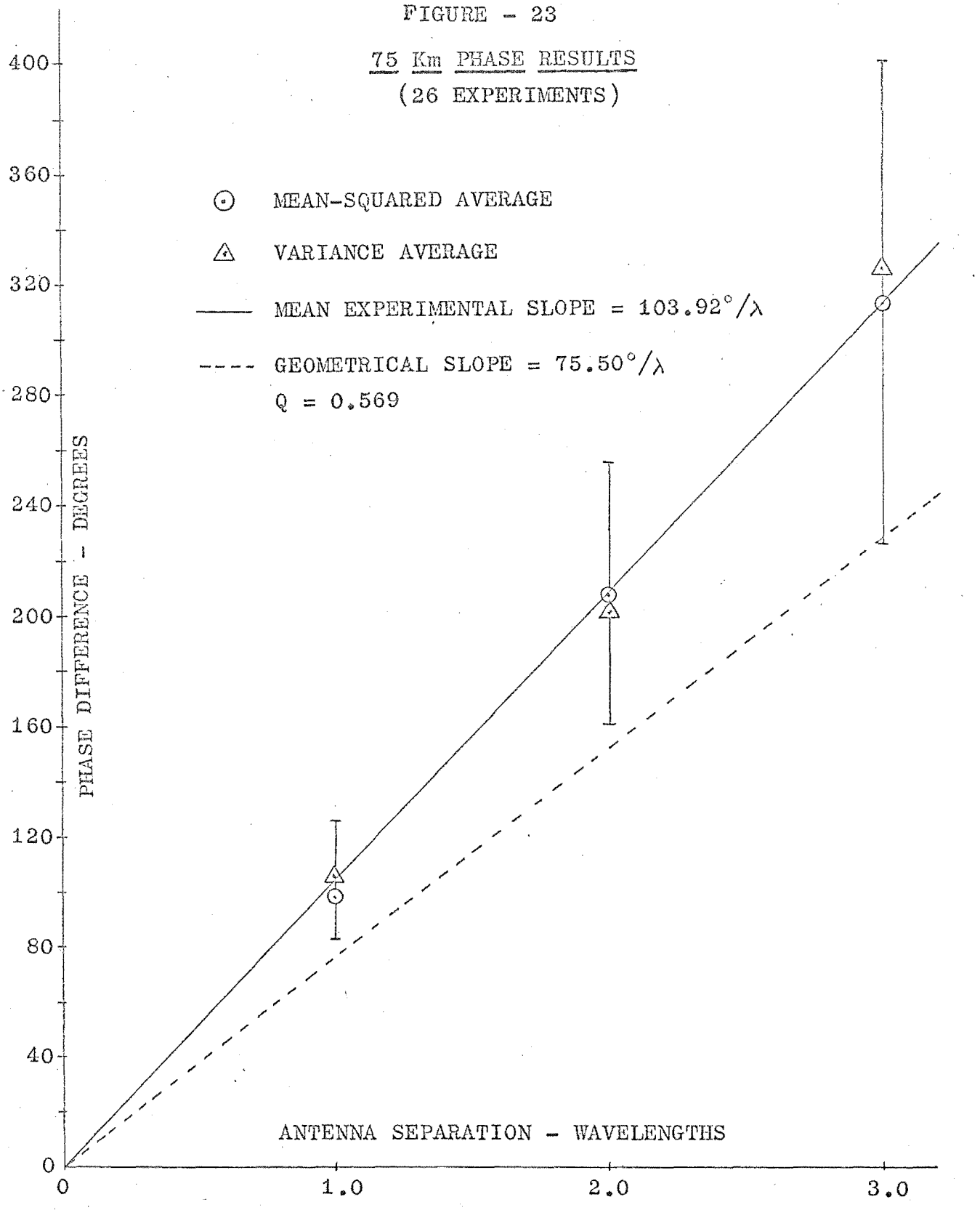

FIGURE - 24

80 Km PHASE RESULTS

(46 EXPERIMENTS)

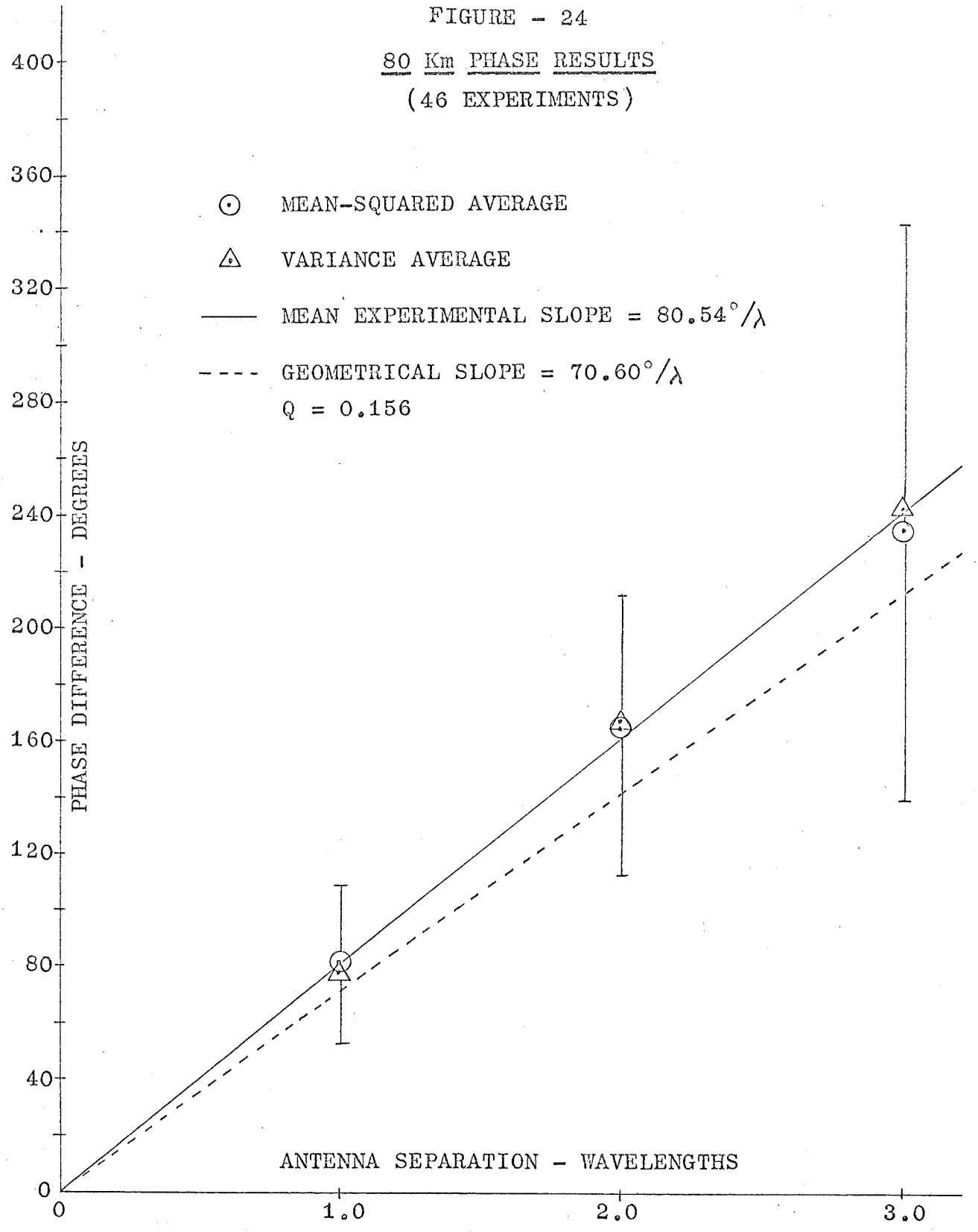

FIGURE - 25

85 Km PHASE RESULTS

(42 EXPERIMENTS)

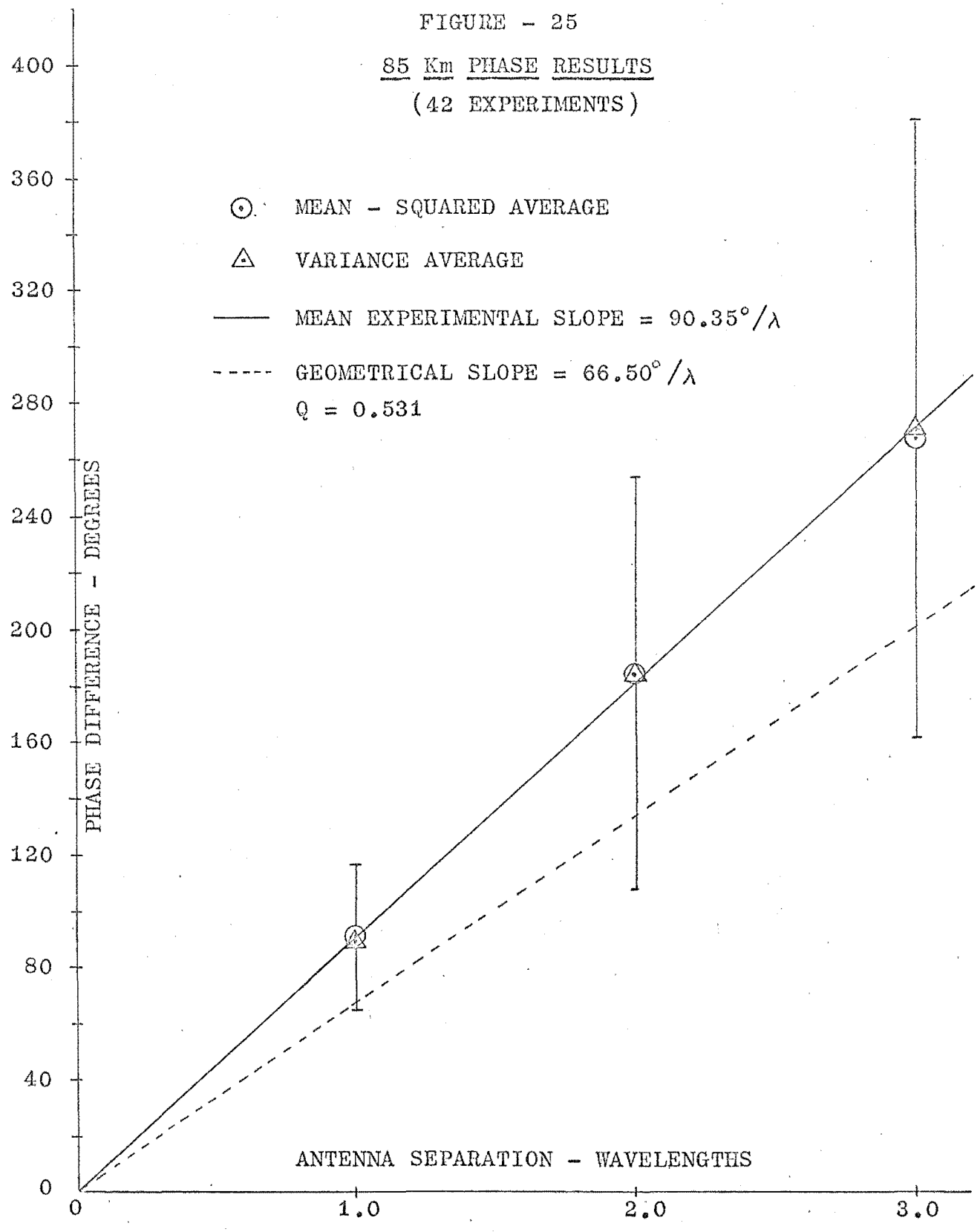

FIGURE - 26

90 Km PHASE RESULTS
(30 EXPERIMENTS)

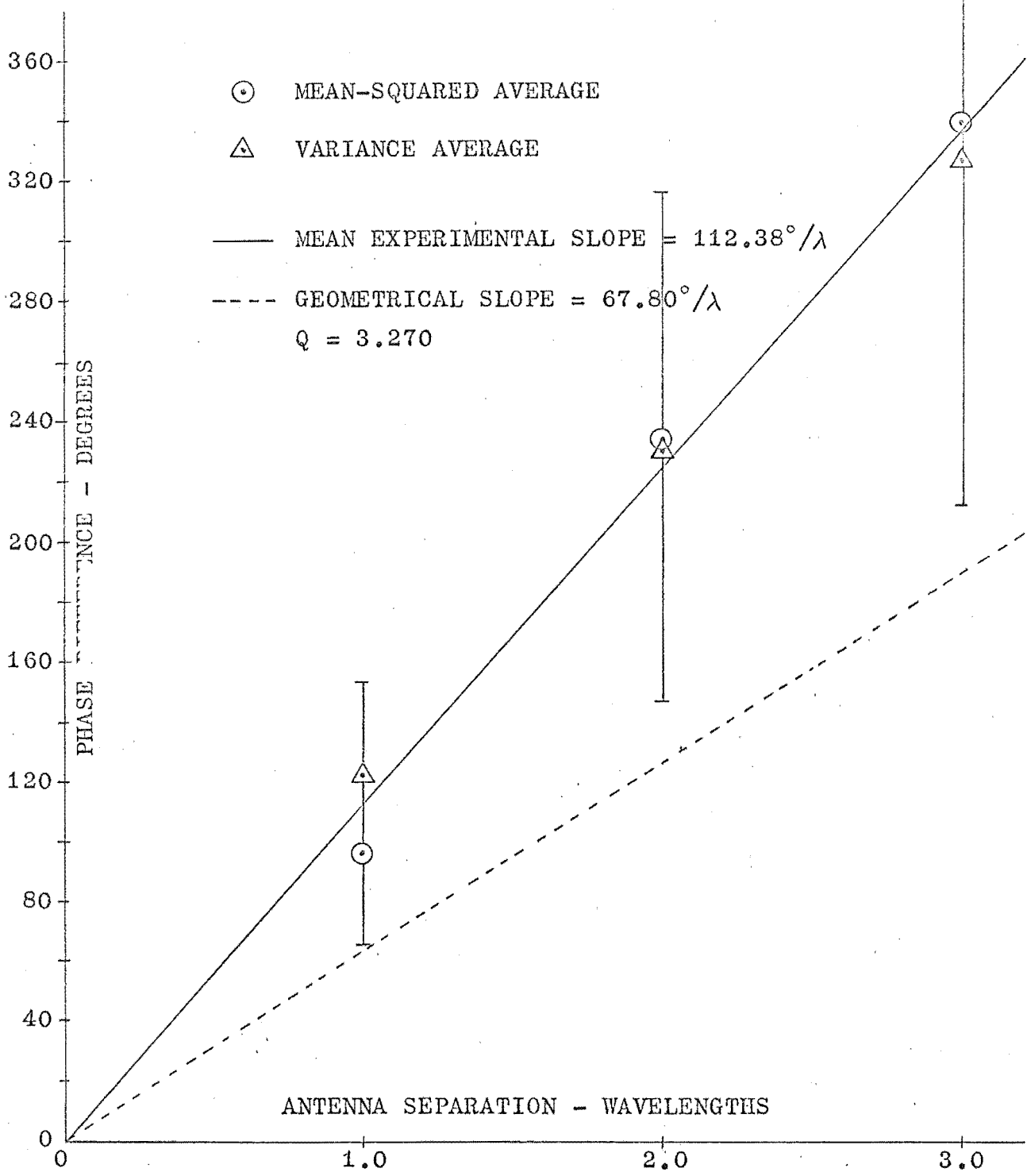

FIGURE - 27

120 Km PHASE RESULTS
(18 EXPERIMENTS)

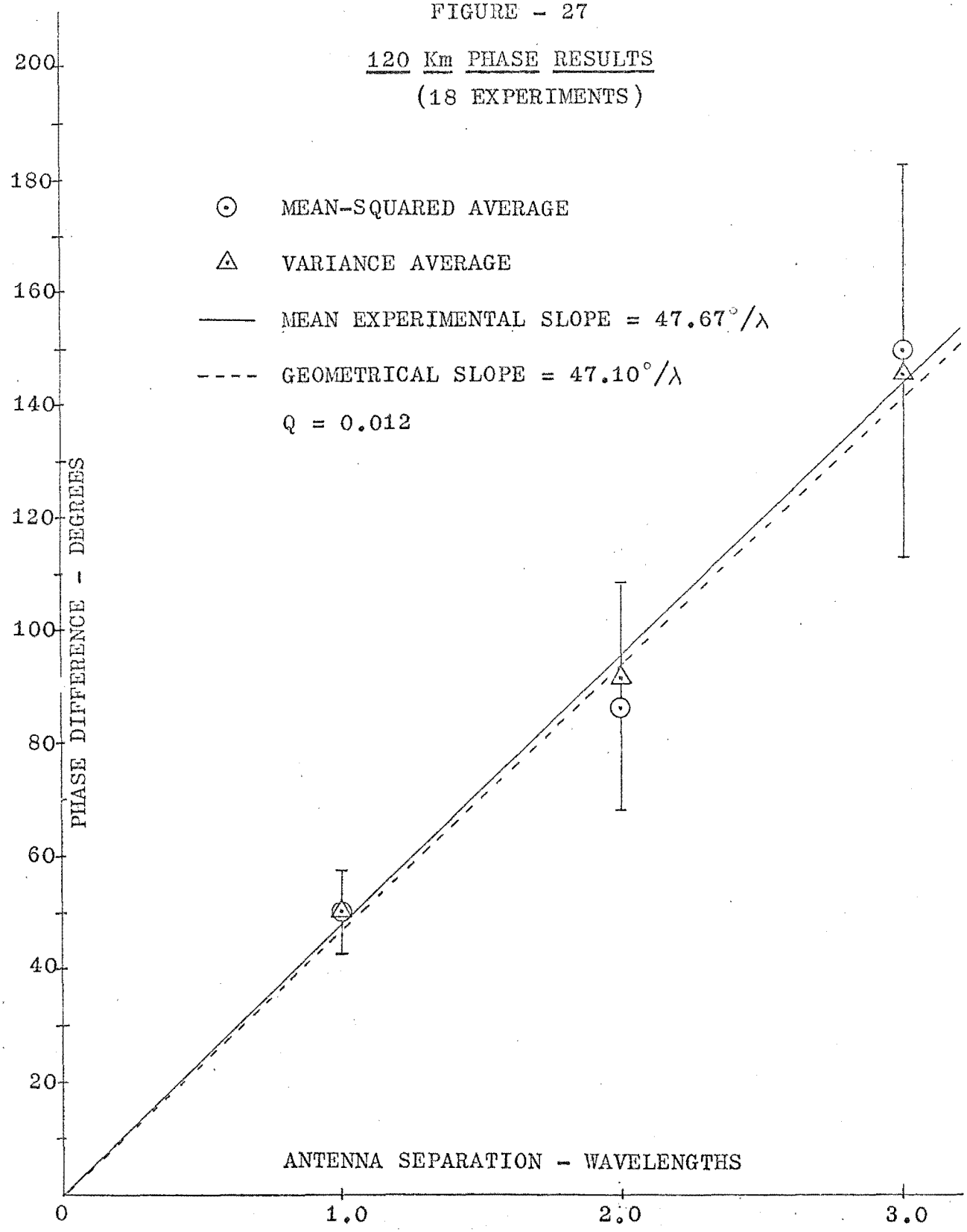

squared and variance) data.

It is clear from an inspection of the curves that the phase difference is a linear function of the antenna separation. Note also that this linear dependence seems to extend to the limits of confidence indicated by the error bars. One concludes that although the apparent angle of arrival shows considerable fluctuations on a day-to-day basis, the phase difference for each experiment was proportional to antenna spacing.

It is comparatively easy to envision the cause for the large day-to-day fluctuations in the phase slope. As an example, one might postulate "tilts" (Bramley 1953) or gravity waves (Hines 1963) in the ionospheric D-region. Under these circumstances, and in view of the large number of individual experiments performed, one would expect the mean phase-slope to coincide with the geometrical phase-slope. This conclusion is, in general, not substantiated by the phase data given in figures (22) to (27). A possible exception to this generalization can be found in figure (27) which shows the results from E-region (over-dense) reflections.

There can be little doubt that the mean experimental phase slope is consistently larger than the

expected geometrical phase slope. This result is, of course, in agreement with the theoretical predictions from equation (38b) in which the argument of the complex field correlation was shown to be

$$\phi = \frac{2\pi r}{\lambda}\left[\frac{\sin\theta_o + 2Q\tan\theta_o}{1+Q}\right] \qquad (38b)$$

Thus, on the assumption that the day-to-day phase-slope fluctuations due to gravity waves or tilts would average out to be the mean experimental slope, it is possible to compute a value for Q from equation (38b). The results are listed on the appropriate graph sheets.

From theoretical considerations, a non-zero value of Q is evidence that the angular spectrum was not randomly phased. Before the experimental results were interpreted in this light, it was deemed prudent to investigate two additional features of the experiment that might conceivably lead to a non-zero value for Q. First, consider that the experimental technique (section III-2) was developed on the assumption that a single magneto-ionic wave component is returned from the scattering volume. In reality, both magneto-ionic wave components will be present in the received signal. In Appendix B it is shown that neither the spatial field correlation

magnitude nor its phase is influenced by the simultaneous presence of the two magneto-ionic components.

A second possibility for obtaining a non-zero Q exists when the received electromagnetic energy is re-radiated by power lines, fences, or other structures in the vicinity of the antennas. To test this hypothesis, a simple experiment was conducted in which an additional dipole antenna was erected midway between the 2λ spaced antennas. (See figure 28). This new antenna configuration yielded three different 1λ spacings and 2 different 2λ spacings. The phase difference results obtained from four consecutive 8-minute experiments are presented in figure (28). No effort was made to fit these data points to a straight line; the only purpose of this illustration is to show the extent to which the data points agree with one another when different baseline configurations were used. Similar results were obtained from tests for the other scattering heights.

From the space diversity tests and from the results of Appendix B one may conclude that the observed non-zero value of Q was not due to "sighting" errors nor to the simultaneous presence of both magneto-ionic modes. The only remaining explanation is that the magnitude of angular correlation in the

FIGURE - 28

SPACE DIVERSITY

115 Km PHASE RESULTS

4 CONSECUTIVE 8 - MINUTE EXPERIMENTS
CONDUCTED ON 13 DECEMBER, 1969.

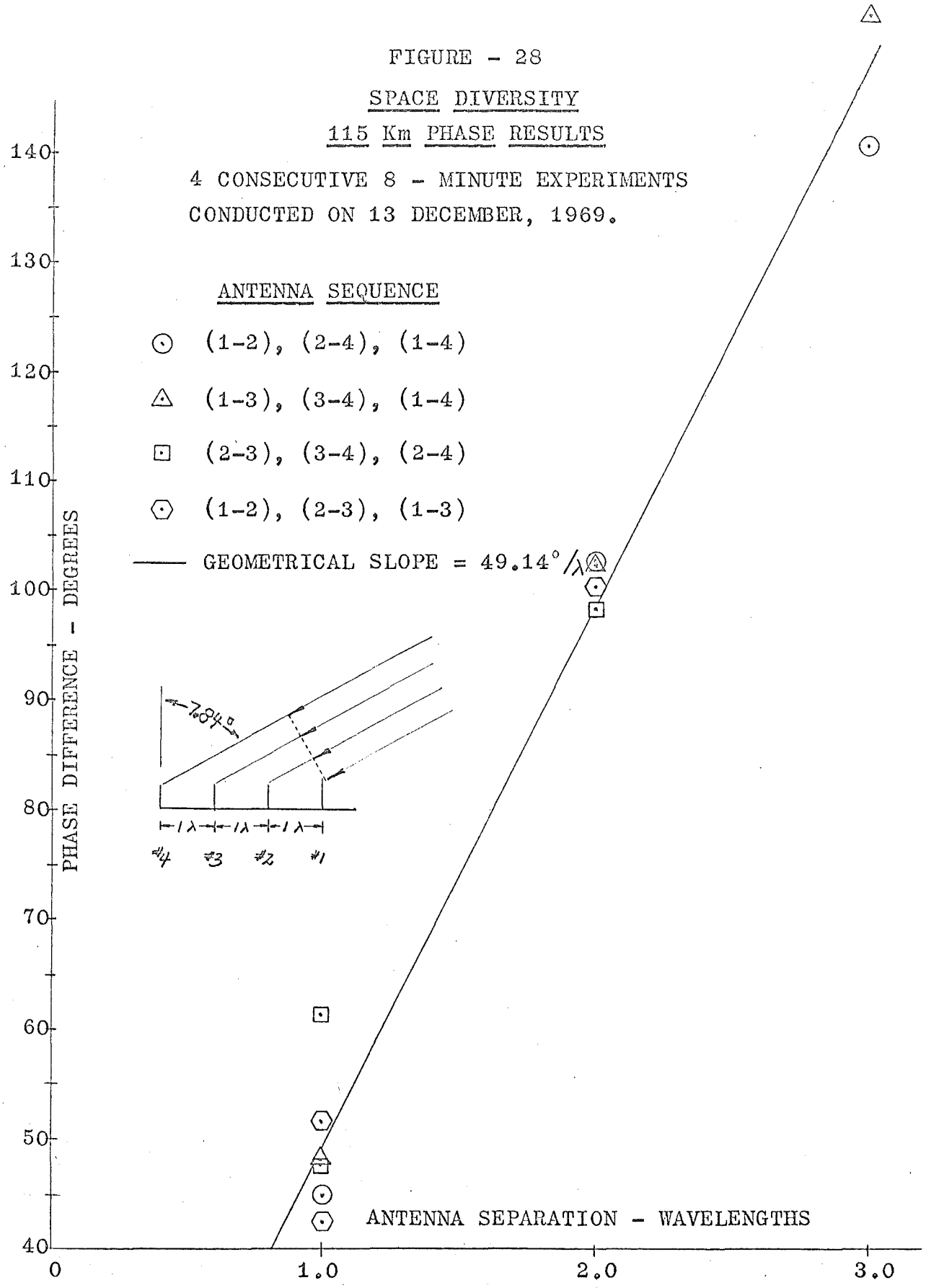

spectrum of plane waves was not zero. However, it might be advantageous to adopt at this time a more qualitative criterion for determining whether the angular spectrum was randomly phased. One could argue that if the mean experimental phase slope agreed "reasonably" well with the geometrical phase slope, then there would be cause to assume that the angular spectrum was randomly phased. On this basis, the results from 70 km, 80 km, and 120 km suggest that, on the average, the angular spectrum might have been randomly phased. For echoes from 75 km, 85 km, and particularly 90 km, there is evidence to show that, on the average, the angular spectrum was not randomly phased.

The results from the correlation fit routine are presented in figures (29) to (34). It will be noted that each of these figures contains two separate graphs: the first of these shows the distribution of the correlation "length" L from individual curve fits, while in the second graph the fit to the average (mean squared and variance) data is presented. The error bars indicate the combined data standard deviation from the mean value.

It is evident from the data shown in figures (29) to (34) that the magnitude of the spatial field

FIGURE - 29

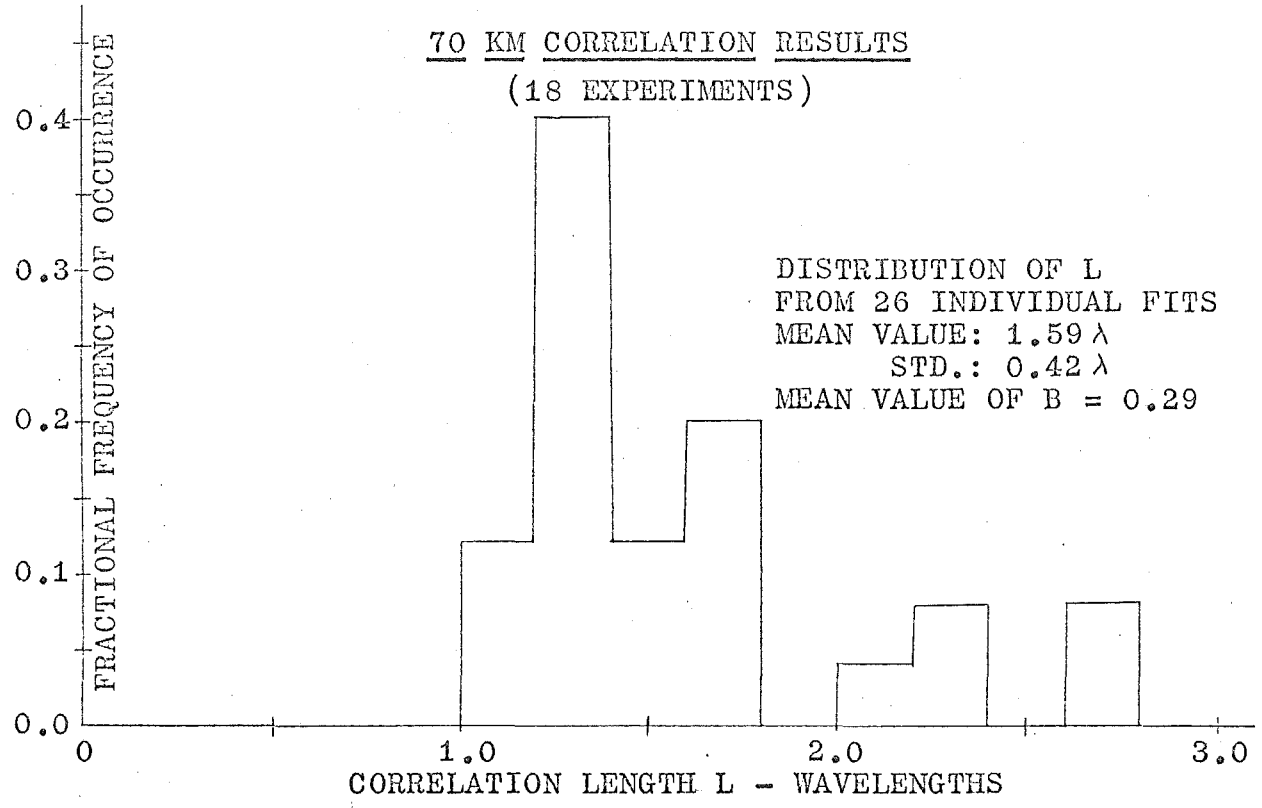
70 KM CORRELATION RESULTS
(18 EXPERIMENTS)
FRACTIONAL FREQUENCY OF OCCURRENCE
0.0
0.1
0.2
0.3
0.4
DISTRIBUTION OF L
FROM 26 INDIVIDUAL FITS
MEAN VALUE: 1.59 λ
STD.: 0.42 λ
MEAN VALUE OF B = 0.29
0
1.0
2.0
3.0
CORRELATION LENGTH L - WAVELENGTHS

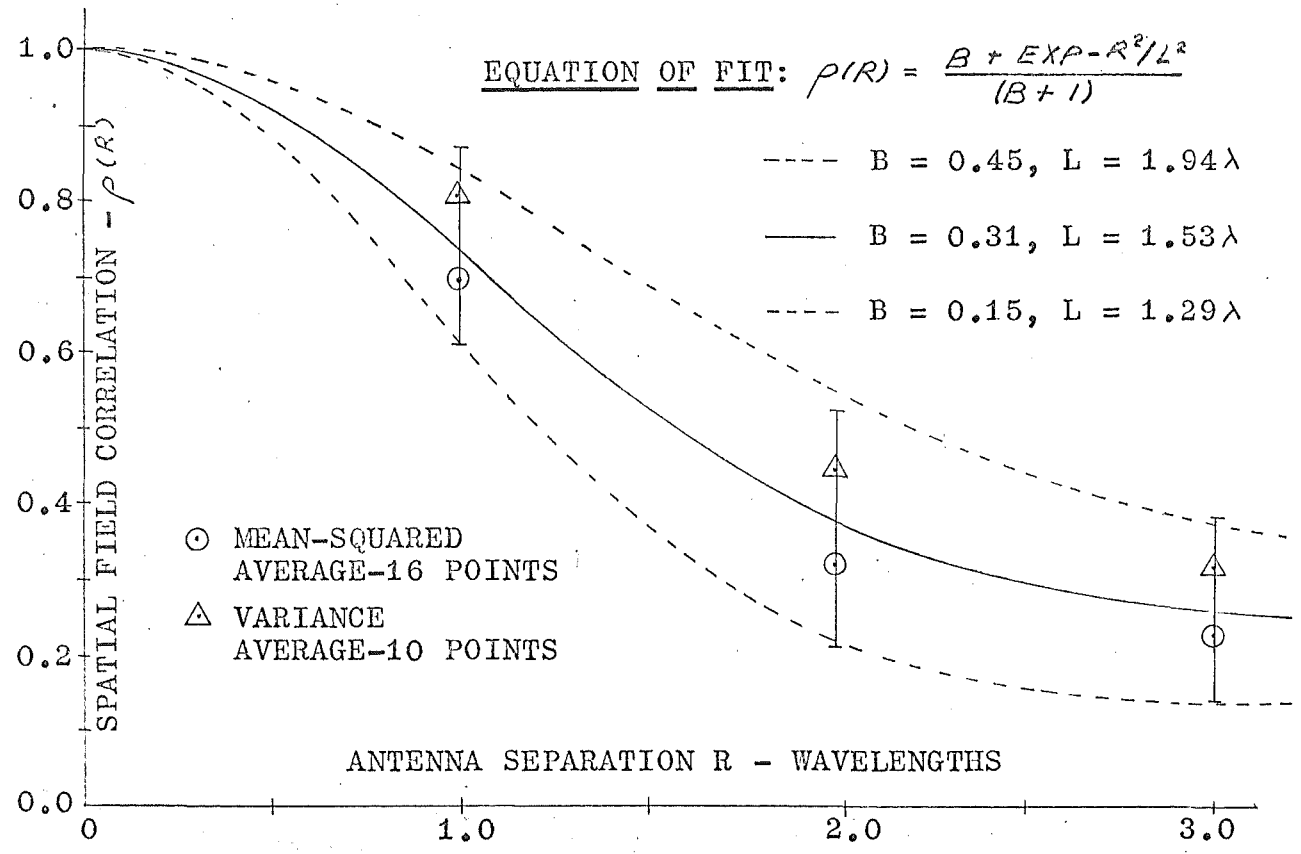
EQUATION OF FIT: ρ(R) = (B + EXP-R²/L²) / (B + 1)
---- B = 0.45, L = 1.94λ
—— B = 0.31, L = 1.53λ
---- B = 0.15, L = 1.29λ
SPATIAL FIELD CORRELATION - ρ(R)
0.0
0.2
0.4
0.6
0.8
1.0
⊙ MEAN-SQUARED
AVERAGE-16 POINTS
△ VARIANCE
AVERAGE-10 POINTS
ANTENNA SEPARATION R - WAVELENGTHS
0
1.0
2.0
3.0

FIGURE - 30

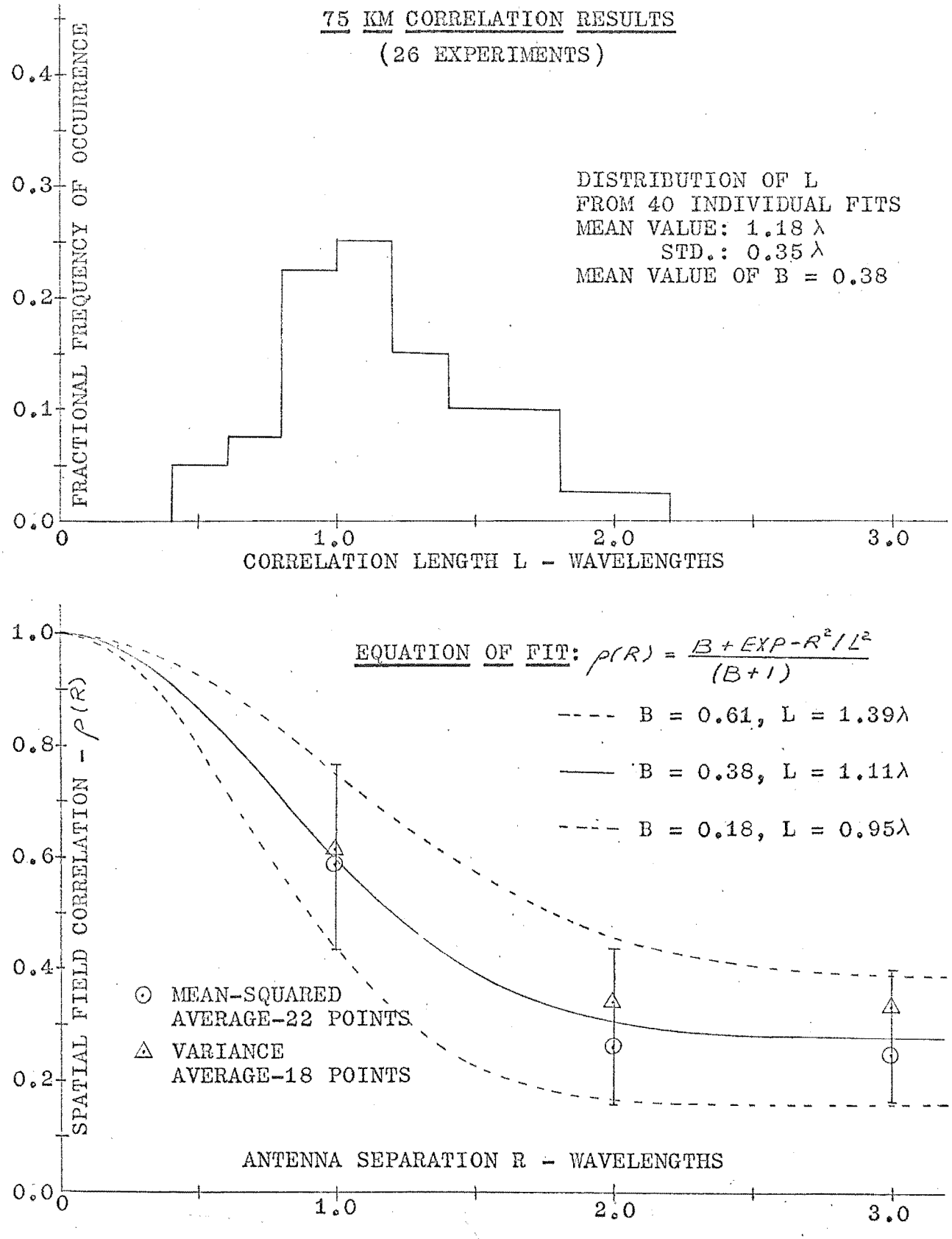
75 KM CORRELATION RESULTS
(26 EXPERIMENTS)
FRACTIONAL FREQUENCY OF OCCURRENCE
0.0
0.1
0.2
0.3
0.4
DISTRIBUTION OF L
FROM 40 INDIVIDUAL FITS
MEAN VALUE: 1.18 λ
STD.: 0.35 λ
MEAN VALUE OF B = 0.38
0
1.0
2.0
3.0
CORRELATION LENGTH L - WAVELENGTHS
SPATIAL FIELD CORRELATION - ρ(R)
0.0
0.2
0.4
0.6
0.8
1.0
EQUATION OF FIT: ρ(R) = (B + EXP-R²/L²)/(B+1)
---- B = 0.61, L = 1.39λ
—— B = 0.38, L = 1.11λ
---- B = 0.18, L = 0.95λ
⊙ MEAN-SQUARED
AVERAGE-22 POINTS
△ VARIANCE
AVERAGE-18 POINTS
ANTENNA SEPARATION R - WAVELENGTHS
0
1.0
2.0
3.0

FIGURE - 31

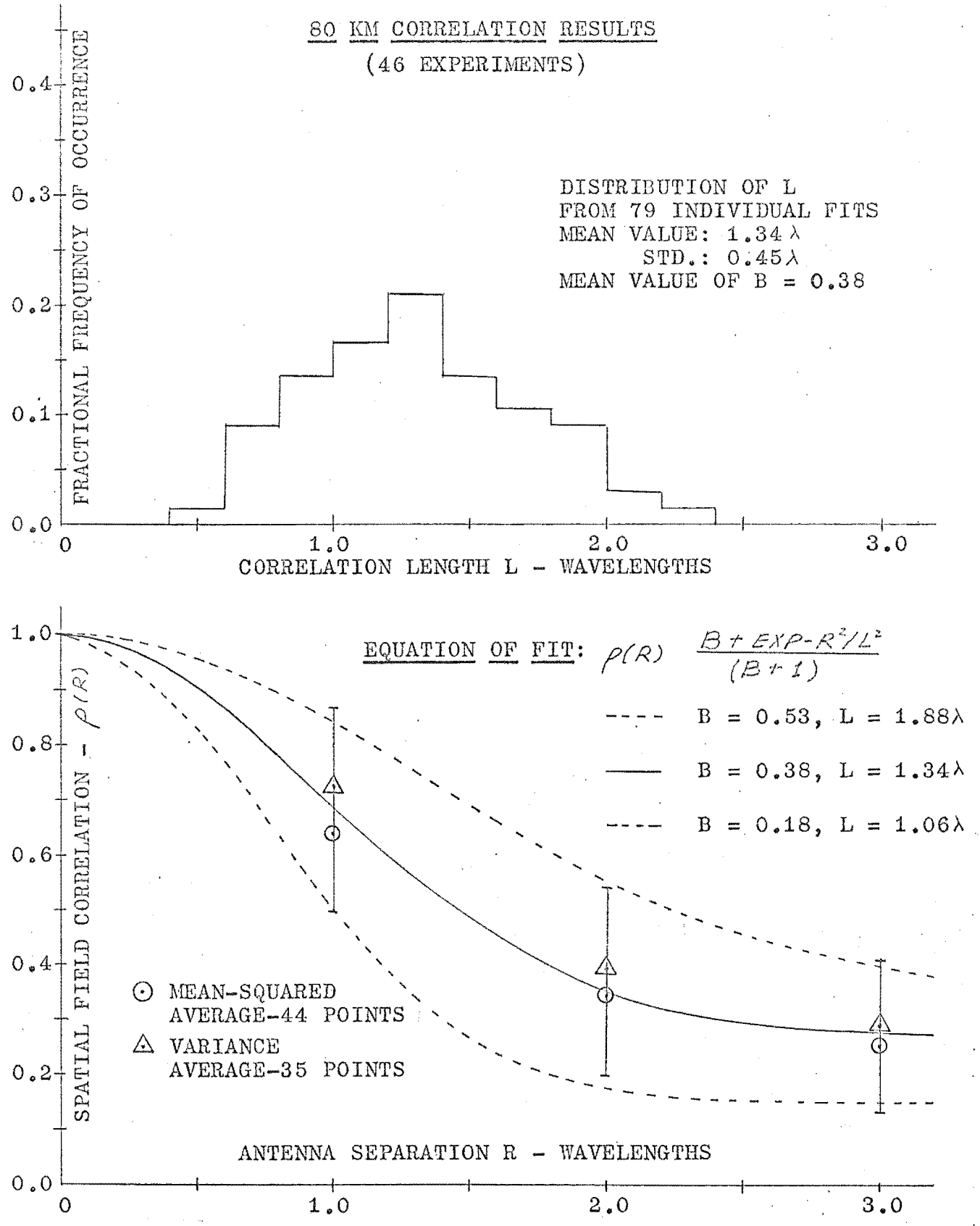
80 KM CORRELATION RESULTS
(46 EXPERIMENTS)
DISTRIBUTION OF L
FROM 79 INDIVIDUAL FITS
MEAN VALUE: 1.34 λ
STD.: 0.45λ
MEAN VALUE OF B = 0.38
FRACTIONAL FREQUENCY OF OCCURRENCE
0.0
0.1
0.2
0.3
0.4
0
1.0
2.0
3.0
CORRELATION LENGTH L - WAVELENGTHS
EQUATION OF FIT: ρ(R) (B + EXP-R²/L²)/(B + 1)
B = 0.53, L = 1.88λ
B = 0.38, L = 1.34λ
B = 0.18, L = 1.06λ
SPATIAL FIELD CORRELATION - ρ(R)
MEAN-SQUARED
AVERAGE-44 POINTS
VARIANCE
AVERAGE-35 POINTS
ANTENNA SEPARATION R - WAVELENGTHS

FIGURE - 32

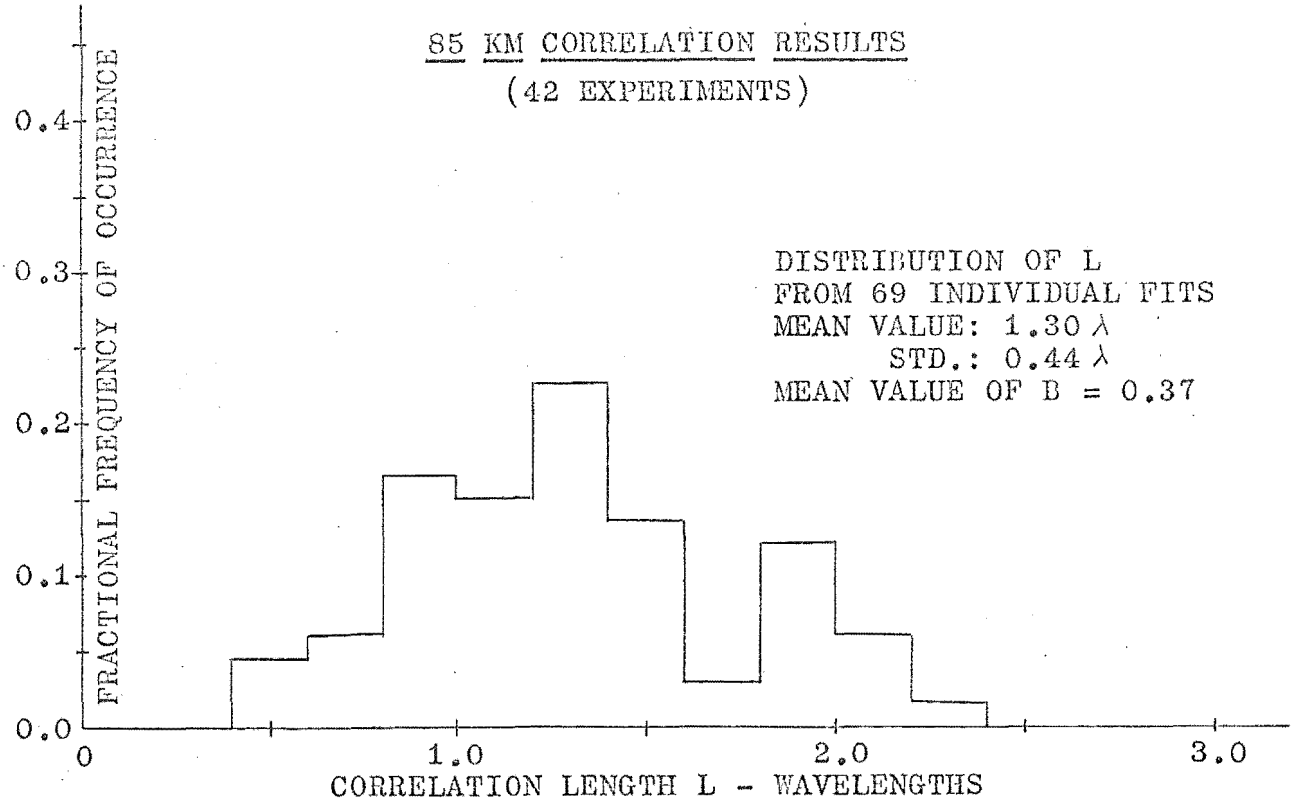
85 KM CORRELATION RESULTS
(42 EXPERIMENTS)
DISTRIBUTION OF L
FROM 69 INDIVIDUAL FITS
MEAN VALUE: 1.30 λ
STD.: 0.44 λ
MEAN VALUE OF B = 0.37
FRACTIONAL FREQUENCY OF OCCURRENCE
0.0
0.1
0.2
0.3
0.4
0
1.0
2.0
3.0
CORRELATION LENGTH L - WAVELENGTHS

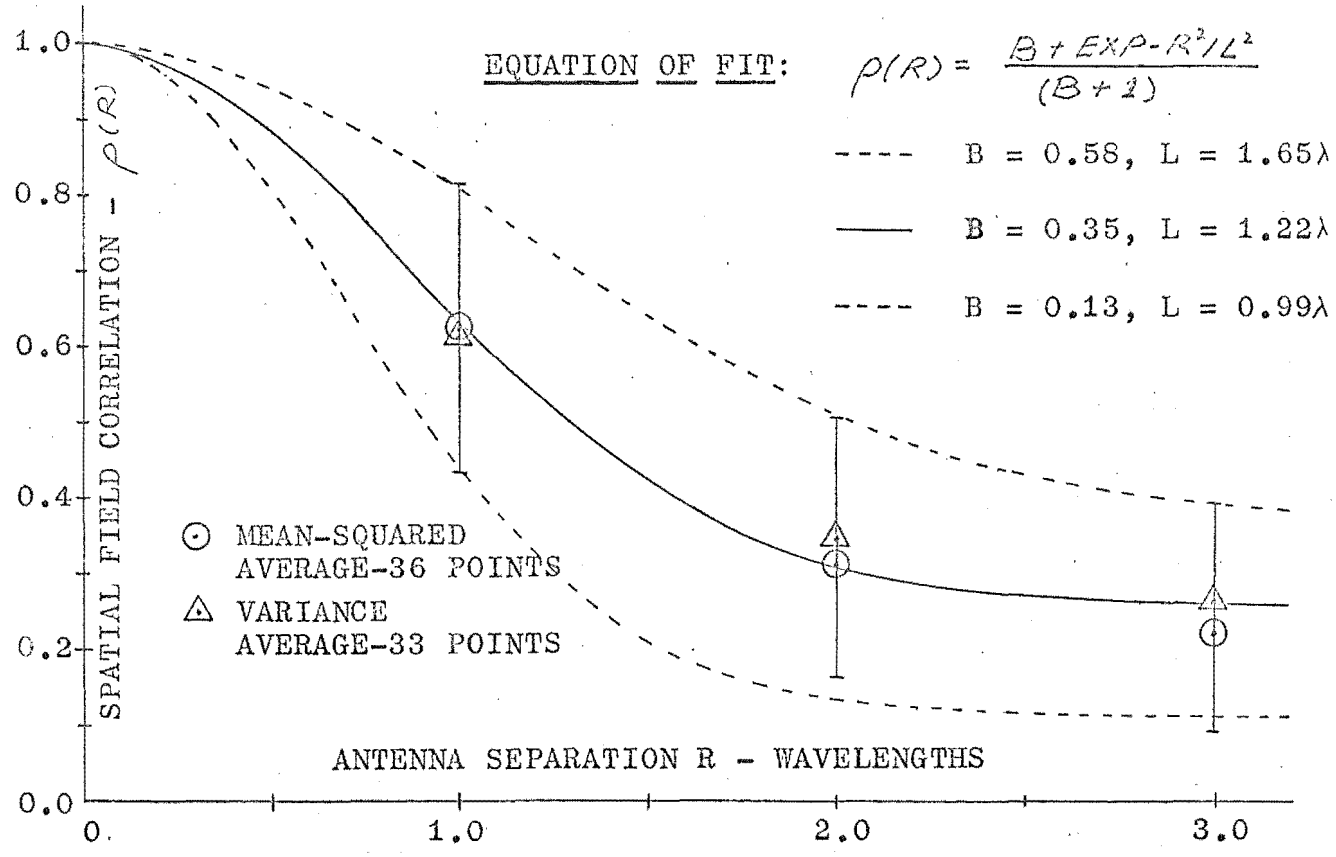
EQUATION OF FIT: ρ(R) = (B + EXP-R²/L²) / (B + 1)
---- B = 0.58, L = 1.65λ
—— B = 0.35, L = 1.22λ
---- B = 0.13, L = 0.99λ
SPATIAL FIELD CORRELATION - ρ(R)
⊙ MEAN-SQUARED AVERAGE-36 POINTS
△ VARIANCE AVERAGE-33 POINTS
ANTENNA SEPARATION R - WAVELENGTHS
0.0
0.2
0.4
0.6
0.8
1.0
0.
1.0
2.0
3.0

FIGURE - 33

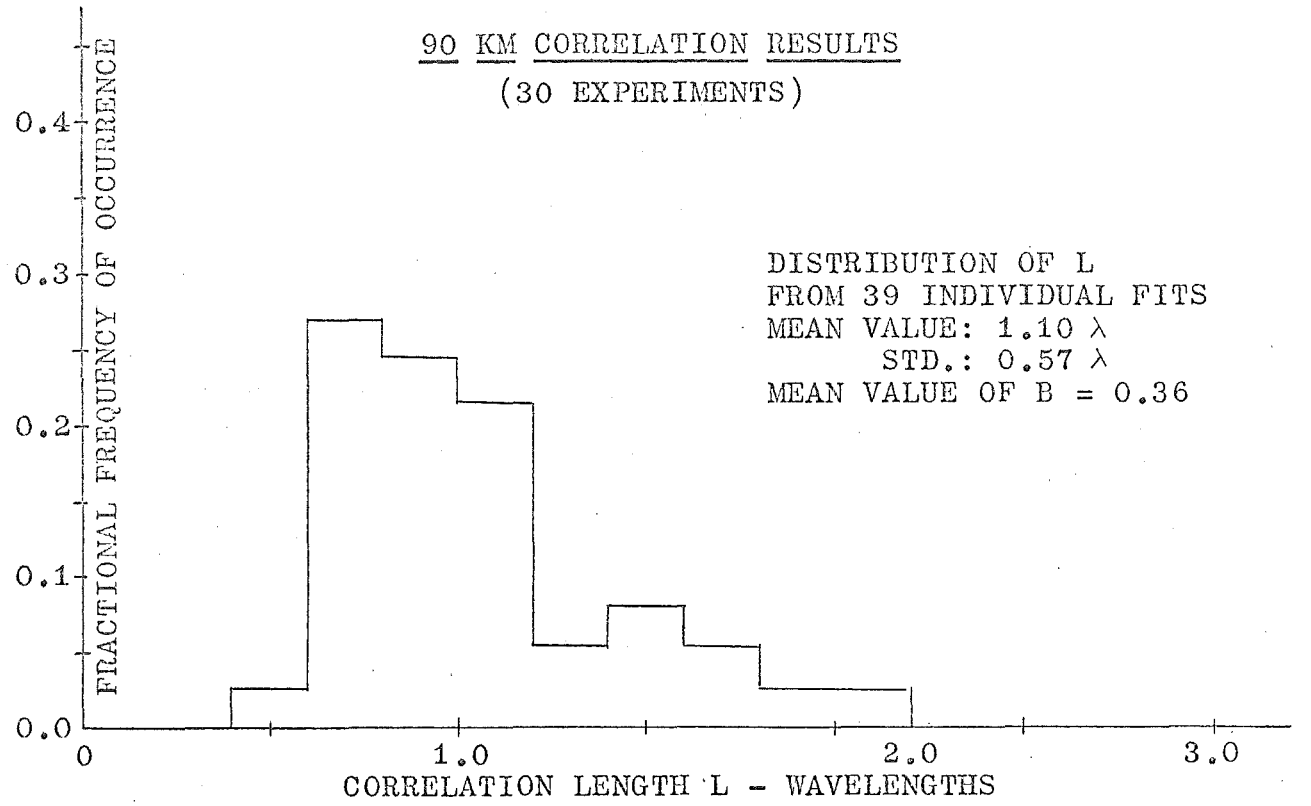
90 KM CORRELATION RESULTS
(30 EXPERIMENTS)
DISTRIBUTION OF L
FROM 39 INDIVIDUAL FITS
MEAN VALUE: 1.10 λ
STD.: 0.57 λ
MEAN VALUE OF B = 0.36
FRACTIONAL FREQUENCY OF OCCURRENCE
0.0
0.1
0.2
0.3
0.4
0
1.0
2.0
3.0
CORRELATION LENGTH L - WAVELENGTHS

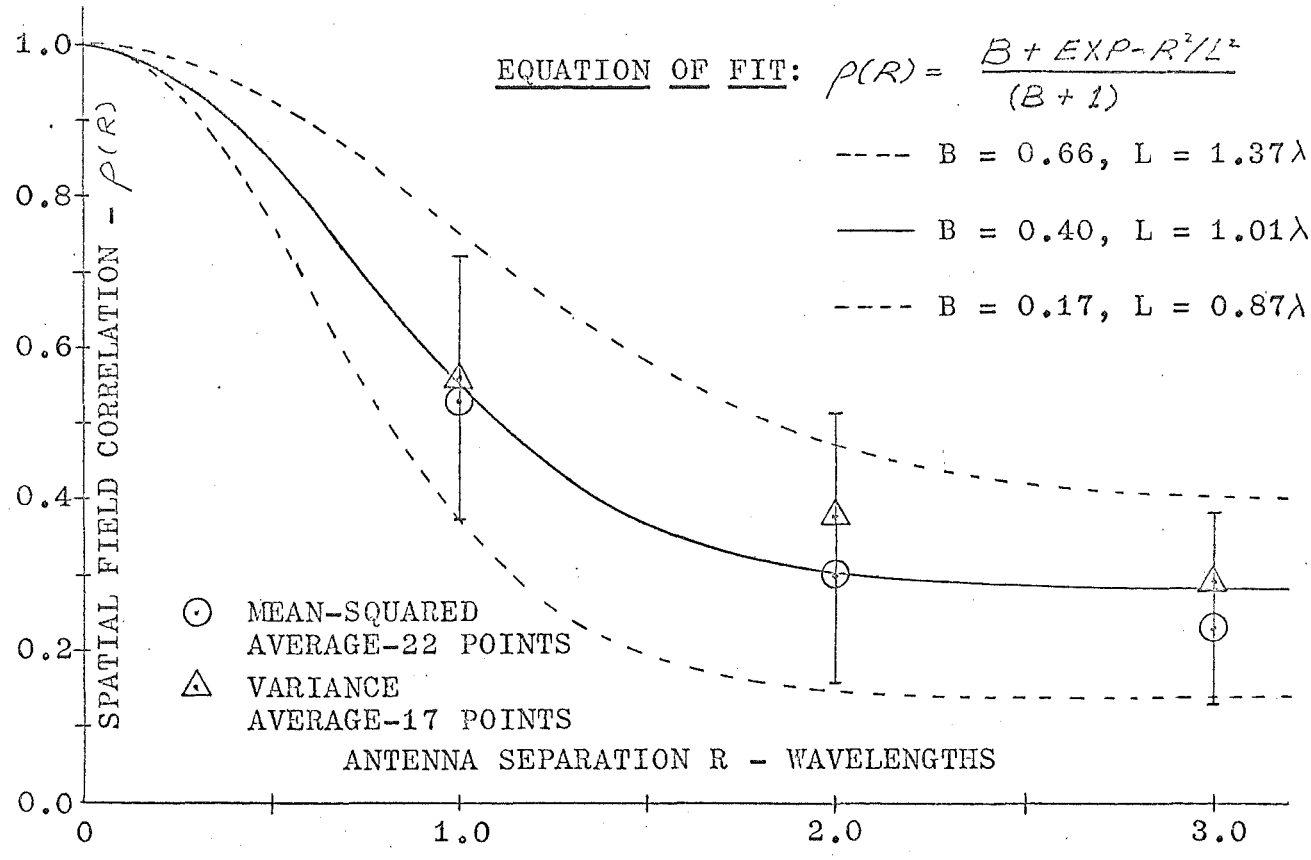
EQUATION OF FIT: ρ(R) = (B + EXP-R²/L²) / (B + 1)
---- B = 0.66, L = 1.37λ
—— B = 0.40, L = 1.01λ
---- B = 0.17, L = 0.87λ
SPATIAL FIELD CORRELATION - ρ(R)
⊙ MEAN-SQUARED
AVERAGE-22 POINTS
△ VARIANCE
AVERAGE-17 POINTS
ANTENNA SEPARATION R - WAVELENGTHS
0.0
0.2
0.4
0.6
0.8
1.0
0
1.0
2.0
3.0

FIGURE - 34

120 KM CORRELATION RESULTS
(18 EXPERIMENTS)

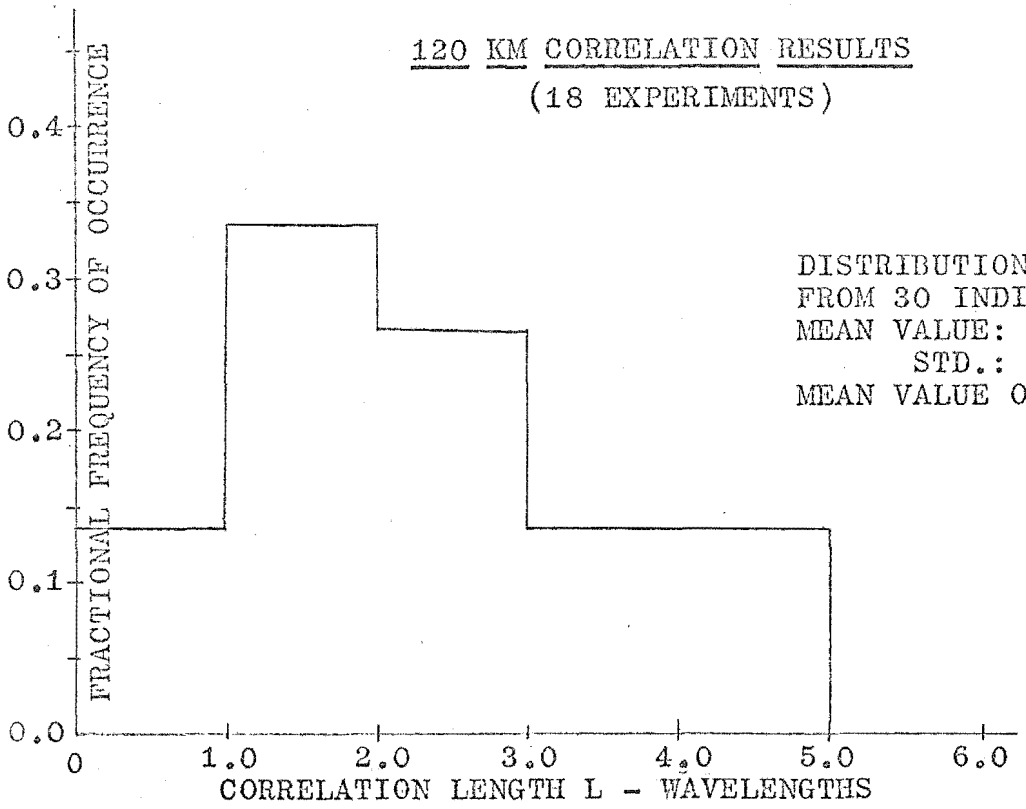

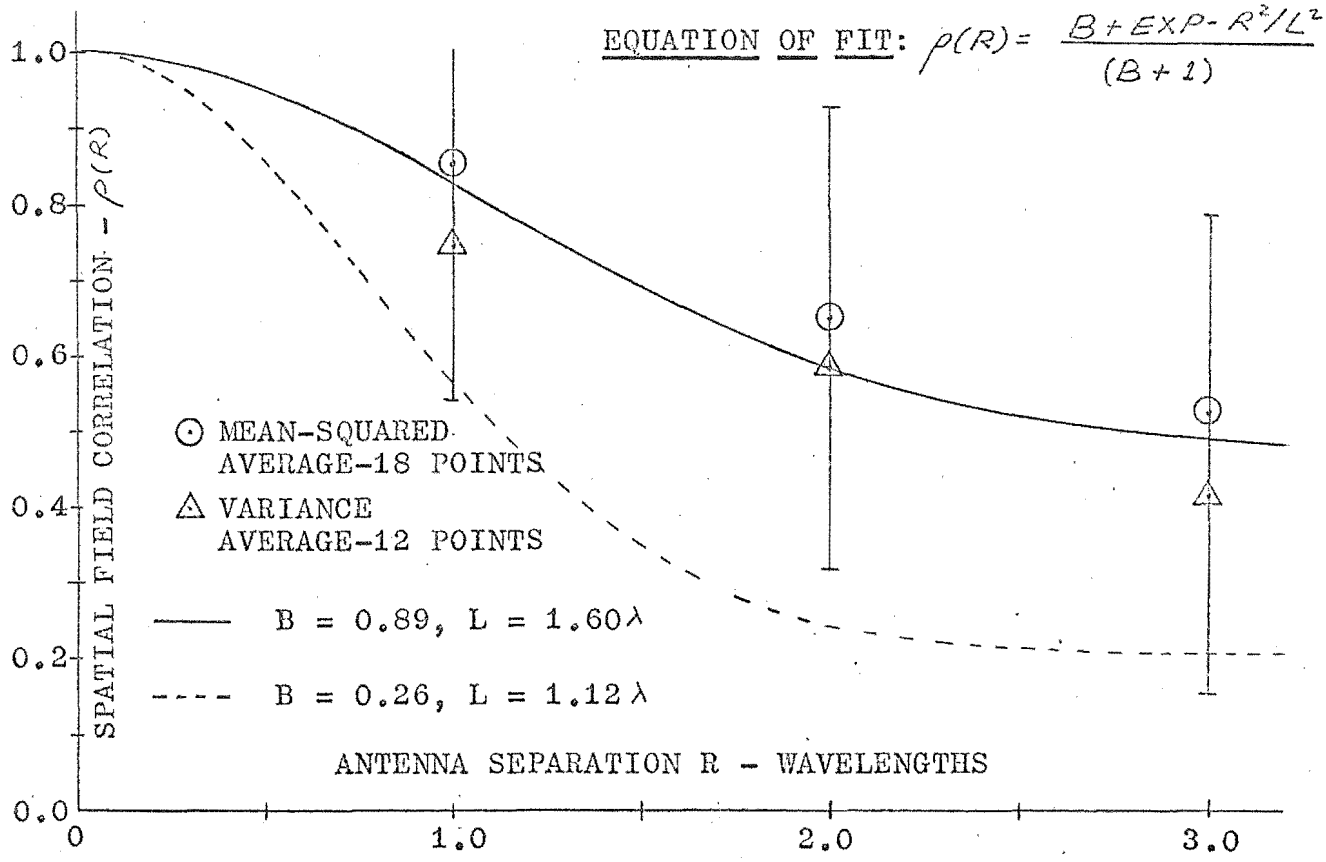

correlation contains the constant component which was predicted from the discussion in section II(3). It also appears from the "mean fit" and from the average of individual fits, that the value of B is approximately the same for all of the D-region heights considered here. A general conclusion from these results is that there exists a plane undiffracted wave in the angular spectrum of D-region echoes, and that approximately 25% of the total power returned from a given scattering height must be associated with this plane wave. The remainder of the total power is contained in a continuous angular spectrum of plane waves.

It was shown earlier that the argument of the spatial field correlation was proportional to the antenna separation. Consequently, the angular power spectrum as received by the three antennas was symmetrical about some angle of arrival. It is, therefore, possible to compute the cone angle in which the scattered power, as well as the power due to the undiffracted wave, must be contained. This computation was carried out, and the results are plotted in figure (35). Also shown in figure (35) is a table which is intended to summarize the overall results from the correlation experiment. The difference between L and ℓ should be noted in particular:

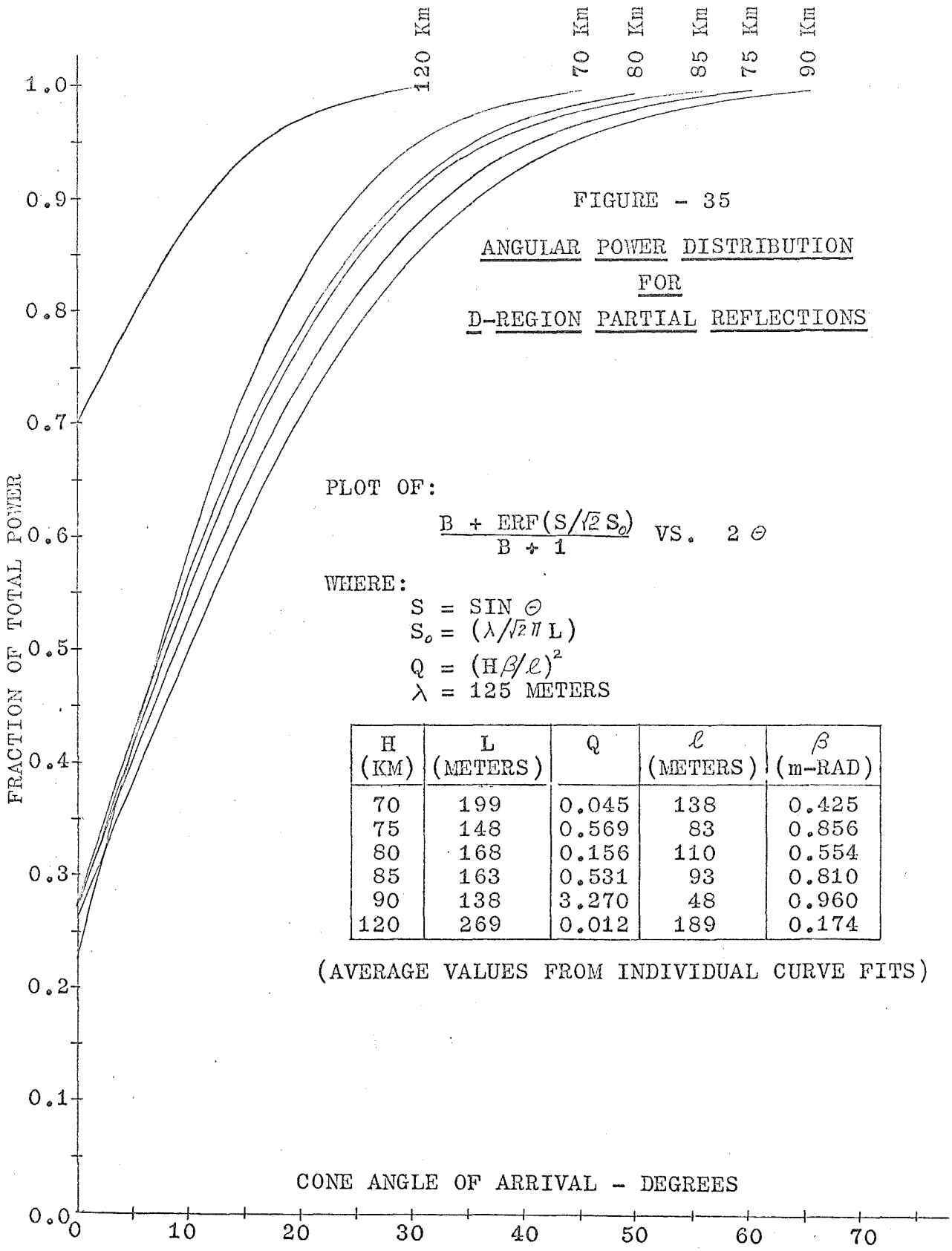

FIGURE - 35

ANGULAR POWER DISTRIBUTION

FOR

D-REGION PARTIAL REFLECTIONS

PLOT OF:

$$\frac{B + ERF(S/\sqrt{2}\,S_o)}{B + 1} \quad VS. \quad 2\Theta$$

WHERE:

$S = SIN\ \Theta$

$S_o = (\lambda/\sqrt{2}\,\pi L)$

$Q = (H\beta/\ell)^2$

$\lambda = 125$ METERS

H (KM)	L (METERS)	Q	ℓ (METERS)	β (m-RAD)
70	199	0.045	138	0.425
75	148	0.569	83	0.856
80	168	0.156	110	0.554
85	163	0.531	93	0.810
90	138	3.270	48	0.960
120	269	0.012	189	0.174

(AVERAGE VALUES FROM INDIVIDUAL CURVE FITS)

L is the spatial separation of antennas which will cause the magnitude of the correlation (of the scattered waves) to decrease to e^{-1}, while ℓ is the correlation "size" of the irregularities in the scattering screen. If Q were identically equal to zero, then $\frac{L}{\ell}$ would be equal to $\sqrt{2}$.

An attempt was made to compare the results from the field correlation experiment with results obtained from a separately conducted amplitude correlation experiment. Unfortunately, it was not possible to obtain "zero time-lag" correlation data with the existing experimental equipment. Consequently, these values had to be inferred from four positive time-lags and four negative time-lags for each of the three available antenna spacings. Three such experiments were conducted for each of the scattering heights treated earlier. In an effort to deduce the zero time-lag amplitude correlation as well as to gain some insight into the general trend of the amplitude correlation as a function of lag-time, the 8 data points for each baseline were fitted with a fourth order polynomial. Since the auto-correlation function has to be symmetrical about the zero time-lag position, the 8 auto-correlation points were fitted with a fourth order polynomial in τ^2, where τ

is the lag time. (Data for the auto-correlation were obtained to a maximum lag-time of 4 seconds). Although it is recognized that a least squares polynomial fit has some rather undesirable features, in this application as a "data filter", the results were quite satisfactory. However, not all of the data obtained could be fitted by this process. Those curves for which the r.m.s. departure of data points from the fit was less than 0.1 are presented in the following figures.

It will be noted that in many instances no sensible zero time-lag correlation could be obtained when data from all three baseline lengths are considered simultaneously. By using only the 1λ and 2λ baseline data, it appears that the zero time-lag correlation decreases exponentially with antenna separation for D-region scattering heights. The results for 120 km, on the other hand, suggest that the decrease with antenna separation is gaussian. This finding appears to be in agreement with the results of Fraser and Vincent (1968). However, the results of three experiments for each height can hardly be considered as conclusive evidence in support of their results.

It is interesting to note that the magnitudes of the spatial correlation distance from the amplitude

FIGURE - 36

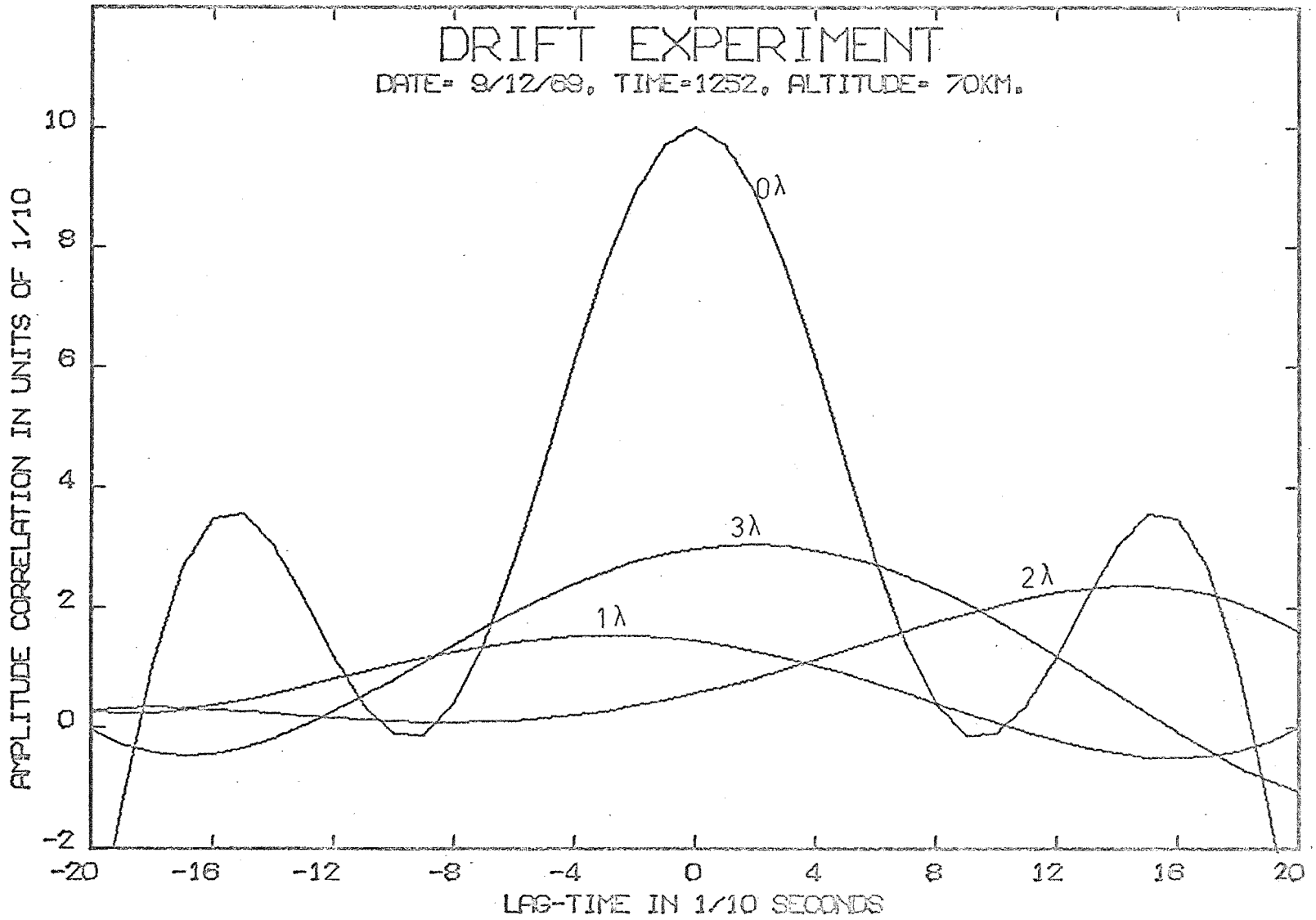
DRIFT EXPERIMENT
DATE= 8/12/69, TIME=1252, ALTITUDE= 70KM.
AMPLITUDE CORRELATION IN UNITS OF 1/10
10
8
6
4
2
0
-2
0λ
1λ
2λ
3λ
-20
-16
-12
-8
-4
0
4
8
12
16
20
LAG-TIME IN 1/10 SECONDS

FIGURE - 37

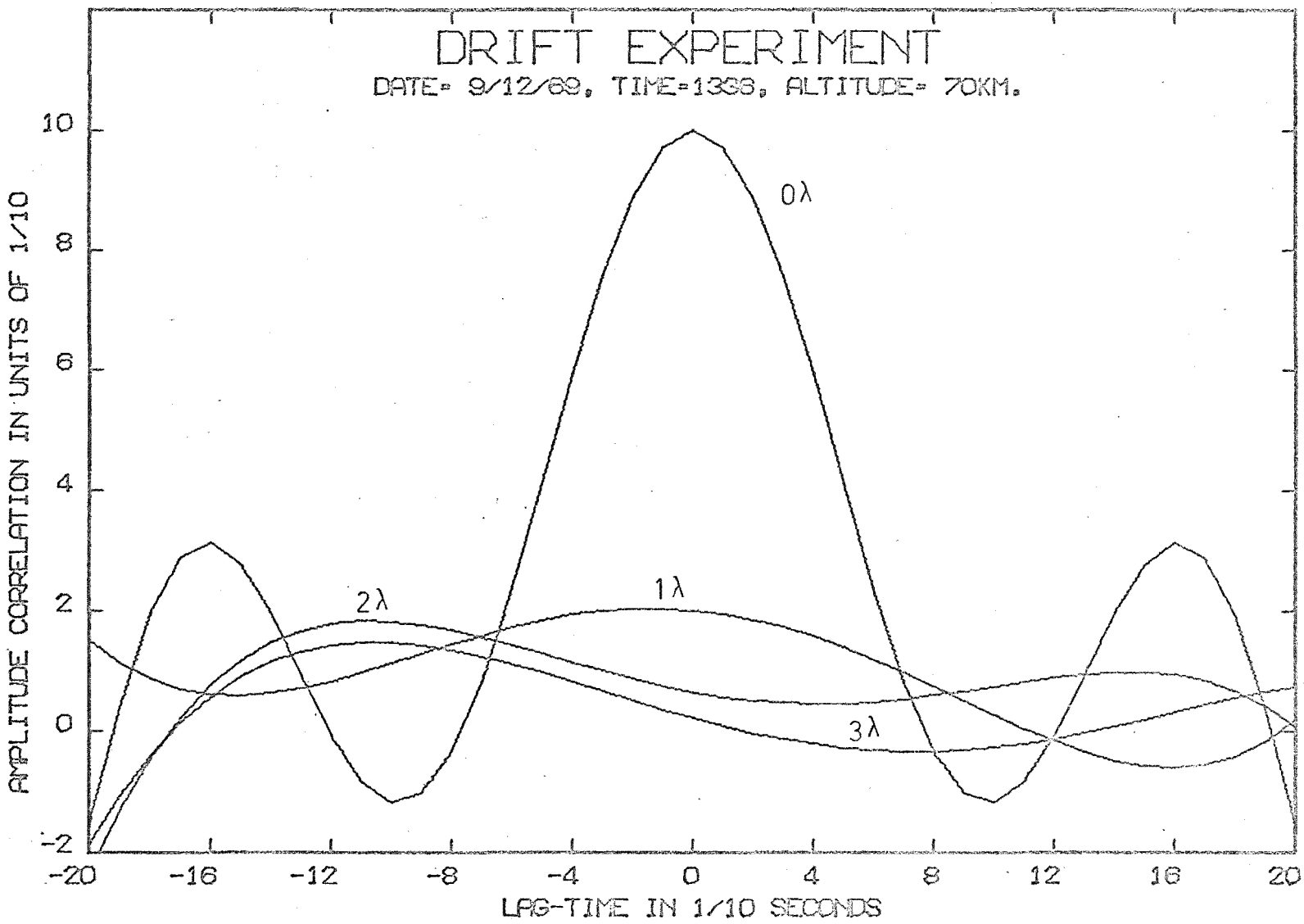
DRIFT EXPERIMENT
DATE= 9/12/69, TIME=1336, ALTITUDE= 70KM.
AMPLITUDE CORRELATION IN UNITS OF 1/10
10
8
6
4
2
0
-2
0λ
1λ
2λ
3λ
-20
-16
-12
-8
-4
0
4
8
12
16
20
LAG-TIME IN 1/10 SECONDS

FIGURE - 38

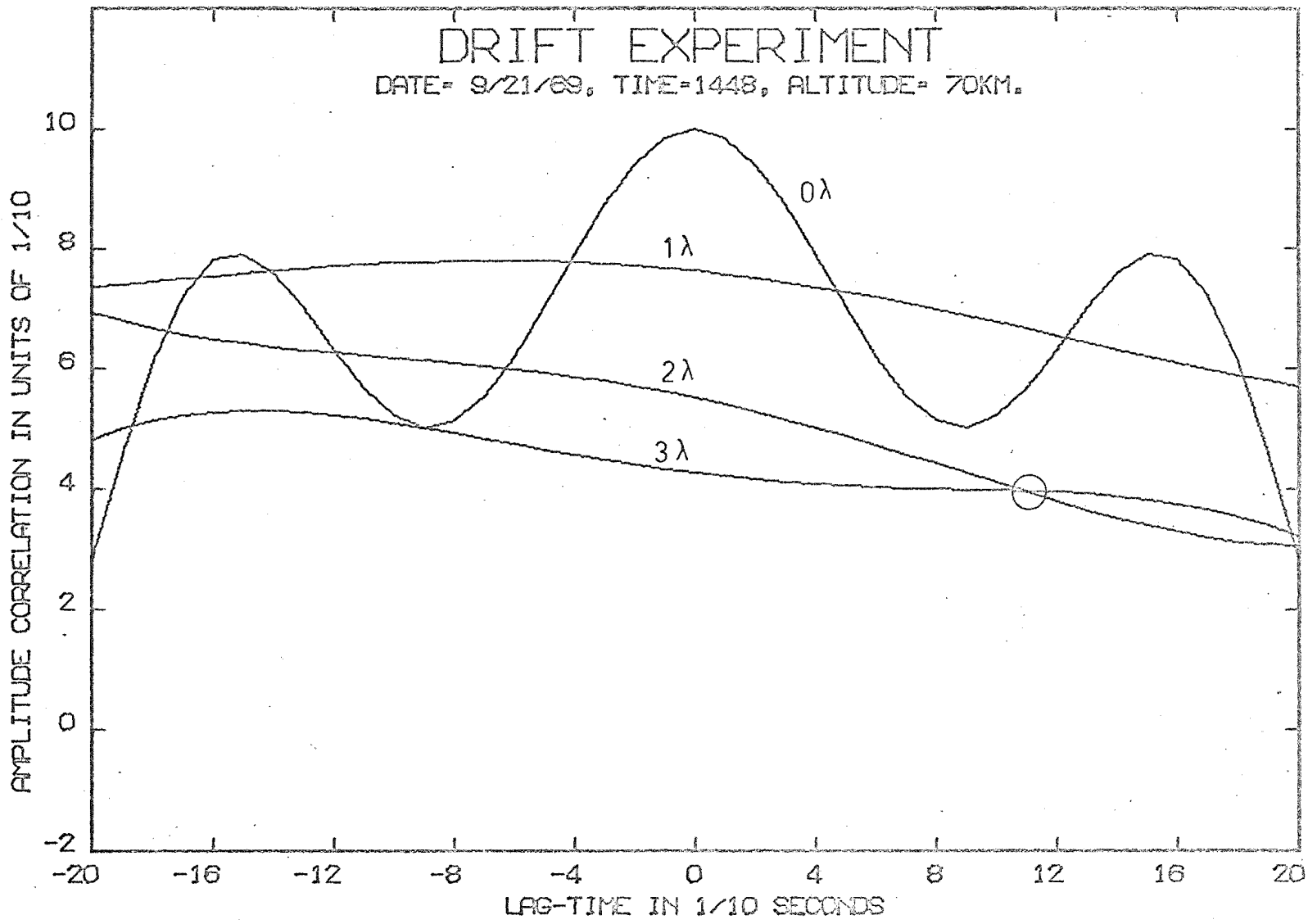
DRIFT EXPERIMENT
DATE= 9/21/69, TIME=1448, ALTITUDE= 70KM.
AMPLITUDE CORRELATION IN UNITS OF 1/10
10
8
6
4
2
0
-2
-20
-16
-12
-8
-4
0
4
8
12
16
20
LAG-TIME IN 1/10 SECONDS
0λ
1λ
2λ
3λ

FIGURE - 39

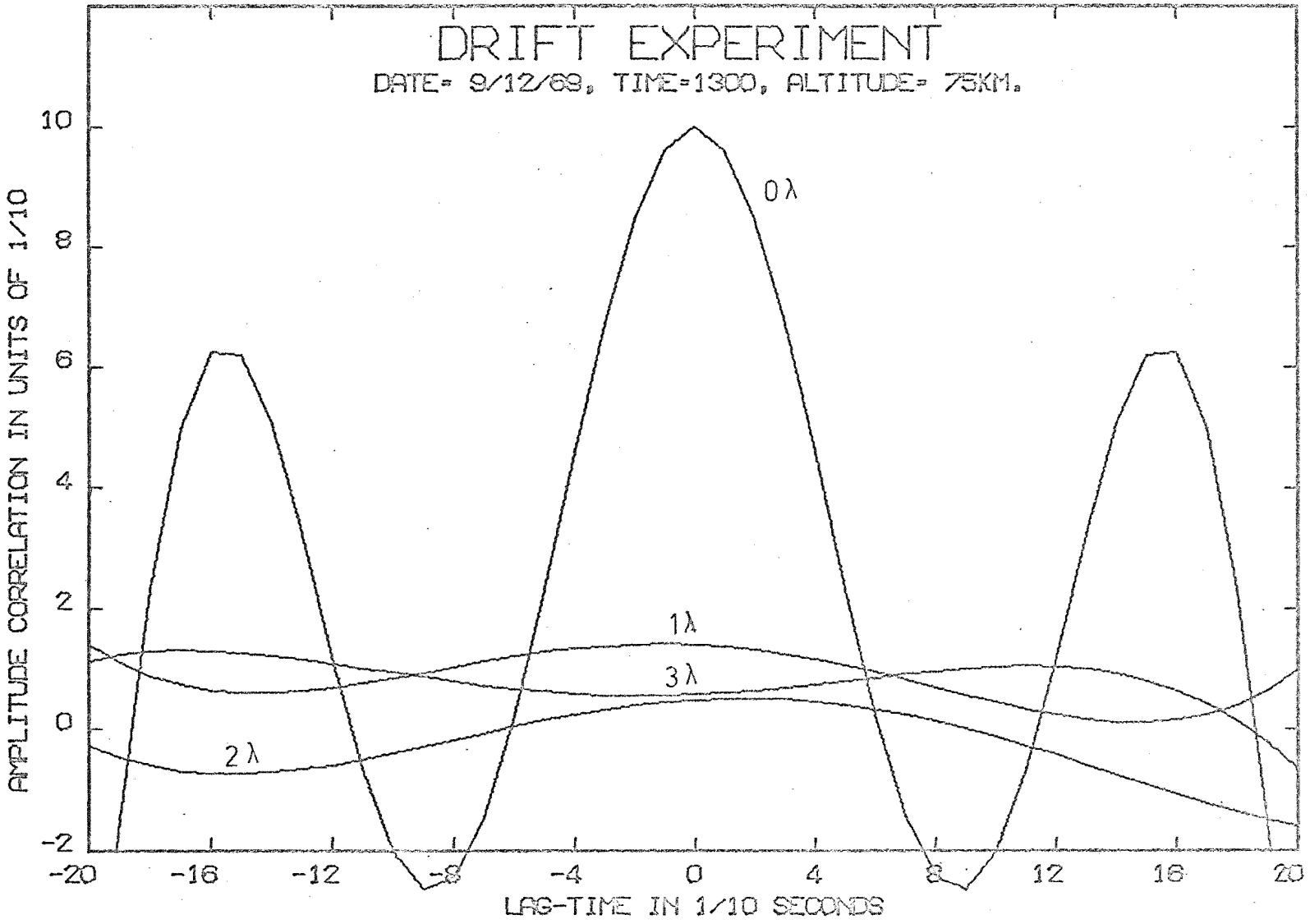
DRIFT EXPERIMENT
DATE= 9/12/69, TIME=1300, ALTITUDE= 75KM.
AMPLITUDE CORRELATION IN UNITS OF 1/10
10
8
6
4
2
0
-2
0λ
1λ
2λ
3λ
-20
-16
-12
-8
-4
0
4
8
12
16
20
LAG-TIME IN 1/10 SECONDS

FIGURE - 40

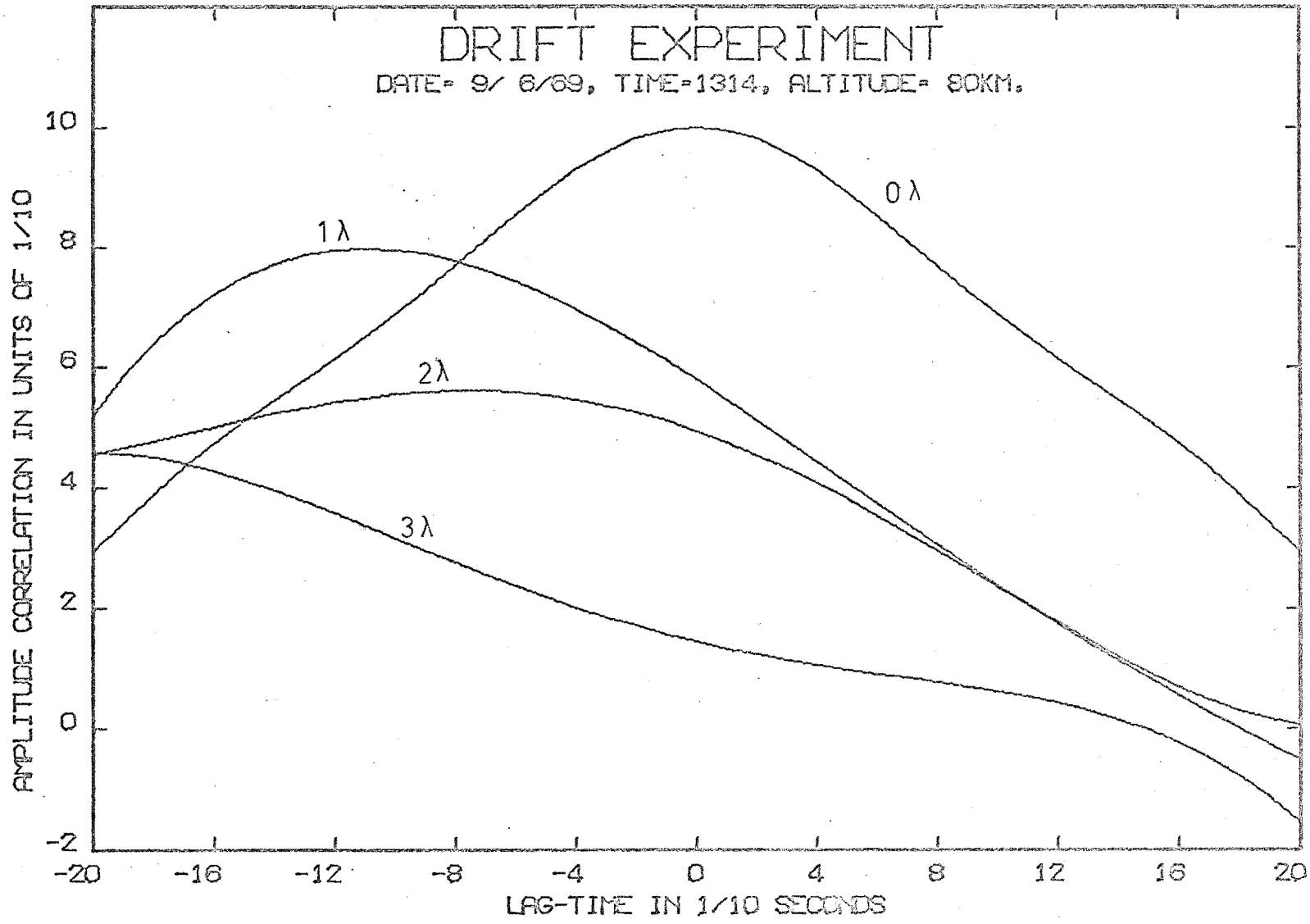
DRIFT EXPERIMENT
DATE= 9/ 6/69, TIME=1314, ALTITUDE= 80KM.
AMPLITUDE CORRELATION IN UNITS OF 1/10
10
8
6
4
2
0
-2
0λ
1λ
2λ
3λ
-20
-16
-12
-8
-4
0
4
8
12
16
20
LAG-TIME IN 1/10 SECONDS

FIGURE - 41

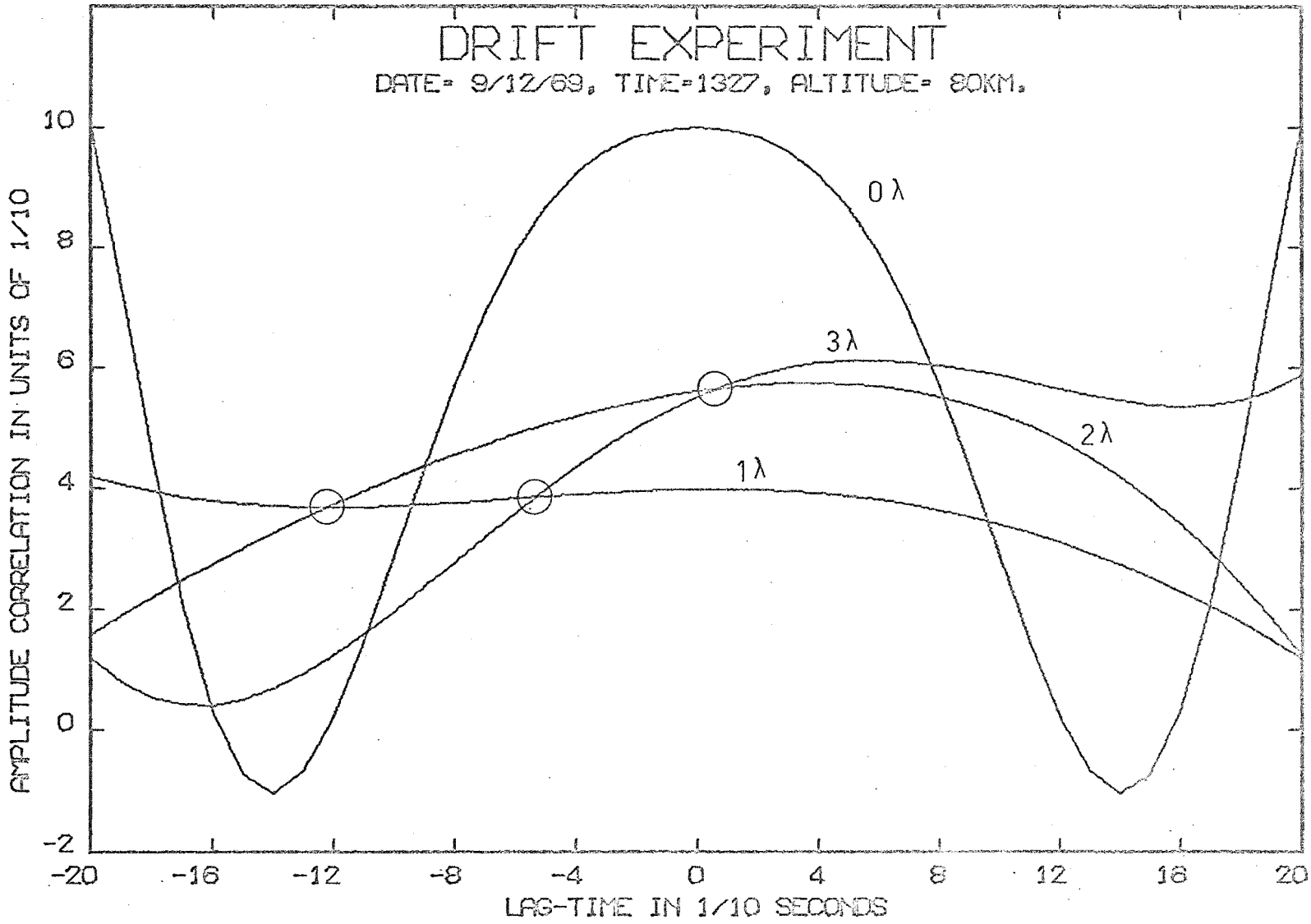
DRIFT EXPERIMENT
DATE= 9/12/69, TIME=1327, ALTITUDE= 80KM.
AMPLITUDE CORRELATION IN UNITS OF 1/10
10
8
6
4
2
0
-2
-20
-16
-12
-8
-4
0
4
8
12
16
20
LAG-TIME IN 1/10 SECONDS
0λ
1λ
2λ
3λ

FIGURE - 42

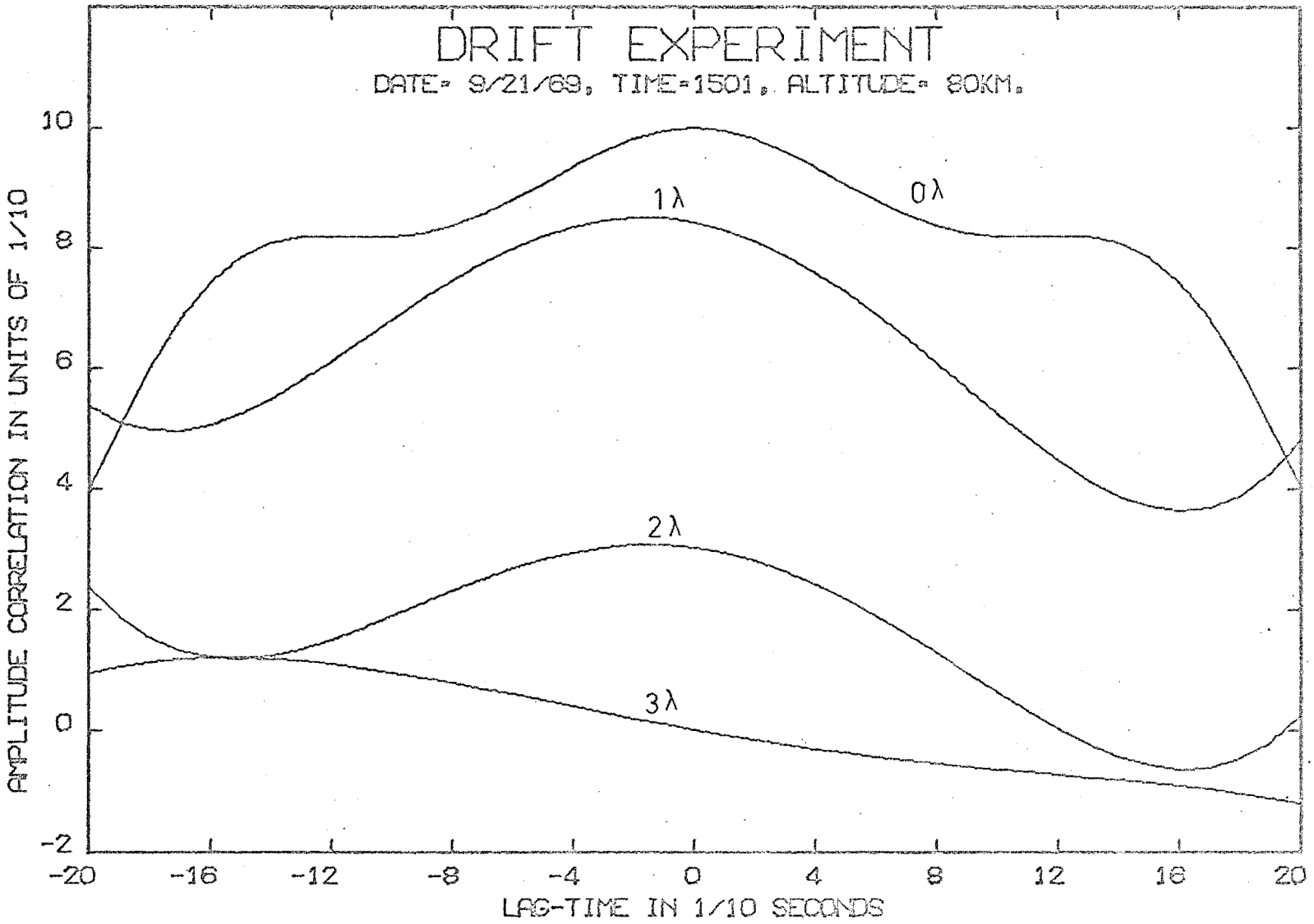
DRIFT EXPERIMENT
DATE= 9/21/69, TIME=1501, ALTITUDE= 80KM.
AMPLITUDE CORRELATION IN UNITS OF 1/10
10
8
6
4
2
0
-2
0λ
1λ
2λ
3λ
-20
-16
-12
-8
-4
0
4
8
12
16
20
LAG-TIME IN 1/10 SECONDS

FIGURE - 43

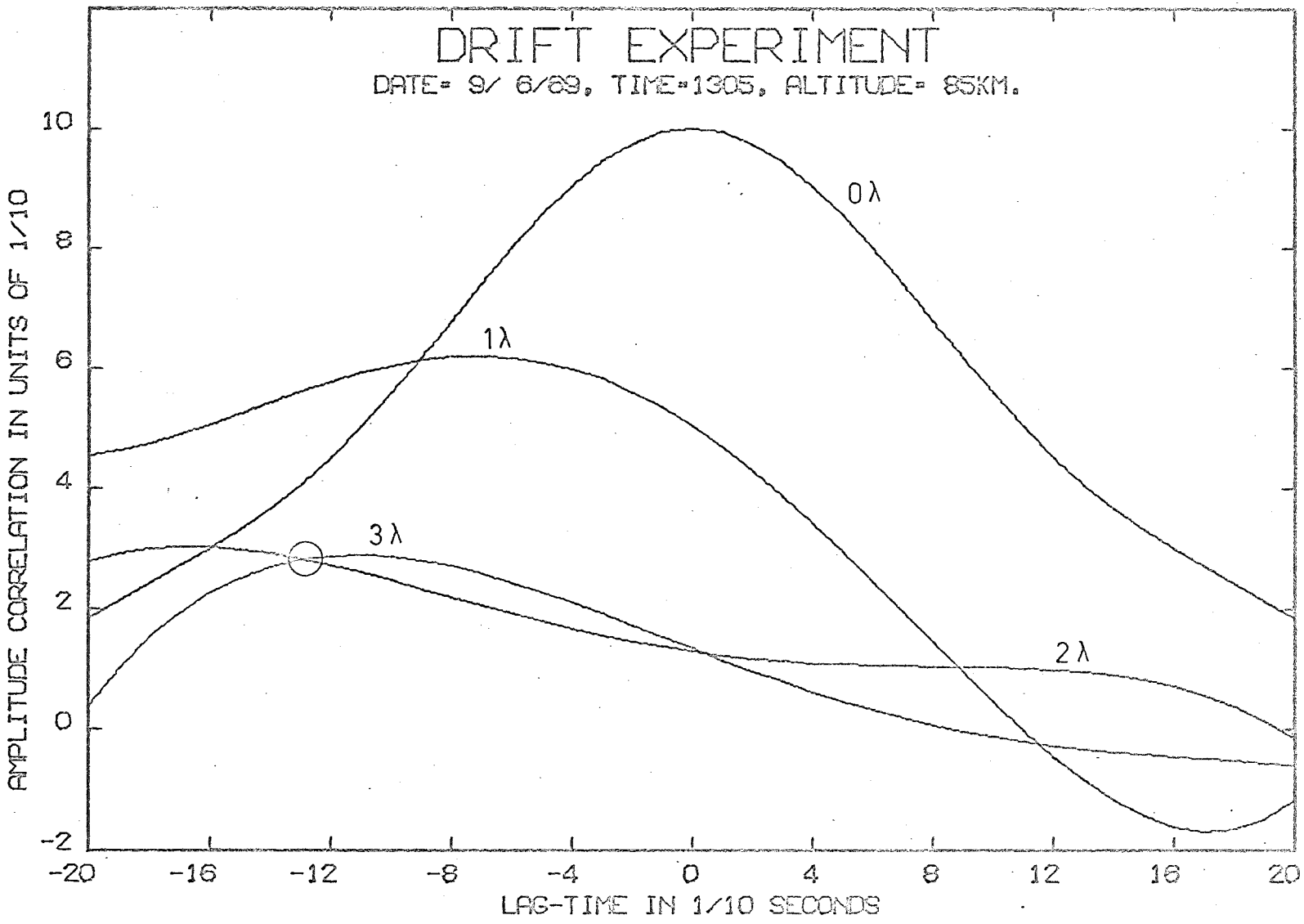
DRIFT EXPERIMENT
DATE= 9/ 6/69, TIME=1305, ALTITUDE= 85KM.
AMPLITUDE CORRELATION IN UNITS OF 1/10
10
8
6
4
2
0
-2
-20
-16
-12
-8
-4
0
4
8
12
16
20
LAG-TIME IN 1/10 SECONDS
0λ
1λ
2λ
3λ

FIGURE - 44

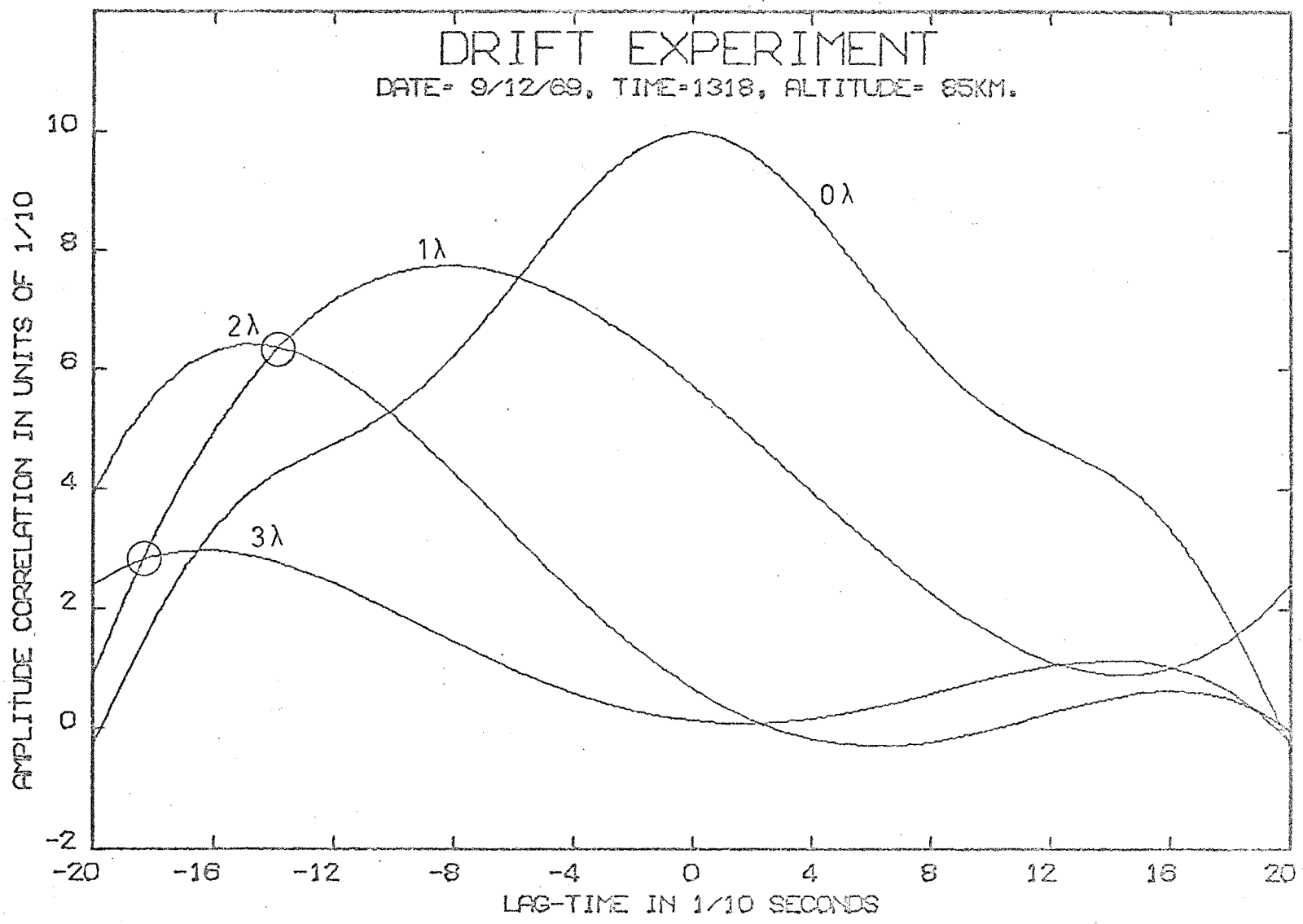
DRIFT EXPERIMENT
DATE= 9/12/69, TIME=1318, ALTITUDE= 85KM.
AMPLITUDE CORRELATION IN UNITS OF 1/10
10
8
6
4
2
0
-2
-20
-16
-12
-8
-4
0
4
8
12
16
20
LAG-TIME IN 1/10 SECONDS
0λ
1λ
2λ
3λ

FIGURE - 45

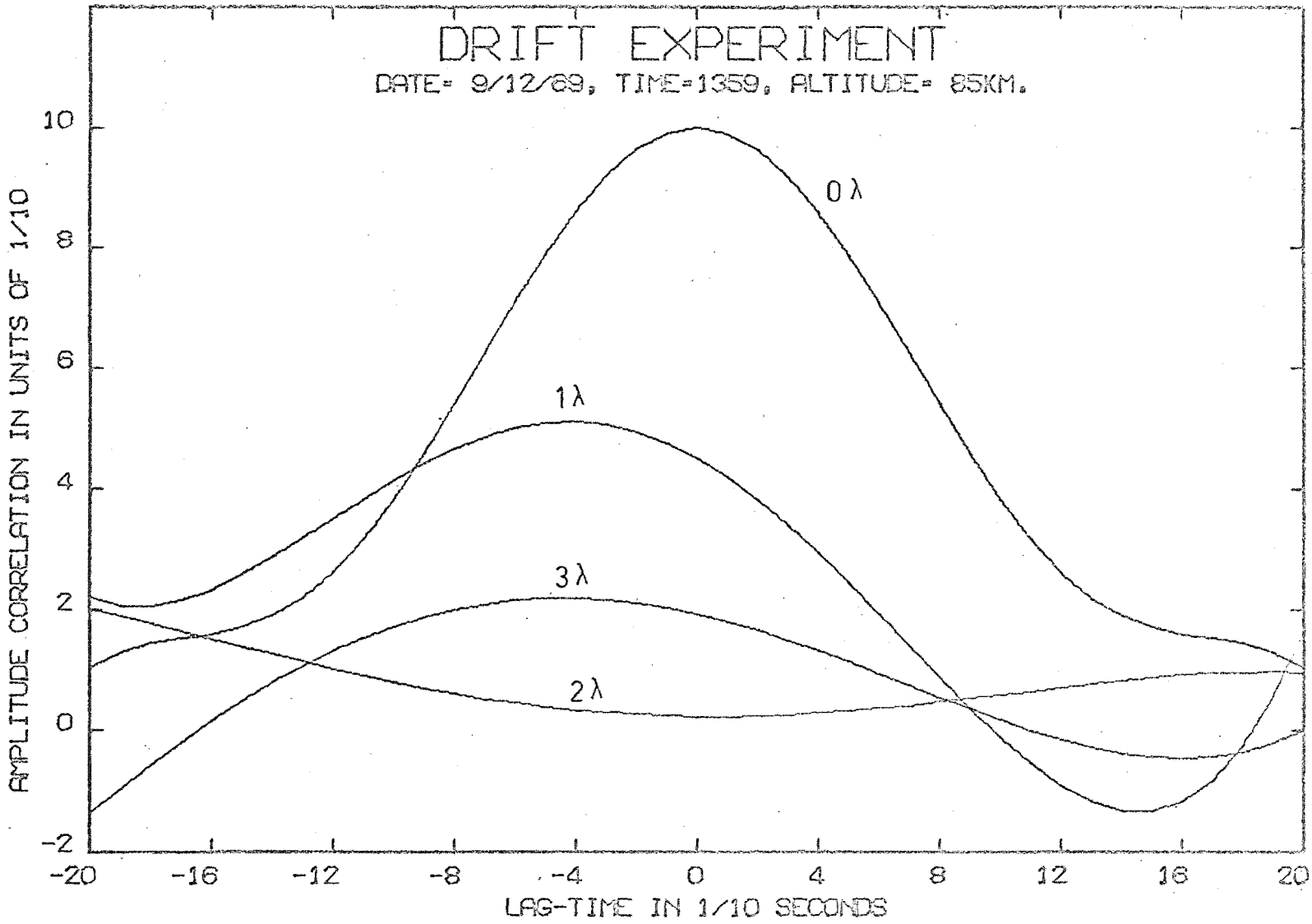
DRIFT EXPERIMENT
DATE= 9/12/69, TIME=1359, ALTITUDE= 85KM.
AMPLITUDE CORRELATION IN UNITS OF 1/10
10
8
6
4
2
0
-2
0λ
1λ
3λ
2λ
-20
-16
-12
-8
-4
0
4
8
12
16
20
LAG-TIME IN 1/10 SECONDS

FIGURE - 46

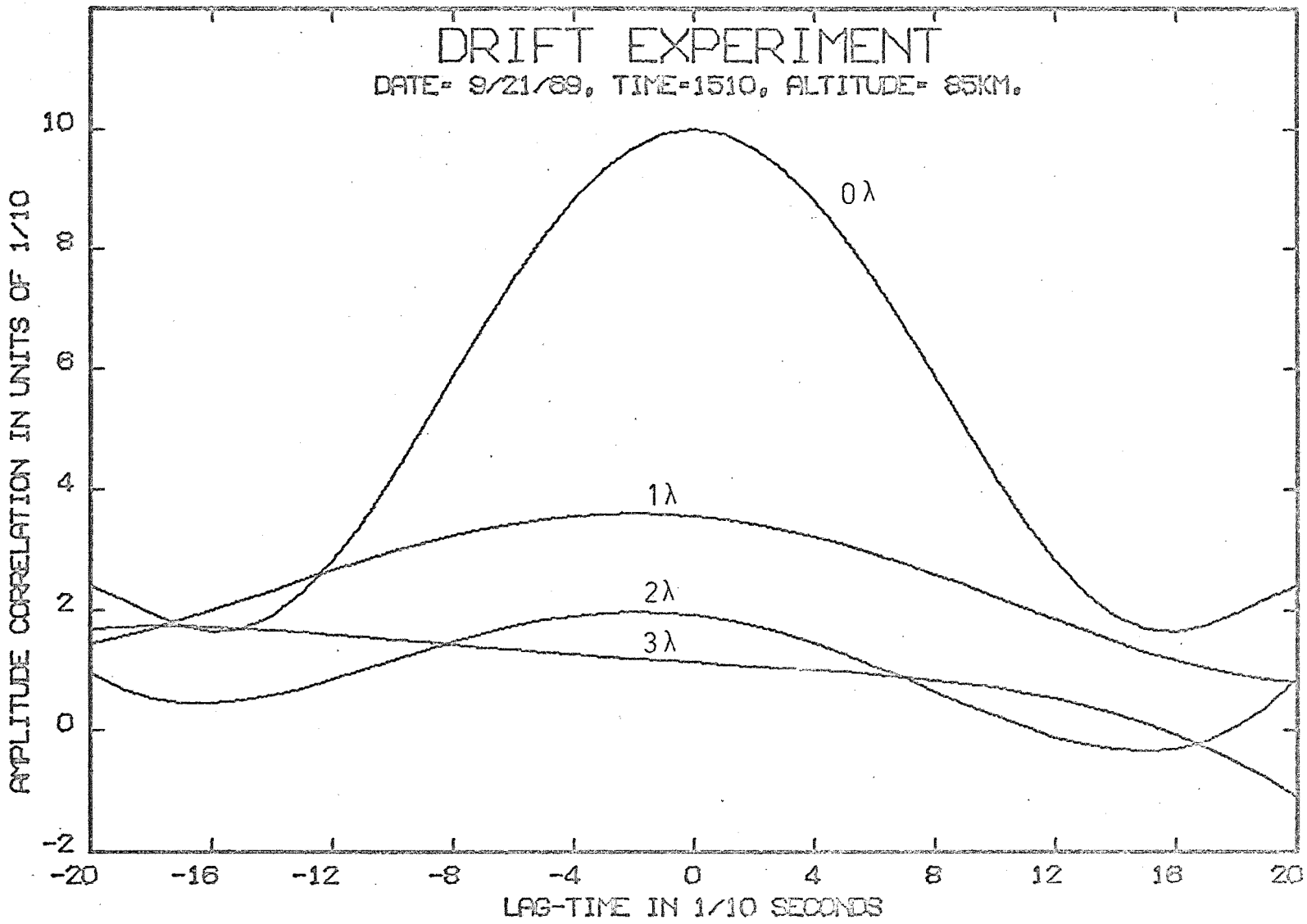
DRIFT EXPERIMENT
DATE= 9/21/69, TIME=1510, ALTITUDE= 85KM.
AMPLITUDE CORRELATION IN UNITS OF 1/10
10
8
6
4
2
0
-2
0λ
1λ
2λ
3λ
-20
-16
-12
-8
-4
0
4
8
12
16
20
LAG-TIME IN 1/10 SECONDS

FIGURE - 47

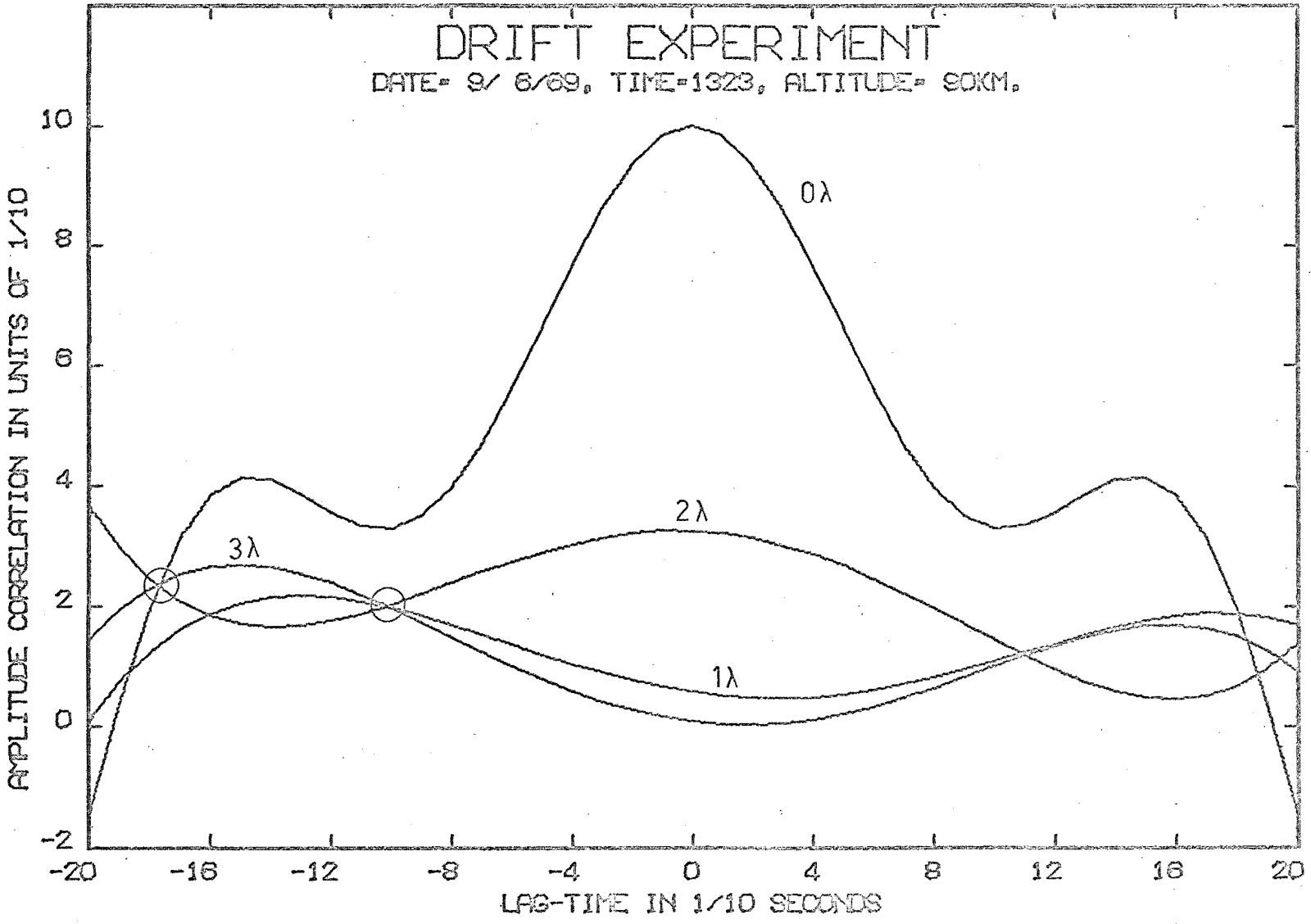
DRIFT EXPERIMENT
DATE= 9/ 6/69, TIME=1323, ALTITUDE= 90KM.
AMPLITUDE CORRELATION IN UNITS OF 1/10
LAG-TIME IN 1/10 SECONDS
10
8
6
4
2
0
-2
-20
-16
-12
-8
-4
0
4
8
12
16
20
0λ
1λ
2λ
3λ

FIGURE - 48

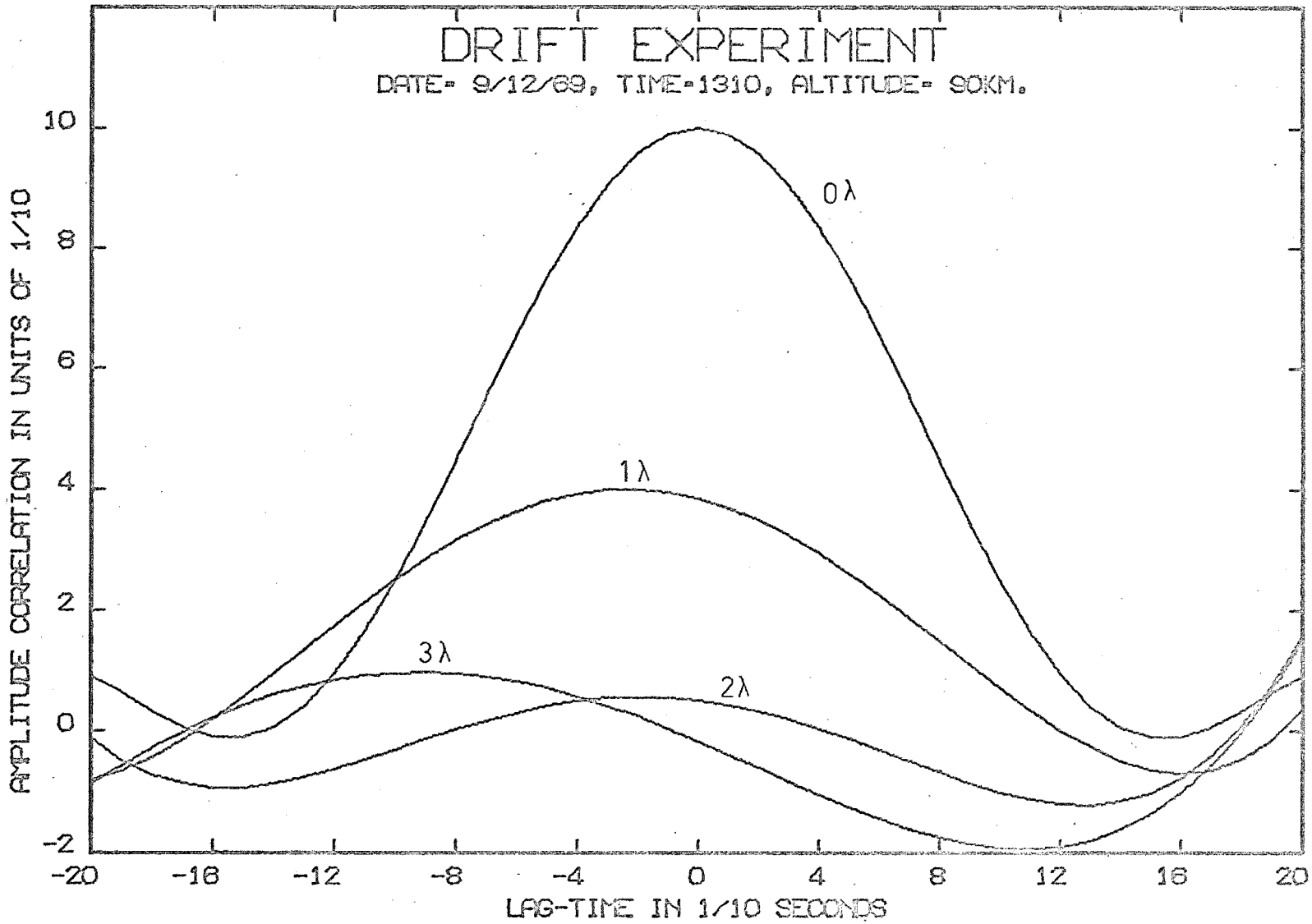
DRIFT EXPERIMENT
DATE- 9/12/69, TIME-1310, ALTITUDE- 90KM.
AMPLITUDE CORRELATION IN UNITS OF 1/10
10
8
6
4
2
0
-2
0λ
1λ
2λ
3λ
-20
-16
-12
-8
-4
0
4
8
12
16
20
LAG-TIME IN 1/10 SECONDS

FIGURE - 49

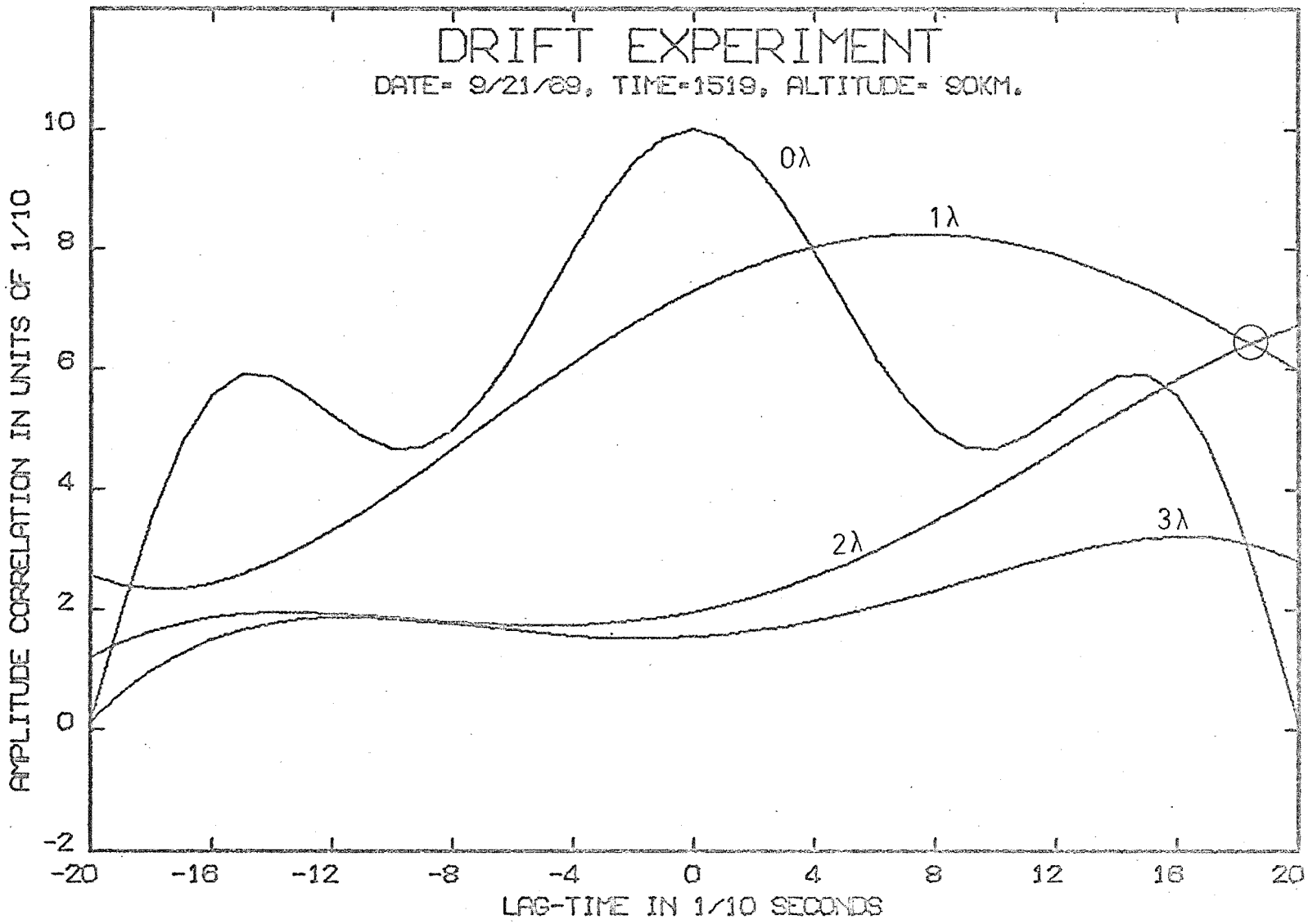
DRIFT EXPERIMENT
DATE= 9/21/69, TIME=1519, ALTITUDE= 90KM.
AMPLITUDE CORRELATION IN UNITS OF 1/10
10
8
6
4
2
0
-2
-20
-16
-12
-8
-4
0
4
8
12
16
20
LAG-TIME IN 1/10 SECONDS
0λ
1λ
2λ
3λ

FIGURE - 50

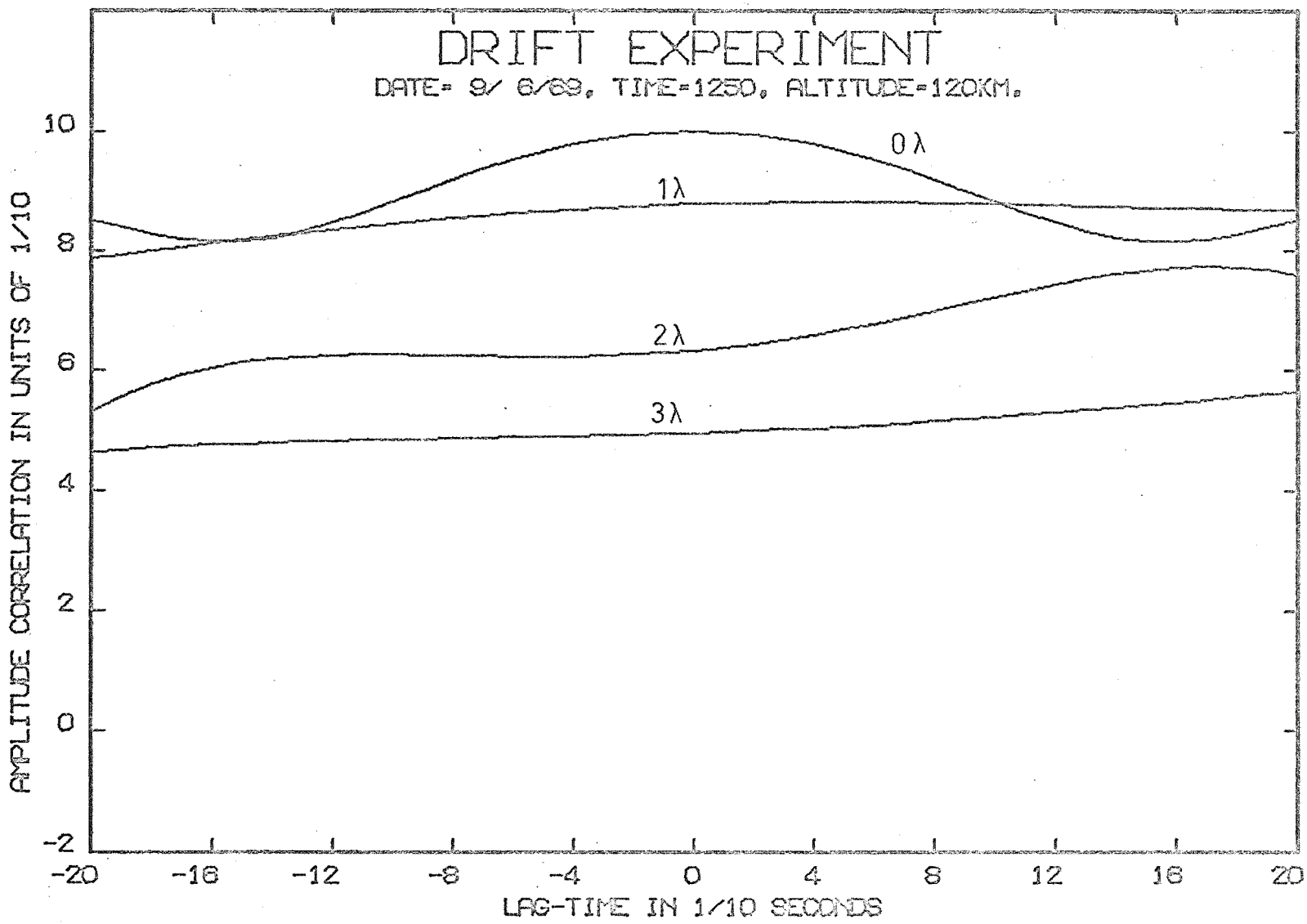
DRIFT EXPERIMENT
DATE= 9/ 6/69, TIME=1250, ALTITUDE=120KM.
0λ
1λ
2λ
3λ
AMPLITUDE CORRELATION IN UNITS OF 1/10
10
8
6
4
2
0
-2
-20
-16
-12
-8
-4
0
4
8
12
16
20
LAG-TIME IN 1/10 SECONDS

FIGURE - 51

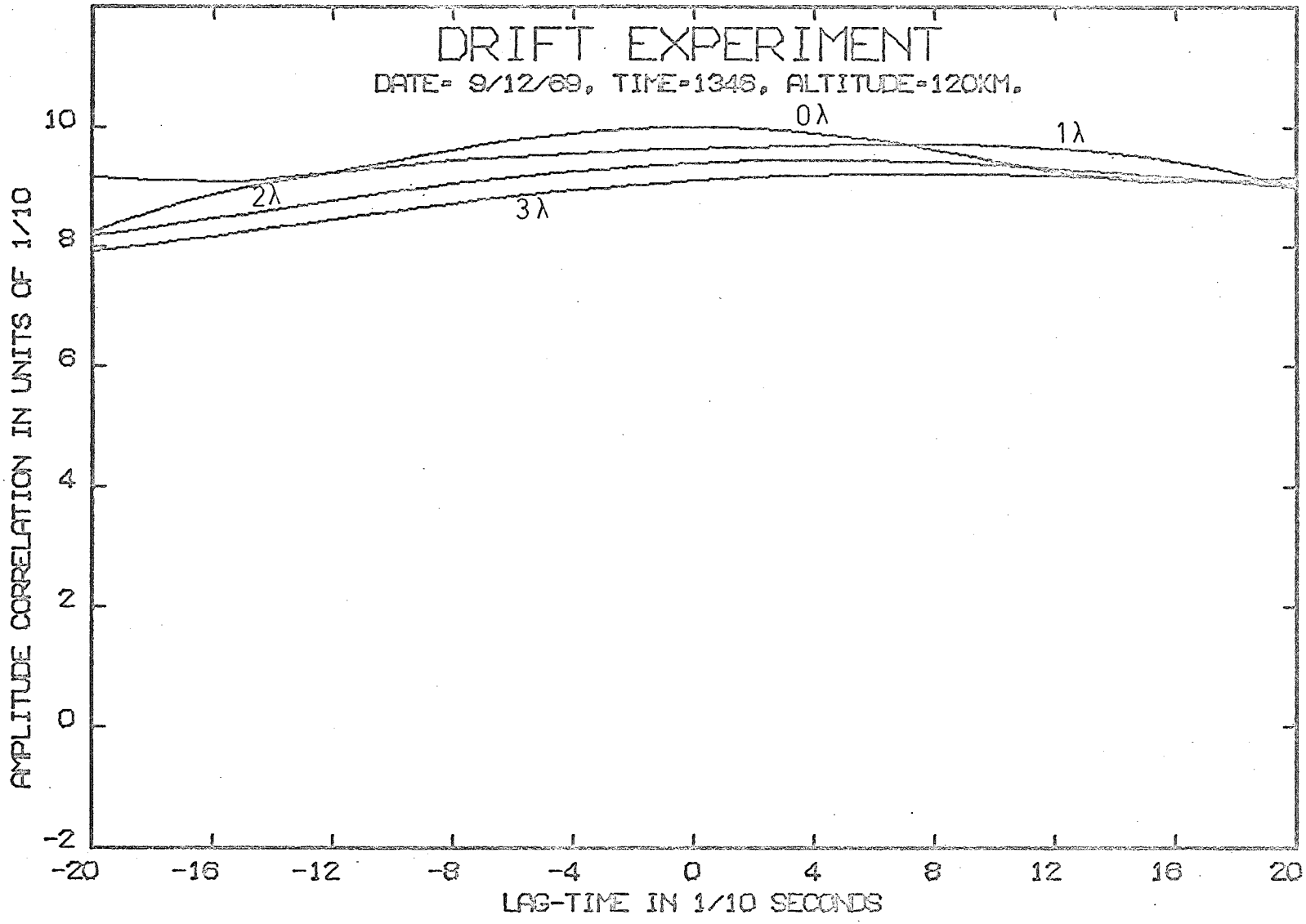
DRIFT EXPERIMENT
DATE= 9/12/69, TIME=1346, ALTITUDE=120KM.
0λ
1λ
2λ
3λ
AMPLITUDE CORRELATION IN UNITS OF 1/10
10
8
6
4
2
0
-2
-20
-16
-12
-8
-4
0
4
8
12
16
20
LAG-TIME IN 1/10 SECONDS

FIGURE - 52

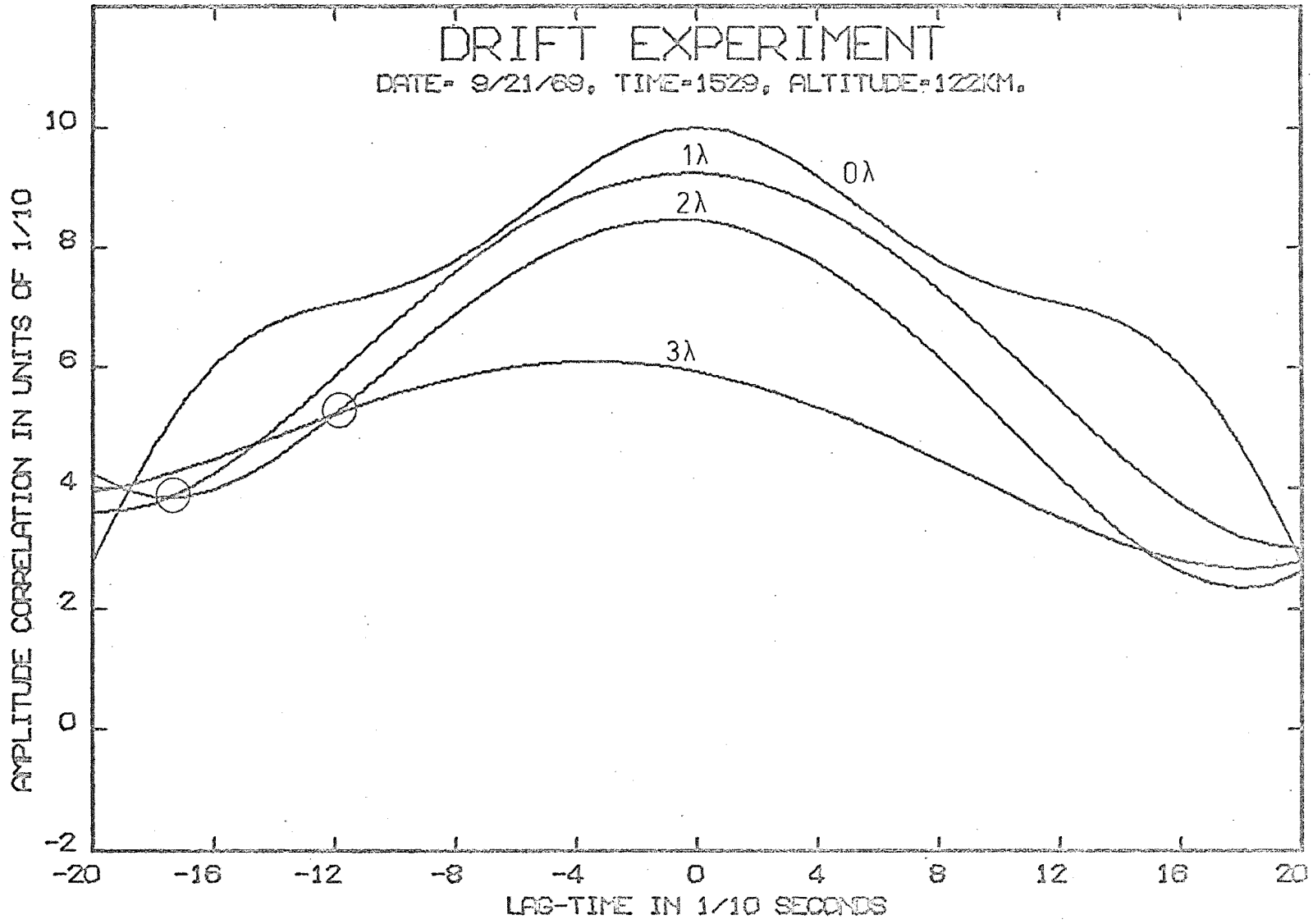
DRIFT EXPERIMENT
DATE= 9/21/69, TIME=1529, ALTITUDE=122KM.
0λ
1λ
2λ
3λ
AMPLITUDE CORRELATION IN UNITS OF 1/10
10
8
6
4
2
0
-2
-20
-16
-12
-8
-4
0
4
8
12
16
20
LAG-TIME IN 1/10 SECONDS

correlation experiments of Fraser and Vincent (1968) are of approximately the same value as are the correlation distances L from the spatial field correlation experiment. Nevertheless, there appears to be a fundamental difference between the results from these two experimental techniques. Bramley (1950) has shown that when the angular spectrum is randomly phased and when the distribution of amplitudes is near Rayleigh, then the spatial field correlation due to the scattered waves should be approximately equal to the square root of the spatial amplitude correlation. Thus, if the angular spectrum were randomly phased, then the results of Fraser and Vincent (1968) would predict that the spatial field correlation should be proportional to $\exp-\frac{r}{2L}$. In actual fact, what is observed is that the spatial field correlation decreases in accordance with $\exp-(\frac{r}{L})^2$. The difference between these two forms is substantial, and one is again forced to conclude that the angular spectrum at D-region heights is probably not randomly phased.

From the table in figure (35), it is evident that at 120 km, Q as well as β are both considerably smaller than for the remaining heights. One would therefore expect that the spatial field correlation

results bear a certain correspondence to the spatial amplitude correlation results for this scattering height.

This agreement is evidenced in the correlation length results obtained by Briggs and Philips (1950), who give this value as 200 meters, and by Feinstein (1954) who finds a best fit to his data for L = 250 meters. The experimental data in both cases were fitted to the square of a pseudo-gaussian correlation function. It appears from the preceding discussion that the results from the spatial field correlation experiment, as well as the implication of these results, are consistent with the findings of other workers.

IV(2). DRIFT EXPERIMENT

Even though the "drift" experiment was primarily intended to give a basis of comparison between the field correlation and the zero-lag amplitude correlation, some rather interesting features are apparent in figures (36) to (52). The first thing to note is the periodicity which is frequently exhibited by the auto-correlation function. One could, of course, argue that this periodicity was artificially introduced by virtue of the polynomial fit. This argument, however, is valid only within the limits imposed by the r.m.s. departure of data points from the smooth curve, which as was stated earlier, was always less than 0.1 and typically not larger than 0.05. Thus, an extreme example of this periodicity is shown in figure (41) which represents the results from an 80 km drift experiment conducted on September 12, 1969.(1) In this particular instance, the r.m.s. departure of data points from the fit was 0.057, and data points

---

(1). It should be noted that in figures (36) to (52) the date is written so that the first number represents the month, and the second the day of the month.

obtains:

$$\rho_A(r) \propto \left[\int_{-\infty}^{\infty} |F(S,t)|^2 \exp-\{2\pi i S r\}\, dS \right]^2 \qquad (70)$$

Results from the field correlation experiment have already been shown to be in disagreement with the proportionality in (70). Furthermore, equation (69) predicts that $\rho_A(r,\tau)$ should have the same functional dependence as does $\rho_A(r,0)$. The only difference should be a time shift between them and possibly a difference in the maximum value due to random decorrelation in time. Even a superficial inspection of the curves in figures (36) to (52) will reveal that the zero lag-time correlation bears little if any resemblance to the shape of the individual drift curves. In several instances, however, the shape of the auto-correlation curve $\rho(0,\tau)$ appears to be similar to the curves for $\rho(r,\tau)$. The curve in figure (40) for 80 km on 6th September, 1969, is an example of this.

If $\rho(r_1,\tau)$ is of the same functional form as is $\rho(r_2,\tau)$, then an intersection of the curves representing these two correlations is possible either if their arguments are equal or if they are multiple valued functions of the argument. The first of these alternatives can obviously not be satisfied for two distinct values of antenna separation r.

Consequently, one is left with the choice that the same functional form is not maintained for $\rho(r_1,\tau)$ and $\rho(r_2,\tau)$ or else that the function has more than one root. That these functions could conceivably have a certain amount of periodicity is suggested by the form of the auto-correlation curves.

In an effort to gain some qualitative appreciation of this dilemma, recall the developments of section II(2) where it was shown that

$$\overline{E(x)E(x+r)^*} = \int_{-\infty}^{\infty} \overline{|F(S)|^2} \exp -i\{2\pi rS\}\, I_1\, dS \qquad (19a)$$

On the basis of a gaussian angular correlation $\rho(\sigma)$ within the spectrum of plane waves, I_1 was shown to be

$$I_1 = \frac{1}{c} \exp -\tfrac{1}{2}\left[\frac{2\pi\beta z(S-\frac{x}{z})}{c}\right]^2 \qquad (29b)$$

where β is a measure of the correlation within the angular spectrum, and $c \doteq 1.0$.

It should be noted that I_1 represents nothing more than a filter function to the angular power spectrum $\overline{|F(S)|^2}$: when $\beta \equiv 0$, then $I_1 \equiv 1.0$, and when β becomes large, then only a portion of $\overline{|F(S)|^2}$ enters into the integration of (19a). The situation becomes far more complex when the angular power spectrum and the "location" x are time dependent. Under these conditions, x in (29b) should be replaced by $x_0 - vt$ where x_0 is the position of the observer,

and v is the velocity of the scatterers in the screen. Likewise, $\overline{|F(S)|^2}$ in (19a) must now be replaced by

$$\overline{F(S,t)F(S',t')^{*}\exp -i\left[2\pi(S-S')vt\right]}$$

By virtue of a non-zero value for t, the quantity $(S-S') = \sigma$ is once more in evidence so that the results obtained in (19a) and (29b) are no longer valid. Instead, a very complicated function will result for I_1 which for non-zero β will be dependent on time as well as on position. On the other hand, if $\beta \equiv 0$, then the traditional relationship for $\overline{E(x,t)E(x+r,t)^{*}}$ will be obtained. Consequently, unless it can be shown that $\beta \equiv 0$, there can be no justification for assuming that the functional form for $\rho_A(r_1,\tau)$ is equal to that for $\rho_A(r_2,\tau)$.

Although it is not the purpose of this work to argue the virtues or disadvantages of ionospheric drift experiments, it should be clear that the results obtained in this program cast considerable doubt on the interpretation of data from amplitude correlation experiments. The burden of proof is therefore shifted to the experimenter who must satisfy himself that the angular spectrum was indeed randomly phased before proceeding with analysis techniques that require this assumption.

IV(3). AMPLITUDE DISTRIBUTION RESULTS

The results from the chi-square test for Rice parameter (a) are presented in figure (53). There can be little doubt that the amplitudes for D-region echoes from scattering heights below 85 km are primarily Rayleigh distributed. This observation is not surprising if a volume scattering process is assumed to be the cause of the partial reflections (Flood 1969). It is to be noted, however, that the probability of observing non-Rayleigh amplitude distributions appears to increase systematically with scattering height. This result implies that there exists a steady signal component in the partially reflected echoes from the D-region. Apparently, the scattering process, especially above 80 km, cannot be due to volume scatter alone. In addition, one is forced to stipulate that the scattering of waves in the D-region is at least partially caused by some coherent process. Such a process would necessitate the existence of large-scale horizontal irregularities which exhibit substantial departures from the mean refractive index. Unfortunately,

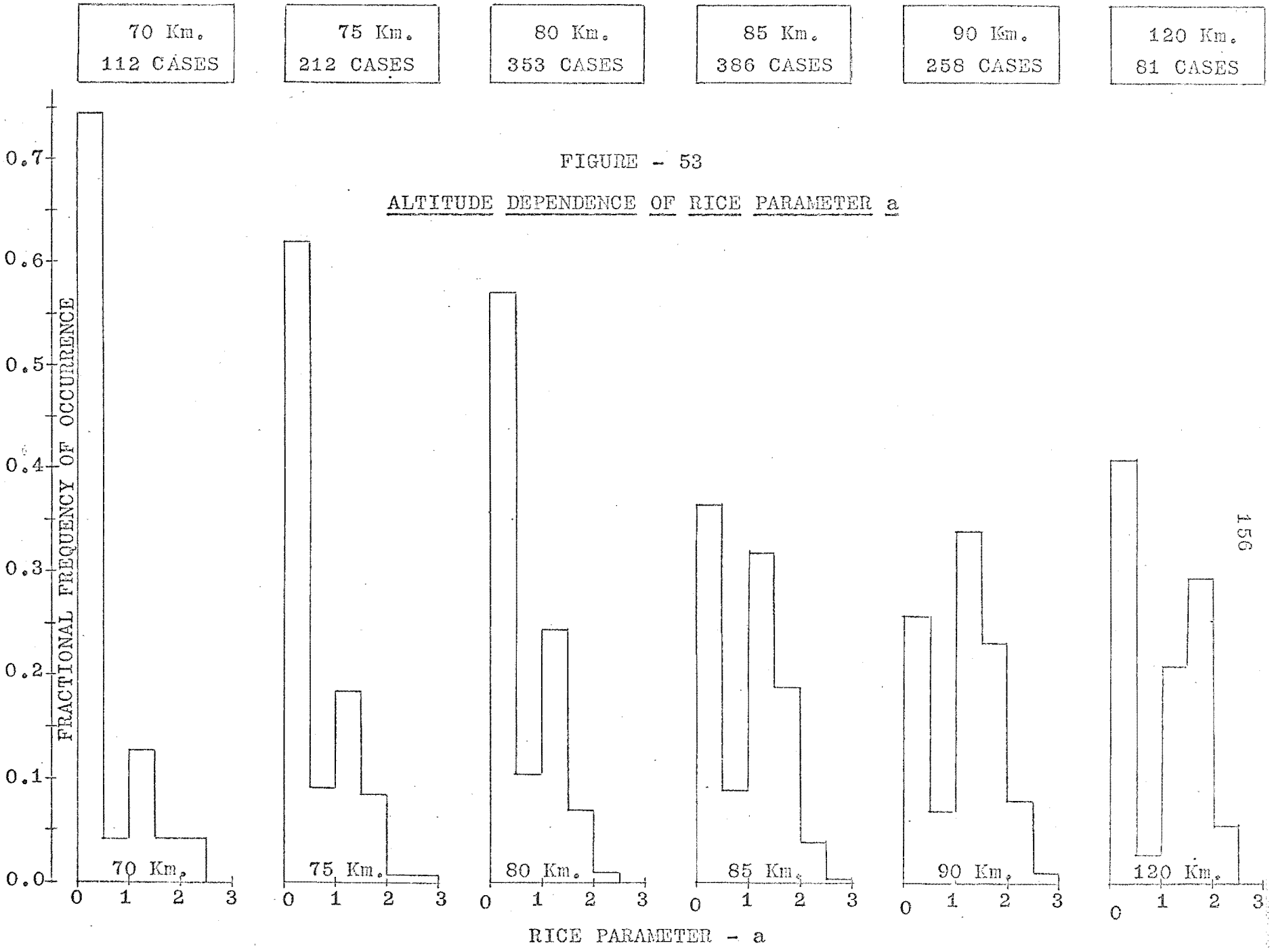

FIGURE - 53

ALTITUDE DEPENDENCE OF RICE PARAMETER a

gradients in electron density of the magnitude required to explain the observed results in figure (53) have never been noticed in the data from rocket experiments. This is surprising in view of the fact that 50% of the time at 85 km and at 90 km, more than one-half of the power in the echo is due to a steady sinusoidal component. Another interesting feature of the results given in figure (53) is the pronounced minimum in the probability that the Rice parameter is between 0.5 and 1.0. These results imply that the distributions were either random or else the power in the steady signal was at least as large as the total power of the random components. A possible explanation for this behaviour is given by Austin (1967) who postulates the existence of a sinusoidal (coherent) reflection screen. Such a screen might conceivably be due to a gravity wave. While Austin's derivation was specifically based on a backscatter geometry, his results may readily be generalized for a bistatic forward scatter geometry. Thus, when ω, k, and A are the radian-frequency, the wave number, and the amplitude (in meters), respectively, of a gravity wave, then it can be shown that

$$\cos(\omega t - kx) = -\frac{1}{2Akh}\left[2x - \overline{d}\right]$$

is the condition for a specular reflection from a point on the screen at height h and distance x from the receiver. (The transmitter and receiver are assumed to be separated by a distance d). It is evident that when $\frac{1}{Akh}$ is larger than, or equal to, 1.0 then only one value of x can satisfy the above relationship. This condition corresponds to a single specular reflection. On the other hand, if $\frac{1}{Akh}$ is smaller than 1.0, three or more values for x will simultaneously satisfy the specular reflection conditions. Under these circumstances Austin (1967) shows that "Rayleigh-like" shallow fading is produced by the combination of the simultaneous reflections. This conclusion is qualitatively verified by Slack (1946) who showed that five independent scatter components produce an amplitude distribution that is similar to a Rayleigh distribution. Although the postulated mechanism explains the minimum in the frequency of occurrence of distributions with Rice parameter between 0.5 and 1.0, it is contrary to the observed altitude dependence of distributions of large Rice parameter. If such a height dependence could be deduced from the specular reflection conditions, then it would stand to reason that the probability of several simultaneous reflections

should be enhanced at large values for h. Since this prediction is certainly not substantiated by the data in figure (53), one must conclude that yet another mechanism is contributing to the overall scattering process in the D-region.

V. SUMMARY AND CONCLUSIONS

The principle aim of the program described in the preceeding sections was to gain a better understanding of partially reflected signals from the ionospheric D-region. As was mentioned repeatedly during the development of this work, much of the currently used theoretical formulation with regard to ionospheric scatter is based on the assumption that the spectrum of backscattered plane waves is randomly phased and that the amplitude of the received signals is Rayleigh distributed. This statement applies to a large variety of ionospheric experiments and in particular to the Gardner-Pawsey differential absorption experiment and to the various drift experiments.

In section II of this work, an attempt is made to give a physical explanation of the "randomly phased angular spectrum". By means of mathematically simple correlation functions the effects due to a "not randomly phased angular spectrum" were isolated. This effect was shown to manifest itself as a "filter function" (equation 29b) which acts on the angular power spectrum $\overline{|F(S)|^2}$. The complex spatial field correlation was then shown to be the Fourier transform

of the product of $\overline{|F(S)|^2}$ and this filter function. The result indicated that the spatial field correlation would be dependent on the antenna separation (r) and also on the specific location of the experiment in the field pattern. It was further shown that a necessary and sufficient condition for the angular spectrum to be randomly phased is to show that the spatial field correlation is independent of the absolute position of the antennas. Under these circumstances, and if the amplitude of the field is Rayleigh distributed, one can meaningfully associate the magnitude of the spatial field correlation with the spatial amplitude correlation.

The experimental portion of this program yielded data from which these two criteria could be assessed. Thus it was shown that the majority of amplitude data analyzed were, in fact, Rayleigh distributed. It was further shown that those data which gave rise to an "off-set" Rayleigh distribution could conceivably be associated with a truly random process. However, the question of how to explain the relatively large number of Rice distributed data remains unanswered.

There can be little doubt that the D-region complex field correlation results are indicative of a significant angular correlation within the spectrum

of plane waves. This statement applies particularly to the scattering heights of 75 km, 85 km, and 90 km, and to a lesser extent to 70 km and 80 km. In contrast, the results obtained from 120 km appear to satisfy the randomly phased angular spectrum requirements.

In section IV some of the implications of the experimental results from this program were discussed. This discussion was restricted to the subject of D-region drift results and it was pointed out that current interpretations might be in serious error. In view of the popularity of ionospheric drift experiments it would appear prudent to substantiate the findings from this program. Two courses of action seem to be indicated. The first of these should involve a multiple station combination experiment in which the spatial amplitude correlation is obtained simultaneously with the complex field correlation. From such an experiment several important facts should emerge:

1. Is the spatial correlation (amplitude or complex field) dependent on absolute position?
2. Is the amplitude correlation simply related to the magnitude of the field correlation?
3. Is the angular correlation within the spectrum of plane waves dependent on absolute location?

Answers to these questions should serve adequately to substantiate or to repudiate the results from the pilot program discussed in this work.

The second course of action is of a theoretical nature and of an immense magnitude. Specifically, computations should be carried out in an effort to relate the magnitude of the complex field correlation to the amplitude correlation under conditions where the angular correlation within the spectrum of plane waves is small but finite. The results from such a study should then be extended to include any possible effects on the interpretation of drift experiments.

While this author would gladly undertake the experimental program suggested earlier and in all likelihood will do so in the future, he has no intentions of competing with anyone brave enough to attempt the second suggested course of action.

APPENDIX A

CIRCUIT DIAGRAMS

FIGURE - A1

2.4 Mc/s RECEIVER

(R.F.-AMPLIFIER, MIXER - OSCILLATOR, I.F.-AMPLIFIER)

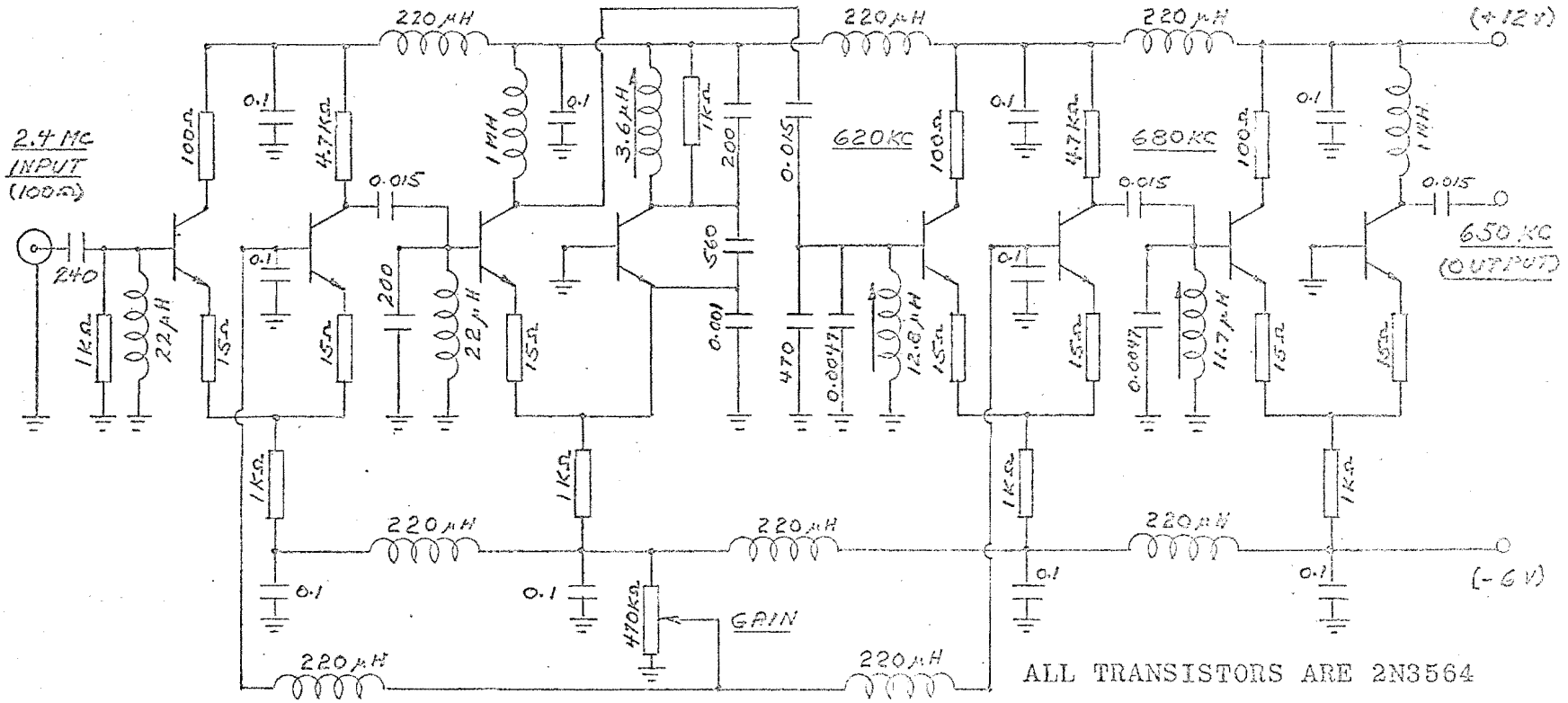

FIGURE - A2

2.4 Mc/s RECEIVER

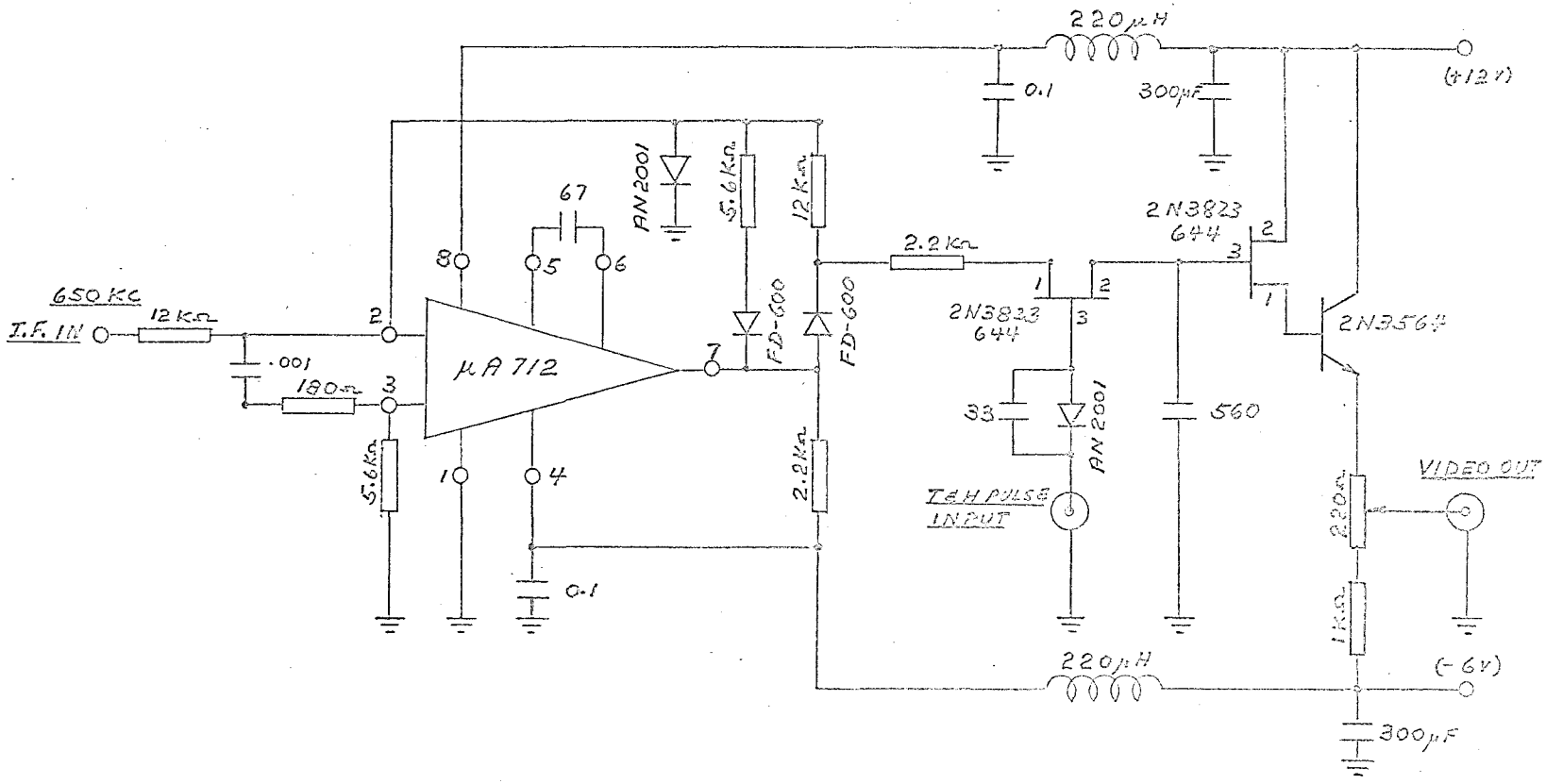

FIGURE - A3

TRACK-AND-HOLD PULSE GENERATOR

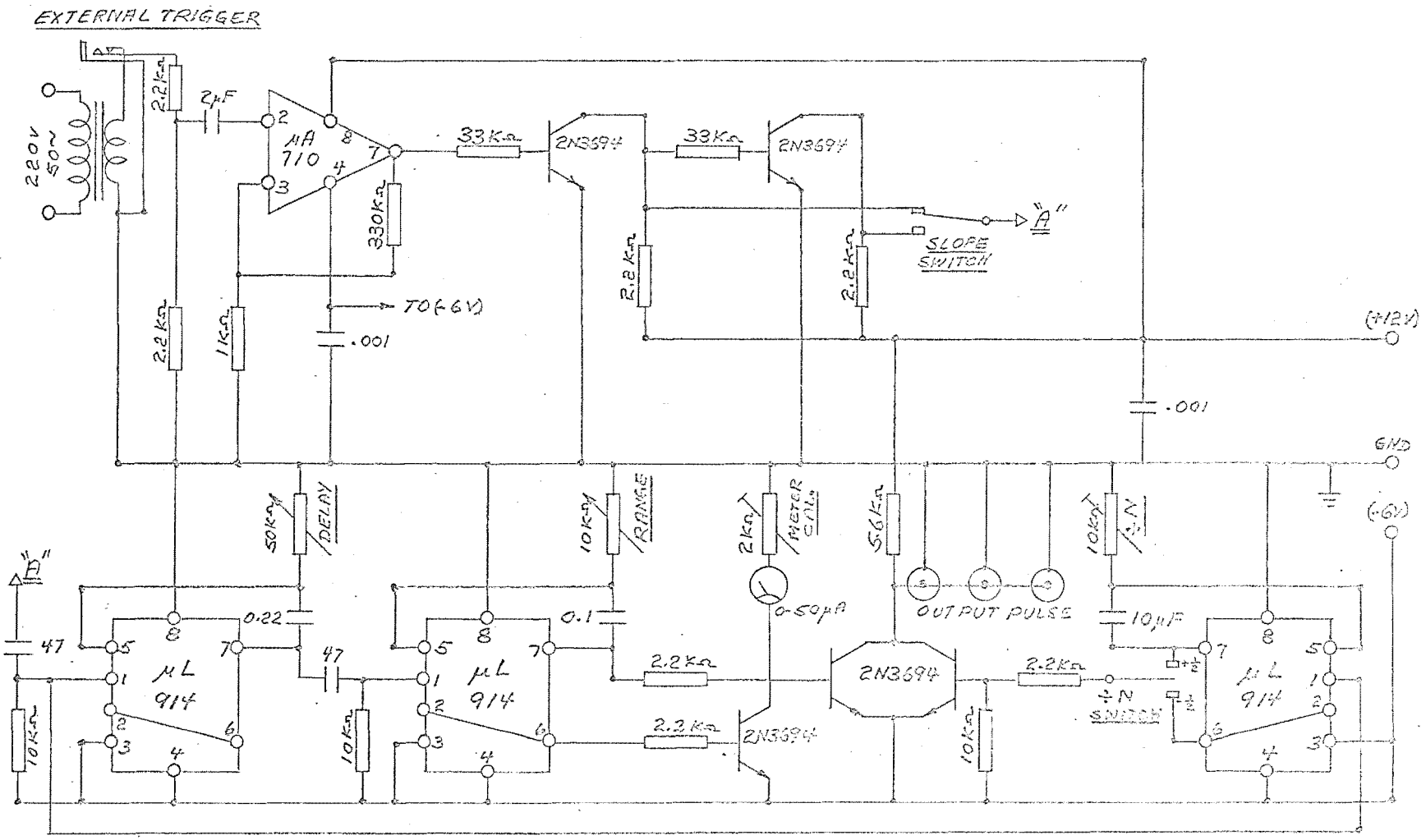

FIGURE - A4

SEQUENTIAL SAMPLER

(DIGITAL CONVERTER INTERFACE LOGIC)

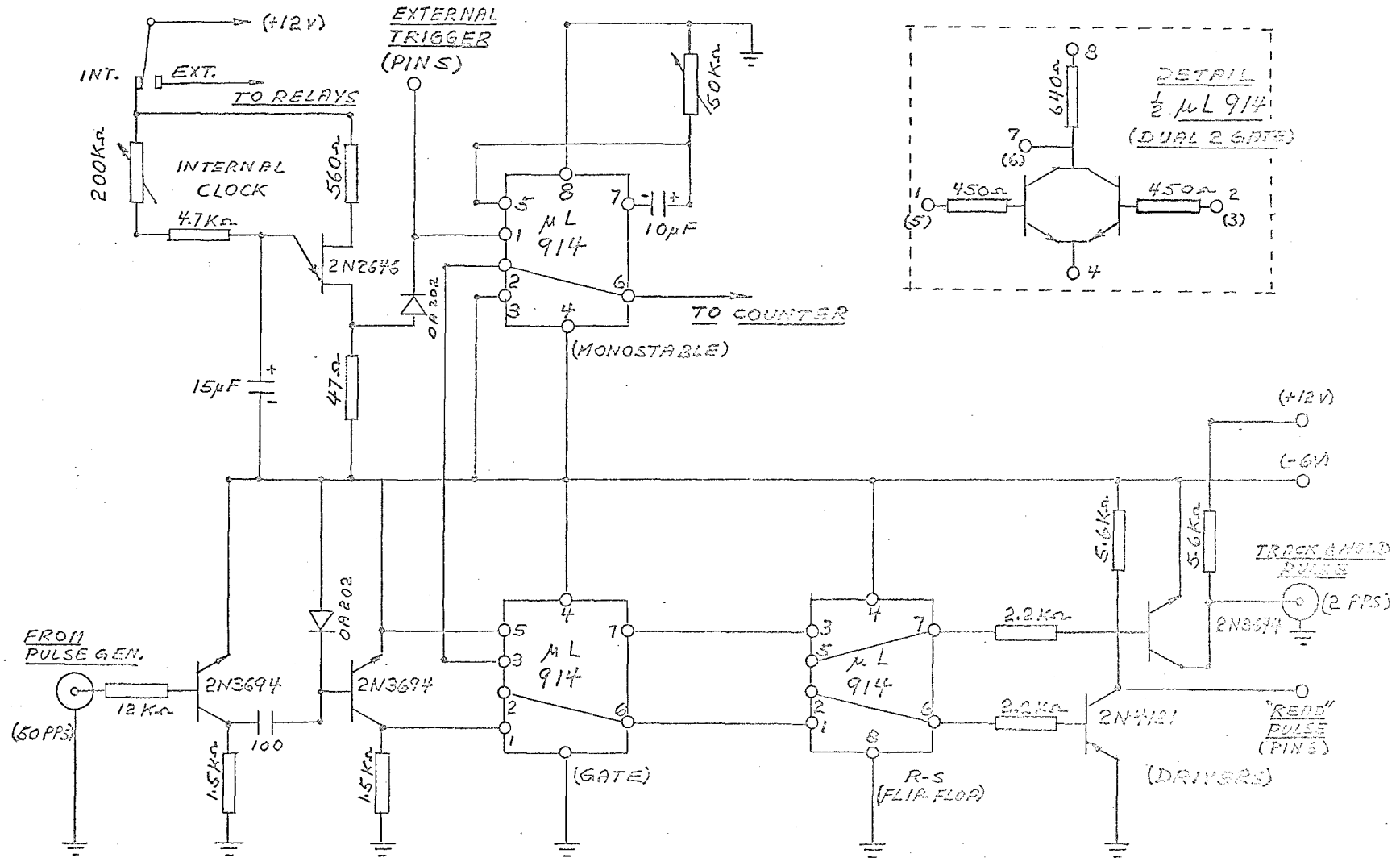

SEQUENTIAL SAMPLER

(COUNTER AND DRIVING LOGIC)

FIGURE - A5

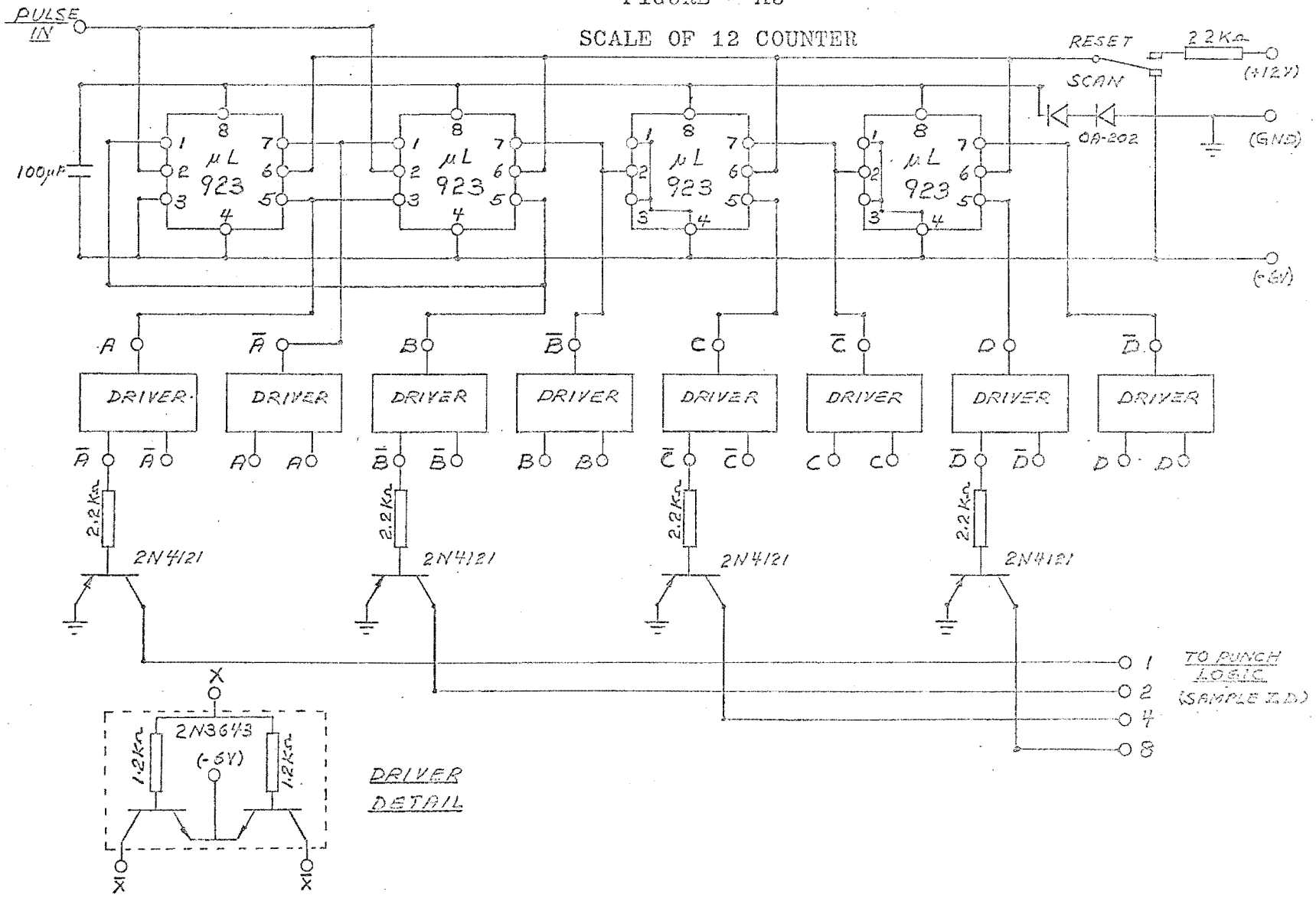

FIGURE - A6

SEQUENTIAL SAMPLER

(RELAY SWITCHING LOGIC)

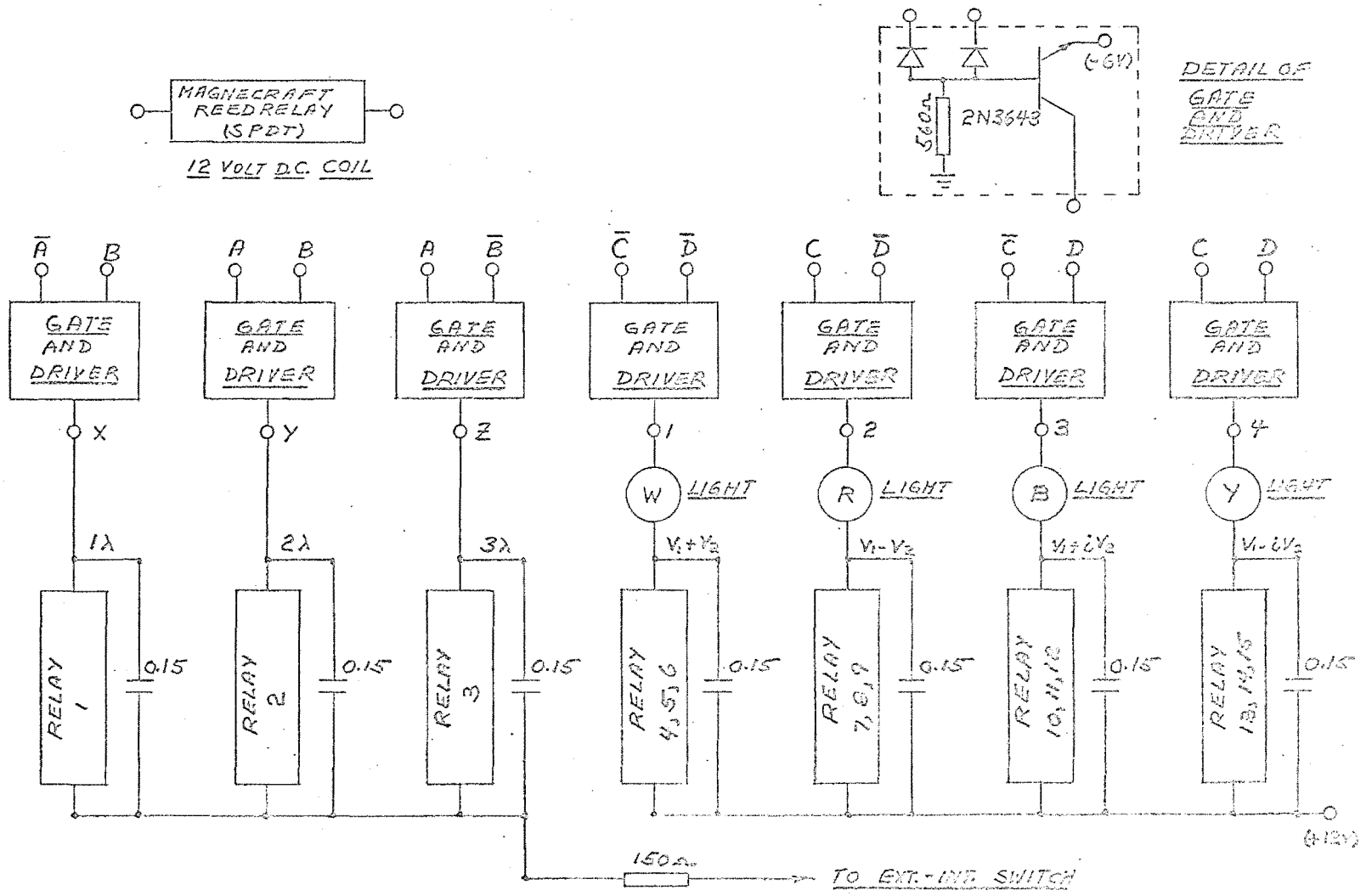

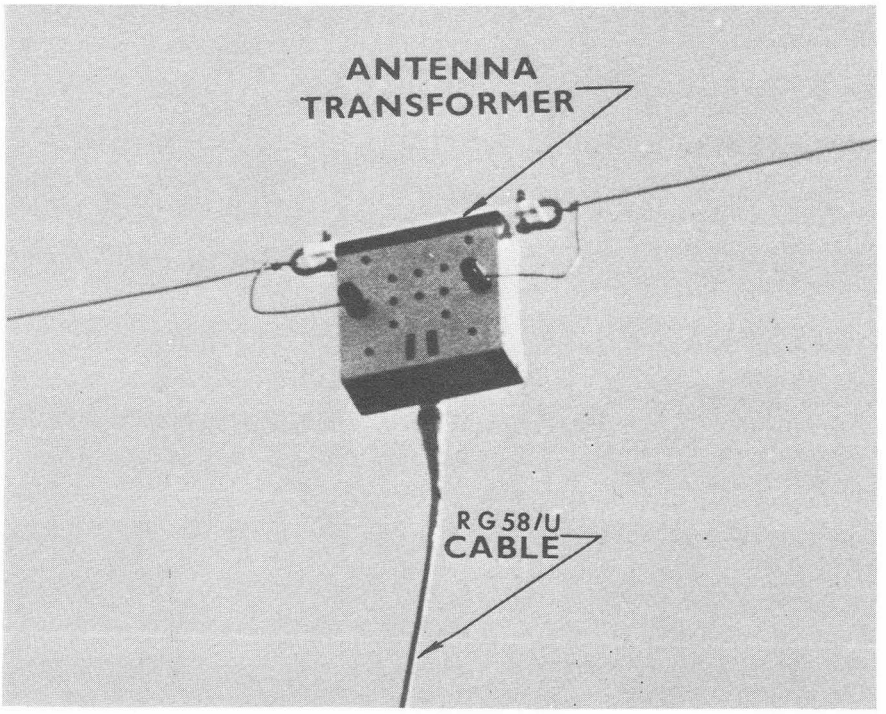

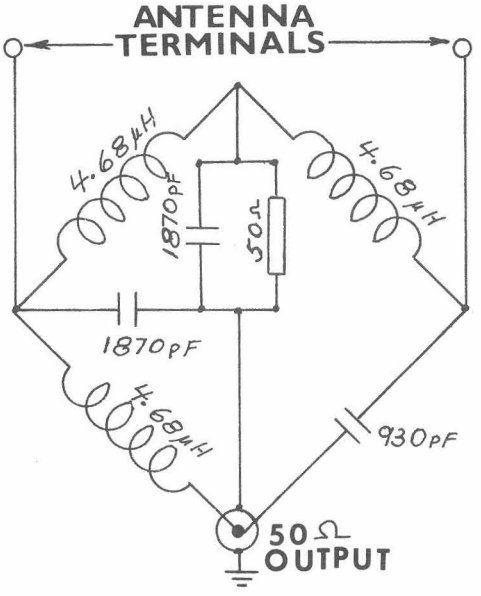

ANTENNA TRANSFORMER
AND
CIRCUIT DIAGRAM
FIGURE - A7

APPENDIX B

DERIVATION OF THE SPATIAL FIELD CORRELATION WHEN BOTH MAGNETO-IONIC MODES ARE PRESENT

The experimental technique described in section III(2) was based on the assumption that a simple plane wave is received by the antennas on the ground. It will be shown in this appendix that the technique employed in the experiment is also applicable when the received electromagnetic energy is elliptically polarized.

Assume that a wave field $\vec{E}$ consists of the vector sum of two magneto-ionic wave components. These components are $\vec{E}_o$ and $\vec{E}_x$, designating the electric field of the ordinary wave and the extraordinary wave, respectively. In a plane of constant phase, these two fields are defined so that

$$\vec{E}_o = A(\hat{x}' + i\hat{y}') \qquad \text{(B-1a)}$$

$$\vec{E}_x = B(\hat{x}' - i\hat{y}')\exp(i\beta) \qquad \text{(B-1b)}$$

In equation (B-1) $\hat{x}'$ and $\hat{y}'$ represent orthogonal unit vectors, and β is the total phase difference between the magneto-ionic components.

Assume next that two antennas are located in the x-y plane and that these are spaced a distance (r) from one another along the y-axis. Assume further that

the x'-y' plane and the x-y plane are inclined to one another by an angle Θ and, for simplicity, that the intersection of the planes coincides with the x-axis. The voltages induced in the two antennas will be designated V_1 and V_2, so that

$$V_1 = (A+B \exp i\beta)\cos\delta - i(A-B\exp i\beta)\sin\delta \qquad \text{(B-2a)}$$

$$V_2 = \left[(A'+B'\exp i\beta)\cos\delta - i(A'-B'\exp i\beta)\sin\delta\right]\exp -i\phi \qquad \text{(B-2b)}$$

In equation (B-2) δ is the angle between the x' axis and the x axis, and $\phi = \frac{2\pi r}{\lambda}\sin\Theta$.

As was suggested in III(2), V_2 will next be modified by changing its phase by some angle α, and the resulting voltage will be added to V_1. Thus:

$$S(\alpha) = (V_1 + V_2 \exp i\alpha) \qquad \text{(B-3)}$$

As before, the receiver output is assumed to be proportional to the magnitude of $S(\alpha)$.

The actual evaluation of the mean squared value of $S(\alpha)$ in terms of the parameters in (B-2) is straightforward but extremely tedious. In order to simplify the resulting expression for $\overline{|S(\alpha)|^2}$ several assumptions were made. To begin with, it was assumed that $\overline{|A|^2} = \overline{|A'|^2}$ and that $\overline{|B|^2} = \overline{|B'|^2}$. In addition, it is assumed that the complex spatial correlation $\rho(r)$ is not dependent on the particular magneto-ionic mode.

Thus:

$$\rho(r) = \frac{\overline{BB'^*}}{\overline{|B|^2}} = \frac{\overline{AA'^*}}{\overline{|A|^2}} \qquad \text{(B-4)}$$

In the derivation for $\overline{|S(\alpha)|^2}$ allowance was also made for the possibility that the magneto-ionic modes are not fully correlated. This possibility was pointed out by von Biel, Flood, and Camnitz (1970). Accordingly, the correlation between the x-wave and o-wave will be defined as

$$\rho_{xo} = \left|\frac{\overline{AB^*}}{\overline{|A|}\,\overline{|B|}}\right| \exp i\beta \qquad \text{(B-5a)}$$

and

$$R_{xo} = |\rho_{xo}| \qquad \text{(B-5b)}$$

Finally, the following identities were assumed:

$$\rho_{xo}\rho(r) = \frac{\overline{AB'^*}}{\overline{|A|}\,\overline{|B|}} \qquad \text{(B-6a)}$$

$$\rho_{xo}^*\,\rho(r)^* = \frac{\overline{B'A^*}}{\overline{|A|}\,\overline{|B|}} \qquad \text{(B-6b)}$$

$$\rho_{xo}^*\,\rho(r) = \frac{\overline{BA'^*}}{\overline{|A|}\,\overline{|B|}} \qquad \text{(B-6c)}$$

$$\rho_{xo}\rho(r)^* = \frac{\overline{A'B^*}}{\overline{|A|}\,\overline{|B|}} \qquad \text{(B-6d)}$$

Within the limitations of these assumptions, it can be shown that

$$\overline{|S(\alpha)|^2} = 2\left[\overline{|A|^2} + \overline{|B|^2} + 2R_{xo}\,\overline{|A|}\,\overline{|B|}\cos(\beta - 2\delta)\right]\left[1 + R(r)\cos(\phi' - \alpha)\right] \qquad \text{(B-7)}$$

where $R(r) = |\rho(r)|$ and $\phi' = \phi + \arg[\rho(r)]$. Equation (B-7)

is of the same form as the corresponding equations in III(2) derived for $\overline{|V(\alpha)|^2}$. Consequently, it has been shown that the magnitude and argument of the spatial field correlation, as derived from this experiment, is not dependent on the simultaneous presence of the magneto-ionic modes.

REFERENCES

Austin, G.L.(1967): "Nature of Radio Waves Reflected from an Undulating Surface"
Am. J. Physics, 35 no. 9 Sept. 1967.

Austin, G.L. and Thorpe, M.R. (1969): "Amplitude Distributions Resulting from Curvature Distributions of a Reflector"
Radio Science, February 1969.

Belrose, J.S. and Burke, M.J. (1964): "A Study of the Lower Ionosphere Using Partial Reflections"(1)
J. Geophys. Res., 69, 2799.

Booker, H.G.; Ratcliffe, J.A.; and Shin, D.H. (1950): "Diffraction From an Irregular Screen With Applications to Ionospheric Problems"
Phil. Trans. Roy. Soc. London, Ser. A 242, 579-607; 1950.

Booker, H.G. (1959): "Radio Scattering in the Lower Ionosphere"
J. Geophys. Res. 64, 2164-2177.

Bramley, E.N. (1951): "Diversity Effects in Spaced Aerial Reception of Ionospheric Waves"
Proc. Inst. Elec. Engrs. (London) 98, 19-25.

Bramley, E.N. (1953): "Direction Finding Studies of Large Scale Ionospheric Irregularities" Proc. Roy. Soc. A 255, 515.

Bramley, E.N. (1954): "Some Aspects of Rapid Directional Fluctuations of Short Radio Waves Reflected at the Ionosphere" Proc. Inst. Elec. Engrs. (London), B, 102, 533 (Paper 1713R).

Briggs, B.H. and Phillips, G.J. (1950): "A Study of the Horizontal Irregularities of the Ionosphere" Proc. Phys. Soc. (London) B, 63, 907.

Budden, K.G.: "Radio Waves in the Ionosphere" Cambridge University Press 1966.

Feinstein, J. (1954): "Some Stochastic Problems In Wave Propagation" Transactions IRE Vol. AP-2 Part I (January 1954) Part II (April 1954)

Fejer, J.A. (1955): "The Interaction of Pulsed Radio Waves in the Ionosphere" J. Atmos. Terr. Phys. 7, 322.

Flood, W.A. (1968): "Revised Theory For Partial Reflection D-Region Measurements" J. Geophys. Res., 73, 5585.

Fraser, G.J. and Vincent, R.A. (1968):
"A Study Of D-Region Irregularities"
NCAR MS-68-186
National Center for Atmospheric Research,
Boulder, Colorado, U.S.A.

Gardner, F.F. and Pawsey, J.L. (1953):
"Study of the Ionospheric D-Region Using
Partial Reflections"
J. Atmos. Terr. Phys. 3, 321.

Golden, J.T. (1965): "Fortran IV Programming and
Computing"
Prentice-Hall 1965.

Haug, A, and Pettersen, H. (1969):
"An Interpretation of Asymmetric
Cross-Correlation Functions in D-
and Lower E-Region Drift Measurements"
The Auroral Observatory, P.O. Box 387,
9001 Tromsø, Norway,
(Accepted for Publication in J. Atmos.
Terr. Phys.)

Parthasarathy, R.; Lerfald, G.M.; Little, C.G. (1963):
"Derivation of Electron Density Profiles
in the Lower Ionosphere Using Radio
Absorption Measurements at Multiple
Frequencies". J. Geophys. Res., 68, 12, 3581.

Ratcliffe, J.A. (1956): "Some Aspects of Diffraction Theory and Their Application To The Ionosphere"
Repts. Progr. in Phys. 19, 188.

Rice, S.O. (1944): "Mathematical Analysis of Random Noise"
Bell System Tech. J. 23, 282-332; 1944.

Rice, S.O. (1945):
Bell System Tech. J. 24, 46; 1945.

Sen, H.K. and Wyller, A.A. (1960):
"On The Generalization Of The Appleton-Hartree Magneto-Ionic Formulas"
J. Geophys. Res., 65, 3931-3950.

Slack, M. (1946): J. Inst. Elec. Engrs. Pt. III, 93, 76.

Smith, R.A. and Bourne, I.A. (1966):
Private Communication At The Symposium of Ground Based Techniques.
Ottawa, Ontario, Canada; 1966.

Uhlenbeck, G.E. (1945):
Radiation Laboratory Report No. 454 (M.I.T.)

Vincent, R.A. (1967): "Lower Ionospheric Irregularities"
Ph. D. Thesis, University of Canterbury, Christchurch, New Zealand, page A27.

von Biel, H.A. (1965): "1965 Solar Eclipse Partial Reflection Experiment"
Final Report Contract DA49-146-XZ-403;
DASA, Washington, D.C., U.S.A. December 1965.

von Biel, H.A. (1966): "D-Region Partial Reflection Experiment Performed During The 12 November 1966 Solar Eclipse"
Final Report Contract DA-49-146-XZ-546;
DASA, Washington, D.C., U.S.A. July 1967.

von Biel, H.A.; Flood, W.A.; Camnitz, H.G. (1970): "A Differential Phase Partial Reflection Technique For The Determination Of D-Region Ionization"
J. Geophys. Res., (in press).

Whale, H.A. and Gardiner, C.W. (1966): "The Effect of a Specular Component On The Correlation Between Signals Received On Spaced Antennas"
Radio Science, vol. 1 (new series) no. 5, p. 557.

Whitehead, J.D. (1962): "Distribution of Echo Amplitudes From an Undulating Surface"
J. Atmos. Terr. Phys. 24, 715-721.